The Application of X-RAY Computerised Tomography for the Advancement of Non-Invasive Imaging in Entomology

Greco, Mark

Award date:
2013

Awarding institution:
University of Bath

THE APPLICATION OF X-RAY COMPUTERISED TOMOGRAPHY FOR THE ADVANCEMENT OF NON-INVASIVE IMAGING IN ENTOMOLOGY

Mark Kerry Greco

A thesis submitted for the degree of Doctor of Philosophy

University of Bath

Department of Electronic and Electrical Engineering

February 2013

COPYRIGHT

_____

Mark K Greco

TO MY WIFE AND DAUGHTERS…

Table of Contents

Dedication……..……...……...…ii

Table of Contents.....…….……iii

List of Figures…….……viii

List of Tables…….xi

Acknowledgements…….....……xii

Thesis Summary……..xiii

Chapter 1 Literature Review…….……..……1

1.1 Introduction…….…….……..…....1

1.2 Non-invasive Imaging……...……..2

1.3 Techniques available for non-invasive imaging……..…..…….…2

1.4 Computed tomography (CT)…….……..…….…….....3

1.4.1 Tomography…….…….…….……3

1.4.2 CT…….…….……..……..…4

1.4.3 Back-Projection…….……..…5

1.4.4 Iterative methods…….…...…8

1.4.5 Analytic reconstruction…….…….…..…..9

1.4.6 Algebraic Reconstruction Technique (ART)……..……..…….9

1.4.7 Multiplicative Algebraic Reconstruction Technique (MART)…….…..….10

1.4.8 Simultaneous Algebraic Reconstruction Technique (SART)……..11

1.5 Limitations of x-ray CT……..…..11

1.6 Types of scanners……..…12

1.6.1 First-Generation Scanners……...…….12

1.6.2 Second-Generation Scanners……12

1.6.3 Third-Generation Scanners…….…….12

1.6.4 Fourth-Generation Scanners…….……12

1.6.5 Modern CT scanners…….…13

Chapter 2 Description of the methods……..…..……14

2.1 Introduction……..……14

2.2 Proof of concept for using X-ray Computer Tomography in insect biology studies……...……..15

2.3 Sample preparation……...…….……16

2.4 Data capture……...……18

2.5 X-ray beam energy……...……..…19

2.6 Scan field size…….…...……19

2.7 Slice thickness……...……20

2.8 Detector number……..…….……20

2.9 Data storage……...…20

2.10 Post-processing…….21

2.11 Data analyses……23

Chapter 3 Application of CT to morphology of locusts, ladybirds and butterflies……..24

3.0 General Introduction…….24

3.1 CT of locust……..……24

3.1.1 Introduction……..……24

3.1.2 Methods……27

3.1.2.1 The insects……..…….…….27

3.1.2.2 Micro-CT scanning…….……..…27

3.1.2.3 Image reconstruction and viewing……27

3.1.2.4 Masking and Segmenting…….……27

3.1.2.5 Production of 3-D printed models…….…….…..…28

3.1.3 Results……..29

3.1.3.1 Imaging…….29

3.1.3.2 The 3-D printed model…….……36

3.2 CT of Ladybird…….……38

3.2.1 Introduction……..……..38

3.2.2 Methods……38

3.2.3 Results……..39

3.3 CT of the Butterfly…….…..48

3.3.1 Introduction……..48

3.3.2 Methods……49

3.3.3 Results……..51

3.4 Discussion……..……52

3.4.1 The locust…….52

3.4.2 The ladybird…….…….53

3.4.3 The butterfly…….……54

3.5 Future Directions……..54

Chapter 4 A specific case for non-invasive CT "The Honeybee Bee Brain"…..…56

4.1 Introduction…….…….56

4.2 Methods……57

4.3 Results……..60

4.4 Discussion……61

4.5 Future Directions……..62

Chapter 5 Application of CT to Insect Behaviour……63

5.1 Introduction……..63

5.2 Methods……66

5.2.1 Hive preparation…….…..66

5.2.2 Diagnostic Radioentomology (CT)……..68

5.2.3 Statistics……68

5.2.4 Distribution of storage cells on combs…….……70

5.2.5 Sugar concentration versus distance from brood centre……..…70

5.3 Results……..…..…71

5.3.1 Honey storage frequency ratios……..……..71

5.3.2 Distribution of storage cells on combs……..…….…..…71

5.3.3 Sugar concentration versus distance from brood centre……..…….....…71

5.4 Discussion……..…..…..…73

5.5 Future Directions……..76

Chapter 6 Conclusion and Future Research……..…..…...…77

Literature Cited……..…..…..…81

Appendices……..…...103

List of Figures

Figure 1 A schematic of focal plane tomography……..……...4

Figure 2 An object of random shape, f(x,y) and its projection are shown for an angle of….……..7

Figure 3 A schematic diagram of how CT values are calculated using the Sum along ray method…….....…….…….8

Figure 4 Sample preparation for MacroCT .……...……17

Figure 5 A schematic diagram of sample positioning for MicroCT.…….…….18

Figure 6 A BeeView post-processing table representing quantitative measurements of wax volume in a managed *A. mellifera* hive……22

Figure 7 Four 3-D views of the desert locust *(S. gregaria*)……29

Figure 8 Four 3-D views of the head and thorax……31

Figure 9 Three views of the head and thorax..……32

Figure 10 Two 3-D views of the segmented tracheal system.……..33

Figure 11 Three MIP volume rendered images of the thorax including details of legs, HAS and tracheae……...…..34

Figure 12 Two 3-D views of the metathorax and anterior abdomen…….……...35

Figure 13 STL file of the segmented tracheal system of the locust's abdominal tracheal system……..…….……..36

Figure 14 The STL image of a section of the segmented tracheal system of the locust's abdominal tracheae……..…….37

Figure 15 Photomicrograph of "stage 1" dissection of *C. septempunctata* with elytra and tergites removed……..…..40

Figure 16 Photomicrograph of "stage 2" dissection of *C. septempunctata* detailing the abdominal portion of the alimentary tract……..41

Figure 17 Photomicrograph of the resected thoracic and abdominal sections of the alimentary tract of *C. septempunctata*……..42

Figure 18 Schematic diagram of thoracic and abdominal sections of the alimentary tract of *C. septempunctata*…...…….43

Figure 19 A 3D, volume rendered, micro-CT image of a male *C. septempunctata* using Maximum Intensity Projection…….……..44

Figure 20 A 2D micro-CT image showing a transverse section through a *C. septempunctata* abdomen…….……..……..45

Figure 21 A 2D micro-CT image showing a transverse section through a *C. septempunctata* abdomen……..…..…..46

Figure 22 A 3D, volume-rendered and segmented image of the radio-opaque malpighian tubules in *C. septempunctata*……..……..47

Figure 23 Three individuals of *M. menelaus*, a late-stage caterpillar (larva), a mid-stage chrysalis (pupa) and a late-stage chrysalis (adult)……..49

Figure 24 Four 3-D images of *M. menelaus*……..…….…..…..…..51

Figure 25 The 3D rendered brain…….……..…..…….58

Figure 26 A 3D volume rendered image of a live honey bee's head capsule…..….59

Figure 27 A 3D volume rendered image with BeeView software of a live honey bee showing the three body segments…..……..60

Figure 28 A 2D axial view of a live honey bee brain showing perfusion of contrast medium…….…...61

Figure 29 A schematic diagram of the three possible pathways as evidenced by the empirical data……...……..…..65

Figure 30 A 3D CT scan of an Apidae hive as prepared for mapping the in-hive honey distribution patterns…….……..67

Figure 31 The standard curve produced for this experiment plotting Hounsfield Units (HU) according to sugar concentrations……...…..69

Figure 32 A 2D CT scan showing patchy distribution of cells containing honey with differing sugar concentrations…….…..…72

List of Tables

Table 1 Options for scanning insects and their colonies…….……100

Table 2 Honey storage frequency ratios……...…101

Table 3 Spearman correlations of Hounsfield Units (HU) vs. distance measures and Kruskal-Wallis tests…….……102

Acknowledgements

I thank my supervisors Professor Cathryn Mitchell and Dr Manuchehr Soleimani for their consistent support. Professor Cathryn Mitchell's academic guidance and encouragement was particularly appreciated. I also especially thank Professor Duncan Bell for his continued and enthusiastic academic support. Professor Nick Mitchell, Professor Chris Budd, Professor Ed Feil, Dr Nick Priest, Professor Nick Britton and Professor Kate Robson-Brown also helped with advice and academic support during my research. My research was also supported by the tireless efforts of Mr Bob Needs, Mr Peter Davis, Dr Tony Herbert, Mr Brian Coates, Dr David Mortimore and Mr Nick Corps. (And of course there are too many to name individually but I collectively thank the many thousands of bees that enthusiastically contributed to my research).

Thesis Summary

Current methods for assessing the health of insects and their colonies are carried out by researchers making dissections on individual insects (which inevitably kills them) or making visual inspections of colonies and then documenting their observations. For colonies, researchers look for behavioural signs which indicate healthy individuals where foragers are regularly bringing in resources or in weak colonies, where there are fewer foragers working with a more lethargic and less purposeful manner. These methods are prone to large errors and they kill many insects in the process. The research detailed in this thesis addresses the subjective and destructive nature of these methods. This thesis also describes new methods using x-ray CT to develop and adopt protocols to accurately study insects non-invasively. Chapter one covers the current literature on tomography and some background on the different CT methods. Chapter two gives a thorough description of the new methods being developed to study insects non-invasively and details techniques that can be adopted by researchers who require non-invasive approaches to their work. Chapter three describes in detail three examples of research that has been conducted on locusts, ladybirds and butterflies to non-invasively study aspects of their morphology. The methods described maintain the integrity of the specimens for future use if so required. Chapter four covers a specific example of a fine detail study on plasticity of the honeybee brain using X-ray MicroCT and discusses the potential for live scanning to observe brain plasticity in insects. Chapter five extends the work from chapter two to show the usefulness of CT for studying insect behaviour by documenting and describing previously unreported honeybee storage behaviour. Chapter six draws conclusions from the other chapters and discusses future research.

CHAPTER 1

Literature Review

1.1 Introduction

Current methods for assessing colony health in insects are carried out by researchers documenting their observations while making visual inspections. Typically, researchers look for behavioural signs which indicate a healthy individuals or colonies where foragers are regularly bringing in resources or weak colonies where there are fewer foragers working in a more lethargic and less purposeful behaviour. In honeybees (*Apis mellifera*) colonies, frames can be removed or observation hives can be used to observe queen activity such as egg policing and ovipositing or worker hygiene behaviour; however, the methods are based on the experience of the observer which can take years to develop. In stingless bees, colony health can be assessed by manually splitting the hive box apart to view internal structures and evidence of queen activity (Dollin 1996a & 1996b); however, due to the subjective nature of the methods, large errors can occur. The process of opening the hive is particularly invasive for stingless bees, because of the central position of the brood chamber. Many hundreds of bees are often killed from one observation alone. The bees' small size makes them vulnerable to drowning in the spilt honey that invariably occurs during the process. Closing the hive after visual inspection also kills bees, and places the queen at risk of being harmed, as they are squashed in the process. Nevertheless, behavioural and morphological studies on insects continue and because many species are cryptic, have propensities to live in cavities and current methods are invasive and prone to large errors, new methods for studying them are emerging. Therefore, it is important to develop methods which can more accurately and less invasively assess colony health.

1.2 Non-invasive imaging

On the 8th of November 1895, Wilhelm Conrad Röntgen (accidentally) discovered an image cast from one of his cathode ray generators. He later repeated the image by taking an X-ray photograph of his wife's hand which revealed her wedding ring and her bones. The photograph initiated great scientific interest in the new found radiation which he called "X-radiation", because he did not know what type of radiation it was, hence the modern term, X-rays. In general, non-invasive imaging is associated with X-rays or medical imaging, which is a non-invasive method for evaluating anatomy and physiology. Although it is now know that X-rays can be invasive (and can damage biological tissues) at higher energies, the term non-invasive is based on the fact that, at the lower energies used in current imaging modalities, they do not create any damaging biological effects.

1.3 Techniques available for non-invasive imaging

As a field of scientific investigation, non-invasive imaging constitutes a sub-discipline of biomedical engineering, medical physics or medicine depending on the context. Methods such as nuclear medicine use radioactive materials to diagnose or treat various pathologies and are generally considered to be invasive. Many of the techniques developed for non-invasive imaging such as X-rays, nuclear magnetic resonance imaging (MRI) and ultrasonography (U/S) also have industrial applications, although the energies used in industrial applications would be considered to be highly invasive for biological samples. In the case of U/S, the probe consists of ultrasonic pressure waves which return echoes from the various tissue interfaces. The echoes show details of the internal structures. U/S waves do not travel through large interfaces or air and thus limits its use. In the cases of X-rays and MRI, either X-radiation or a magnetic field respectively pass through the subject/sample to identify, separate and quantify different tissue types such as bone, muscle or fat. In general, MRI is the best modality for differentiating soft tissues, is non-invasive and has very long image acquisition times

whereas X-rays are better for resolving smaller structures and have much faster in image acquisition times.

1.4 Computed tomography (CT)

1.4.1 Tomography

Tomography is the method of imaging a single plane, or "slice", of an object resulting in a tomogram. In 1917, the mathematician Radon devised a formula which became known as the "Radon Transform" and in 1921 Bocage used this formula to develop focal-plane tomography. Focal-plane tomography was introduced into X-ray transmission imaging in the 1920's (Bocage 1921). Bocage achieved this by passing X-rays through various objects and moving the X-ray source and target so that only the desired layer was maintained in sharp focus while other layers were blurred out (Fig. 1). The visual effect was similar to that of a narrow depth-of-field in photography, where a desired focal plane remains sharp and all the other objects in the field are blurred (Hsieh 2003).

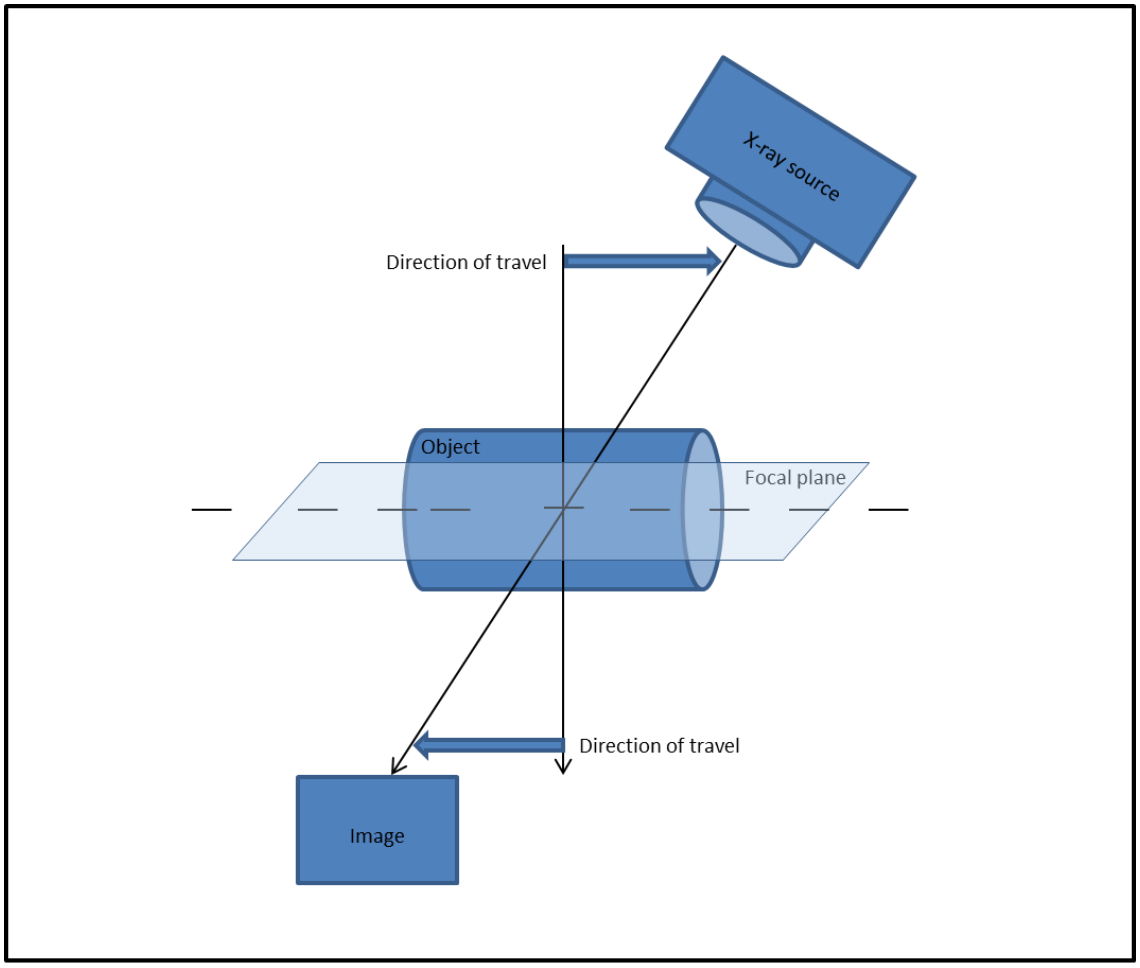

Figure 1: A schematic diagram of how focal-plane tomography is achieved.

1.4.2 CT

The main disadvantage of focal plane tomography is the presence of the unwanted (blurred) information on either side of the desired plane. In CT, the X-rays, used to acquire the data, do not enter other sections of the object. They only pass through the layer being examined, so that unwanted planes are completely omitted. Also, if a sufficient number of views or projections are taken, the distribution of attenuation coefficients within the layer may be determined. The reconstruction of the image from its projections is performed by a computer. In the mid-1960s Godfrey Hounsfield considered whether he could reconstruct a three-dimensional representation of the contents of a box from a set of readings taken through the box at randomly selected directions. He found that by considering the three-dimensional object within the box as a

series of slices, reconstruction was easier than treating the content as a volume. He tested the theoretical principle by working with a matrix of numbers set to zero with a square in the middle where each number was set at 1000. He entered these data into a computer programme to get simulated absorption values and then reconstructed the picture. In 1973 he was instrumental in building the first medical head CT scanner which was funded by EMI (Hounsfield 1973). Later on, he developed a linear greyscale equation based on X-ray attenuation:

$$HU = 1000 \times ((\mu X - \mu water) / \mu water)) \quad [1]$$

Where HU is the Hounsfield Unit, μX is the X-ray attenuation coefficient of a tissue and μwater is the X-ray attenuation coefficient of distilled water at standard temperature and pressure. After using this equation, water is given the value of zero and air is given the value of -1000 which means that tissues with μX higher than water have a positive value and tissues with a lower μX than water have a negative value. This made it possible to attribute a HU value for different tissues based on their X-ray attenuation coefficients.

1.4.3 Back-Projection

First attempts at CT used a method of reconstruction known as back-projection. Reconstruction was performed by back-projecting an object's profile across a plane, i.e. the magnitude of each ray-sum is applied to all points that make up the ray (Fig 2). Generally, Back-Projection does not produce a good reconstruction because each ray-sum is applied to all points along the ray which includes those of high and low densities and this creates star type artifacts (Brooks and Di Chiro 1976).

The algorithm that is currently being used in almost all applications of sum-along-ray tomography is the filtered back-projection algorithm. The algorithm is accurate and works well with fast implementation (Kak and Slaney 1988) and it is based on the Radon transform:

$$g(\phi,s) = \int_l f(x,y)\,dl \quad [2]$$

Where, g(∅,s) as a 1-D projection at an angle (∅) and g(∅,s) is the line integral of the image intensity, f(x, y), along a line l that is distance s from the origin and at angle ∅ off the x-axis.

All points on this line satisfy the equation:

$$x*\sin(\emptyset) - y*\cos(\emptyset) = s \quad [3]$$

Therefore, the projection function g(∅,s) can be rewritten as:

$$g(\phi,s) = \iint f(x,y)\delta(x\sin\phi - y\cos\phi - s)dxdy \quad [4]$$

The collection of these g(∅,s) at all ∅ (Fig 2) is called the Radon Transform of image f(x,y).

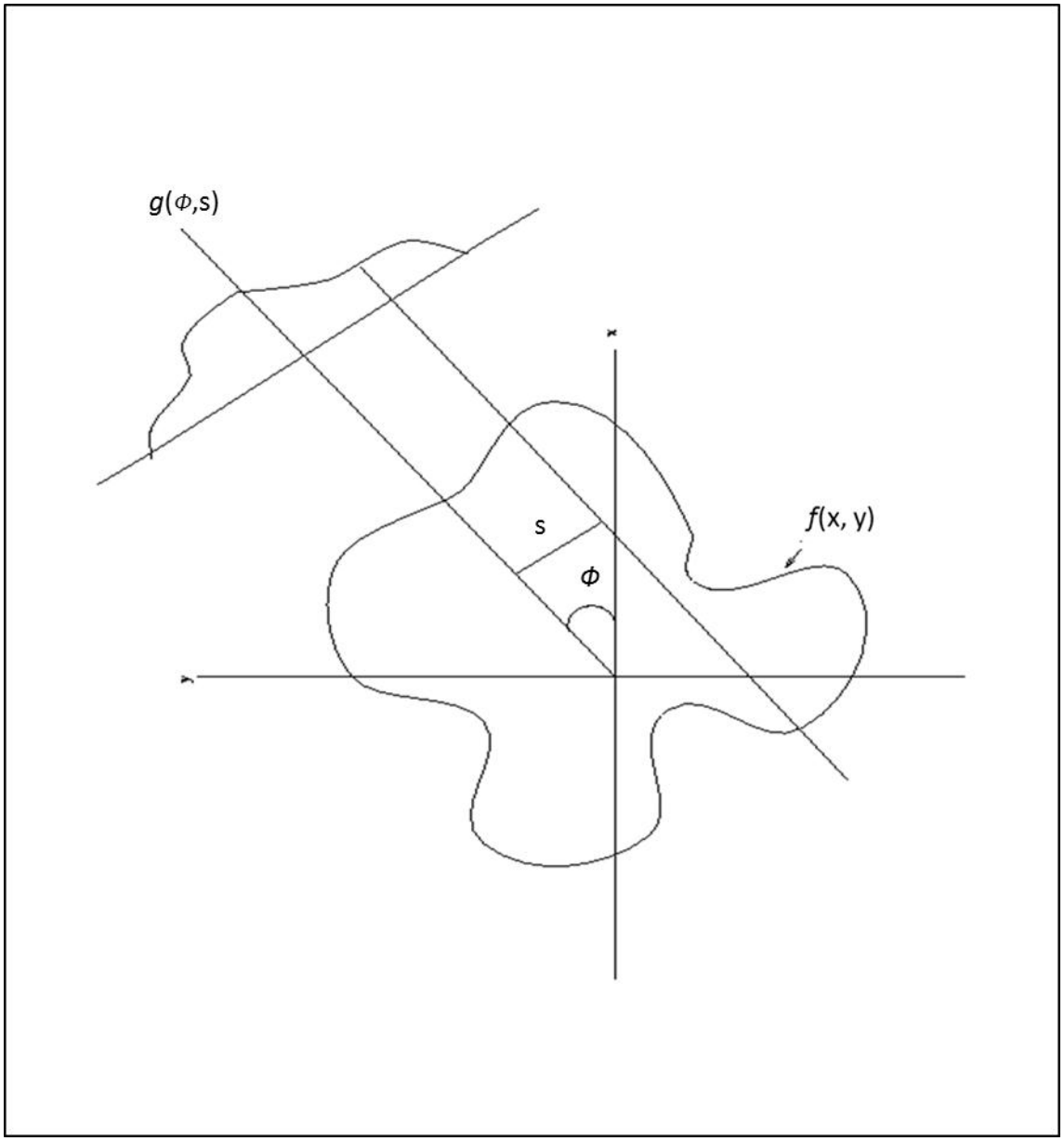

Figure 2: An object of random shape, *f*(x, y) and its projection are shown for an angle of ∅. Figure adapted from Kak (1979).

When given the Fourier transform of a projection at enough angles the projections can be assembled into a complete estimate of the two-dimensional transform and then inverted to arrive at an estimate of a random object (Fig 3).

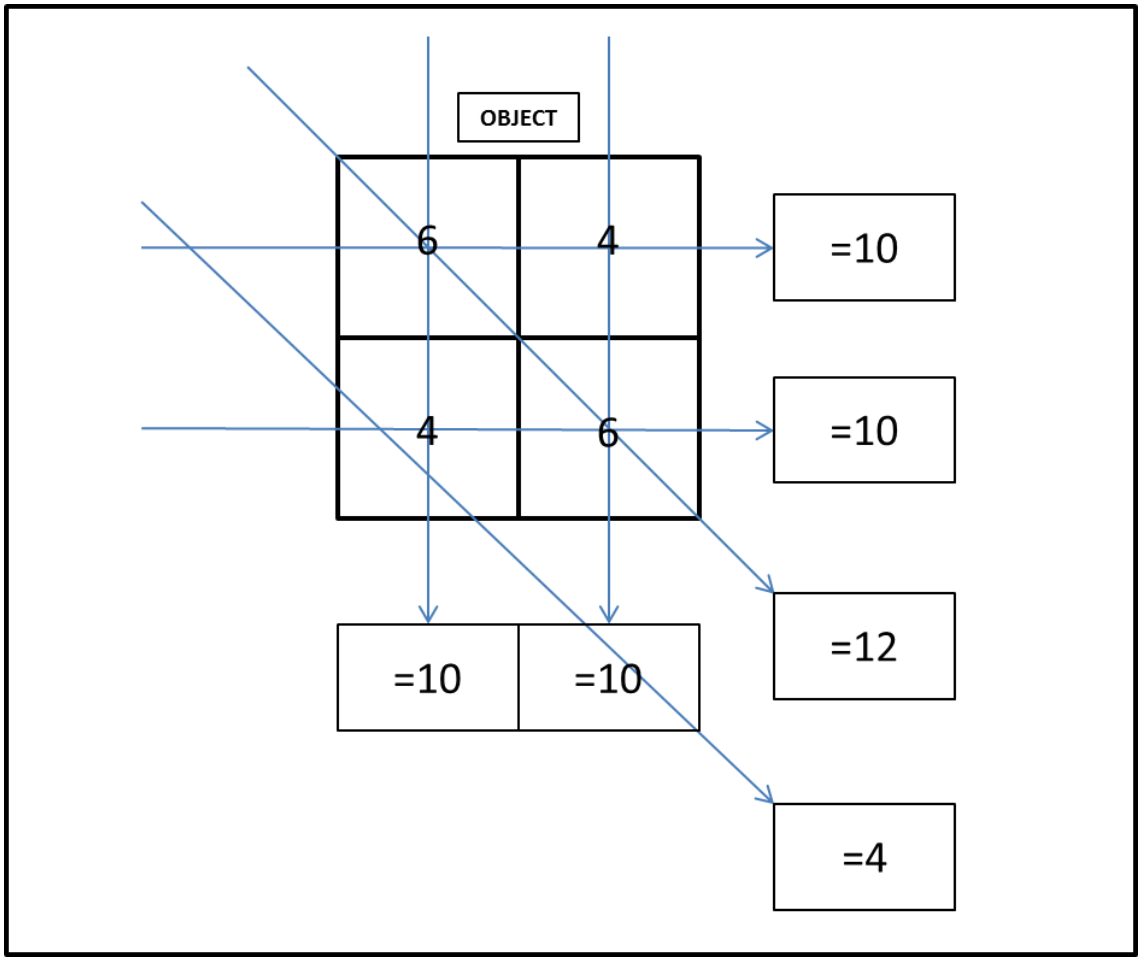

Figure 3: A schematic diagram of how CT values are calculated using the Sum along ray method. Arrows indicate direction of X-ray beam. In this simple illustration, the object has been divided into 4 pixels that have density values of either 6 or 4 HU's.

1.4.4 Iterative methods

Applying corrections to repeated iterations "iterative method" can overcome artefacts that occur with back-projections markedly. The strategy of iterative methods is to apply corrections to arbitrary initial cell densities in an attempt to match the measured ray-projections (Brooks and Di Chiro 1976) and because former matchings are lost as new corrections are made, the procedure is repeated until the calculated projections agree with the measured ones to within the desired accuracy.

1.4.5 Analytic reconstruction

Analytic reconstruction is based on ray sum projection data and again the spatial resolution needs to be limited to just the slice required (Brooks and Di Chiro 1976). In analytical reconstruction, a "band limit" is created so that the image will contain known frequencies. This means that the image can be reconstructed on an array of points, the projections can be sampled at the same interval and that Fourier transforms can be replaced by discrete Fourier series.

1.4.6 Algebraic Reconstruction Technique (ART)

ART is one of the iterative methods and the algorithms follow an intuitive form. For example, with X-ray CT, when the beam passes through the object each projected density is compared back across the reconstruction space in which the densities are iteratively modified. The iterations can bring each reconstructed projection into agreement with the measured projection. The ART algorithm consists of altering the grayness of each pixel intersected by the ray in order to make the ray sum agree with the corresponding element of the measured projection. Assuming that the image being reconstructed is enclosed in a square space of (n x n) array of pixels, $\rho_j (j = 1,\ldots,n^2)$ is grayness or density number, which is uniform within the pixel but different from other pixels. The ART algorithm was first published by Gordon et al. (1970). Rather than trying to handle a given system of equations as a whole, the ART works by an iterative process and has been shown to converge to the least squares solution. Another example is for ionospheric observations (Bust et al. 1997; Mitchell et al. 1998). The one described below is the ART algorithm with relaxation from Censor (1983). An initial guess, x_j^o, is obtained from the background ionosphere and for the k + 1th iteration:

$$x_j^{k+1} = I_j^k + \lambda_k \quad \frac{y_{i-\sum_{m=1}^{n} \Delta_{im} x_m^k}}{\sum_{m=1}^{n} \Delta_{im} \Delta_{im}} \Delta_{ij} \qquad [5]$$

where λ_k, the relaxation parameter, is a number or series of numbers used to control the convergence of the algorithm, $\Delta_{ij}$is the length element of raypath *i* through pixel *j*, *im* is the loop over m from 1 _ *n* for each *i*, and n is the total number of pixels in the grid. The current iterate, x_j^k, is refined to a new value, x_j^{k+1}, by considering a single ray, *i*, and changing the electron density value of the pixels, *j*, intersected by the ray. The discrepancy between the measured TEC and the TEC calculated through the current image is then redistributed among the pixels along the ray in proportion to the length of intersection with each pixel Δ_{ij}. The algorithm then cycles through all raypaths until convergence is achieved.

1.4.7 Multiplicative Algebraic Reconstruction Technique (MART)

The MART technique involves a multiplicative correction to the voxel intensity based on the ratio of the recorded pixel intensity *P*i and the projection of voxel intensities $\sum_j W_{ij} I_j^k$ from the previous iteration k:

$$I_j^{k+1} = I_j^k \left(\frac{P_i}{\sum_j W_{ij} I_j^k} \right)^{\mu W_{ij}} \qquad [6]$$

where μ is a relaxation parameter usually chosen between 0 and 2. Each voxel's intensity is corrected to satisfy one projection or pixel at a time, with a single iteration being completed after every projection has been considered. This method has been shown to provide the maximum information based entropy solution, to represent the most probable reconstruction image based on the recorded projections (Atkinson and Soria 2007). Elsinga et al. (2006) indicate that this algorithm is preferable to that of ART because of the artefacts created in the reconstructed field when using ART.

1.4.8 Simultaneous Algebraic Reconstruction Technique (SART)

A variation on algebraic approaches SART yields reconstructions of good quality and numerical accuracy with only one iteration (Kak and Slaney 1988). The main features of SART are to reduce errors in the approximation of ray integrals of a smooth image by finite sums, the traditional pixel basis is abandoned in favour of bilinear elements. Also, for a circular reconstruction region, only partial weights are assigned to the first and last picture elements on the individual rays. To further reduce the noise resulting from the unavoidable but considerably smaller inconsistencies with real projection data, the correction terms are simultaneously applied for all the rays in one projection. This is in contrast with the ray-by-ray updates in ART. In addition, a heuristic procedure is used to improve the quality of reconstructions. Also, a longitudinal Hamming window is used to emphasise the corrections applied near the middle of a ray relative to those applied near its ends.

In SART, superior reconstructions are obtained by using a model of the forward projection process that is more accurate than what can be obtained by the choice of pixel basis functions. This is done by using bilinear elements which are the simplest higher order basis functions. The basic functions obtained from bilinear elements are pyramid shaped, each with a support extending over a square region of multiple pixels.

1.5 Limitations of x-ray CT

A limitation of iterative methods is the need to select a finite iteration time. This means that there is a practical necessity of stopping before the best possible solution has been achieved. The result is that although some high-frequency detail is lost, some noise is reduced (Shepp and Logan 1974).

A major limitation of analytic methods is the assumption of band-limiting when it includes frequencies that are higher than the limit selected. If these frequencies are present in the projections after sampling intervals, they will reappear as “aliasing” (Bracewell 1965) and will cause a blurry edge to objects.

Processing speed is also a limitation in CT. Iterative methods require more time per iteration than a complete analytic reconstruction. X-ray dosage is a major consideration and therefore, faster processing means reduced doses. For live objects, motion artifacts occur and faster processing helps to reduces these.

1.6 Types of scanners

1.6.1 First-Generation Scanners

The original CAT scanner required pressing the patient's head against a rubber membrane and into a water-filled box. The box rotated in 1-degree increments while a single, narrow X-ray beam and single-detector assembly collected data during a five- to six-minute scan.

1.6.2 Second-Generation Scanners

Second generation scanners used 20 narrow beams and detectors, which allowed a complete scan in the time the patient could hold a breath.

1.6.3 Third-Generation Scanners

In third generation scanners, the beam was widened into a fan shape to cover the entire width of the patient. An array of 250 detectors was linked to the X-ray tube, which rotated together around the patient in approximately than five seconds.

1.6.4 Fourth-Generation Scanners

Fourth generation scanners were in use by 1976. They used a large, stationary ring of detectors that required only the X-ray tube to rotate around the patient. Faster computers and detectors made it possible to scan at 1cm/sec.

1.6.5 Modern CT scanners

Nowadays, synchrotron beamlines can complete scans and reconstruct 3-D images in a matter of seconds and CT scanners can complete a 1cm scan in as little as one-third of a second and recent techniques have been developed to enable scanning software to produce 3D images and physical 3D models (Udupa and Herman 2000). To produce 3D images, many slices are acquired, then reconstructed using software to produce a 3D model, which can then be manipulated and virtually dissected along infinite planes (Appendix 1). It is generally accepted that the term MacroCT applies to CT applications using human body scanners for "macroscopic" studies (resolution down to 0.5mm) and that MicroCT applies to laboratory or Synchrotron CT applications at the "microscopic" level (resolution down to 1.0µm).

Given the need to develop new methods for the study of insects, the overall aim of my thesis was to test the hypotheses that:

1. MacroCT can be used to non-destructively image behaviour in insect colonies;
2. MicroCT can be used to image the anatomical features of insects;
3. CT facilitates the study of insect physiology

The research described in this study was conducted as proof of concept for testing the three hypotheses above.

CHAPTER 2

Description of the methods

2.1 Introduction

In recent years, CT has been adopted to visualise macroscopic characteristics of insects and their behaviour (Tollner, 1991; Fuchs *et al.*, 2004; Greco *et al.*, 2005, 2006, 2009; Perna *et al.*, 2008). Also, with the improvements in spatial resolution and tissue differentiation that are occurring with MacroCT, conventional micro-focus and synchrotron based MicroCT, new methods for the non-invasive imaging of insects are emerging (e.g., Hörnschemeyer *et al.*, 2002; Betz *et al.* 2004Johnson *et al.*, 2004, Wirkner & Prendini 2007; Tafforeau *et al.*, 2006;; Greco *et al.*, 2008; Heethoff *et al.*, 2009). The basic principles of conventional micro-focus source MicroCT are similar to those used in medical CT scanners; however, it is now possible to achieve spatial resolutions down to a few micrometres (Bettuzzi *et al.*, 2004; Feeney *et al.*, 2006). Diagnostic radioentomology (CT) is the collective term used for the non-invasive study of insects using X-radiation (radiographs, MacroCT, and MicroCT). Traditional methods for colony health and the morphological classification of bees have been conducted with the aid of observation hives and dissecting light microscopes, respectively. These techniques are, understandably, limited. For example, observation hives offer only a view of one side of one frame within an entire hive and the use of light microscopy when used for amber inclusions (e.g., Wille and Chandler, 1964; Michener, 1982; Engel, 1995, 1996, 1997, 2000; Rozen, 1996; Camargo *et al.*, 2000; Oliveira, 2002; Hinojosa-Díaz and Engel, 2008), particularly with specimens preserved in opaque pieces (Lak *et al.*, 2008, 2009), are grossly limited. Schlüter and Stürmer (1982) attempted to address methods of examining insect inclusions in opaque amber pieces and to supplement traditional light microscopic study of even clear specimens. Those researchers and Gerling and Hermann (1978), Gerling *et al.* (1981) and Velthuis and Gerling (1983) produced traditional radiographs which provided the first, albeit limited, steps toward enhanced visualisation of cryptic bee behaviour and fossil material. More

recently, detailed information for the study of bees has been obtained with the use of scanning electron microscopy (SEM) (e.g., Serrão, 2001, 2005) and transmission electron microscopy (TEM) (e.g., Araujo *et al.*, 2005). While SEM and TEM studies currently provide the highest level of detail, sample preparations are laborious and are often invasive to completely destructive (e.g., Serrão, 2001). SEM and TEM can be used for the investigation of amber inclusions (e.g., Grimaldi *et al.*, 1994; Engel, 2001); however, these methods are generally not suitable because they require destruction of the material. The development of non-invasive imaging methods such as CT, therefore, offers promise to scientists who need to preserve their specimens or observe behaviour non-invasively.

2.2 Proof of concept for using X-ray Computer Tomography in insect biology studies

Computer Tomography (CT) has been used as a non-invasive method to visualise internal and external human morphology since the early 1970s and, more recently, has been used to study soil ecology and movement in cryptic insects (Tollner 1991; Harrison et al. 1993; Fuchs et al. 2004; Johnson et al. 2004). Modern, medical MacroCT scanners can achieve image resolutions of 0.3 mm and MicroCT scanners can achieve as little as 0.5 μm. CT is inherently non-invasive, because it does not create or promote any physical changes within the sample being studied. Essentially, the x-rays scan through an object/sample and the resultant beam is captured by a series of detectors. The information from the captured beam is then stored as a digital dataset, which can be reconstructed to produce two dimensional and three dimensional images of the object's/sample's structure (Udupa and Herman 2000). The stored information can also give an indication of the different densities that apply to the different structures within the object/sample (Udupa and Herman 2000). The doses used while scanning are measured and the x-ray beam's energy is too low to generate a significant biological effect (Kanao et al., 2003; Brenner and Hall 2007). As described above, current methods for observing nest structures, nesting behaviour and internal morphology of bees are invasive.

Prior to the research presented here, nobody had used CT to scan colonies of insects, so it was unknown whether CT would be sensitive enough to detect behaviour in colonies or to identify components such as individual insects, larvae or pupae. Therefore, I decided to test this by scanning a honeybee (*Apis mellifera*) hive with the purpose of observing their honey storage behaviour using MacroCT. The descriptions below apply jointly to MacroCT and MicroCT.

2.3 Sample preparation

One of the strengths of using CT for observing insects is that there is minimal or no sample preparation required. Generally, the only requirement to perform a CT experiment is that the sample needs to be positioned securely on the scanner bed for MacroCT (Fig. 4) or in the scanner sample stage for MicroCT (Fig. 5). For MacroCT of live colonies within beehives, scans generally take less 30 sec so individual bee movements do not cause any significant movement artefacts. There are also recent developments in movement correction software that will overcome these minor artefacts in the near future.

Figure 4: Sample preparation for MacroCT. Essentially the only preparation required is that the sample (bee hive) is positioned securely on the scanner bed.

Movement artefacts are more significant when scanning live bees in MicroCT scanners. MicroCT scans of individual bees can take as long as 30 min. Even securely fastened bees continue to move slightly during scans, so it is useful to either anaesthetise them with medical grade CO_2 and/or cool them down in a freezer for 10 min prior to scanning. A combination of cooling and CO_2 can keep individual bees motionless for approximately 25 min. If assessment of a particular body segment is required, reducing the scan field size to that segment will take less time, thereby reducing the need for CO_2 and/or cooling.

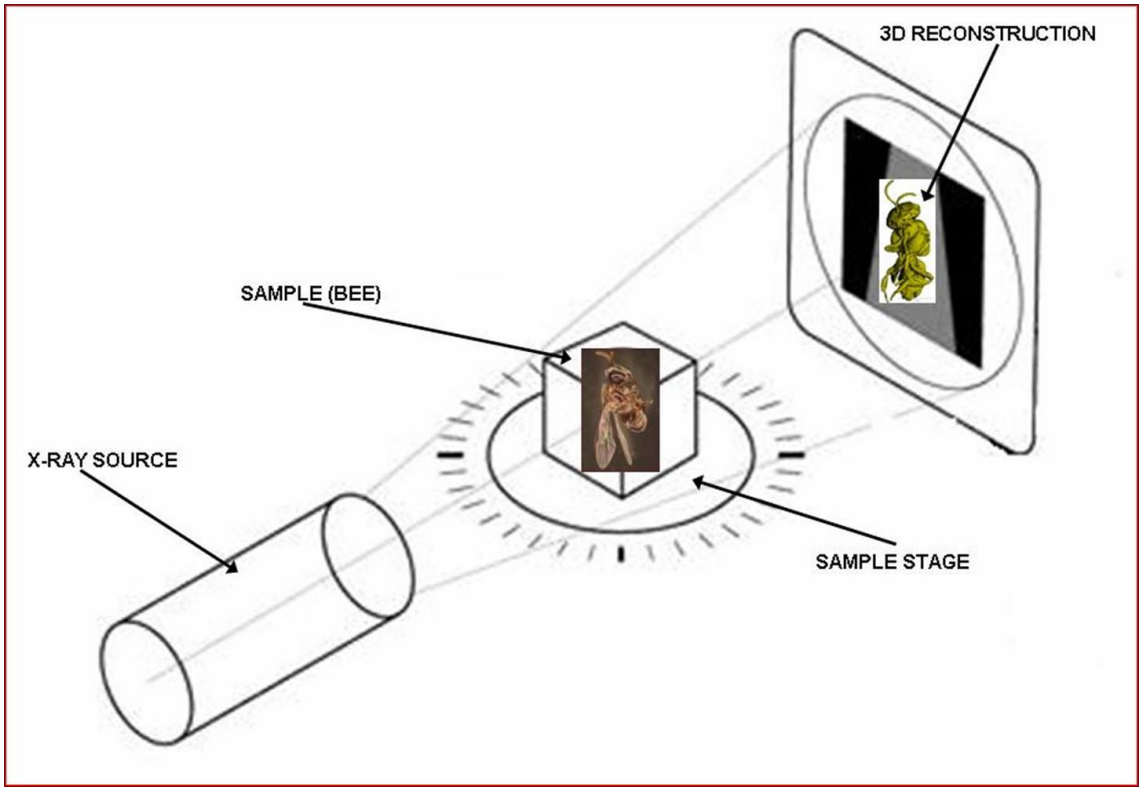

Figure 5: A schematic diagram of sample positioning for MicroCT. Essentially the only preparation required is that the sample (bee) is positioned securely on the sample stage so that the sample remains motionless during the scan.

2.4 Data capture

Once a sample has been positioned appropriately the scanner's proprietary software will guide the researcher on how to perform the required scan. During the scan, the x-ray beam passes through the sample to an array of detectors that record the x-ray beam attenuations produced from the sample's unique characteristics as a digital dataset in raw volume format. The raw volume data set can later be processed to provide 2D and 3D images of the sample as well as quantitative measurements such as volume of the sample's components or structures. The initial choice of scan parameters will influence the resolution of the final 2D and 3D images and the sensitivity of the quantitative measurement's resolution. The scanner's proprietary software will offer many choices for parameter selection; however, for best image resolution and quantitative

measurements, the most significant parameters to select are x-ray beam energy (amperage and voltage), scan field size, slice thickness and detector number.

2.5 X-ray beam energy

The x-ray beam's energy is determined by the amount of current (amperage) and the force of that current (voltage) selected to create the beam. The amperage determines the number of x-ray beam photons available during the scan (flux); thus, increasing the amperage will increase the intensity of the beam. The voltage determines the x-ray beam strength during the scan; thus, increasing the voltage will increase the strength of the beam. Large *A. mellifera* beehives require high energy levels (e.g. 120 mA at 150 kV), smaller stingless bee hives require lower energy levels (e.g. 80 mA at 120 kV) and individual bees can be scanned using even lower energies (e.g. 100 µA at 40 kV) to achieve appropriate image quality and quantitative measurements. For energy efficiency, x-ray dose minimisation and radiation safety it is useful to use the lowest energy levels to achieve the required results. Generally larger and denser samples require higher energy levels than smaller, less dense samples. Researchers will need to assess the energy level requirements independently and reduce amperage and voltage accordingly for their particular study.

2.6 Scan field size

The maximum scan field available during a scan is the fixed circular area of the scanner dimensions multiplied by the fixed length of the scanner's longitudinal travel. Researchers can select a smaller scan field size to include only the sample's region of interest (ROI). Thus, the adjusted scan field size becomes the raw volume data set in which the sample's ROI is contained. It is this raw volume data set that can be processed later to provide the 2D and 3D images and quantitative measurements. Smaller scan field sizes produce better spatial resolution than larger scan field sizes, because each detector will have less information to record and process. Shorter scan field travel will

reduce scanning times and, thus, reduce the likelihood of movement artefacts. Therefore it is better to select the smallest scan field necessary to cover the sample's ROI.

2.7 Slice thickness

Once the scan field size has been determined, slice thickness should be selected for the required spatial resolution. Smaller slice thicknesses result in higher spatial resolution, because there are more slices per unit of sample material. Slice thickness can be reduced to 0.3 mm for MacroCT and 0.5 µm for MicroCT. Researchers should be aware that smaller slice thicknesses produce more slices per unit of sample material and, thus, larger datasets. Larger datasets create the need for more powerful computer hardware and software during post-processing analyses.

2.8 Detector number

Higher numbers of detectors produce higher spatial resolution because there are more detectors receiving and processing information per unit of sample material. Some scanners offer a selection for the number of detectors used during the scanning process. Researchers should be aware that higher numbers of detectors require longer scanning times. Also, more pixels per slice and, thus, larger file sizes per slice are produced. Larger file sizes create larger data sets and the need for more powerful computer hardware and software during post-processing analyses.

2.9 Data storage

Once the sample has been scanned with the appropriate parameters, the resulting dataset needs to be stored appropriately. Scanners have limited space for data storage and usually auto-delete data sets that have not been stored permanently or exported. There are numerous storage devices available that can store electronic datasets (CDs, DVDs, flash drives etc.); however, external hard drives are the largest and most robust forms of

data storage devices. Appropriate storage of data sets is an important component of CT scanning which should be considered when planning an experiment. In particular, some behaviour experiments can continue for months and regular scanning can produce data sets of considerable size. A typical beehive behaviour experiment over six months can accumulate two 900 Mb datasets per month, totalling 10.8 Gb of storage space and MicroCT datasets of single insects can often be as large as 100-200Gb each.

2.10 Post-processing

Once datasets are appropriately stored, they can be post-processed to enable sample analyses. Post-processing can be performed directly on the CT scanner; however, this prevents the use of the scanner for other examinations or prevents other users from accessing the scanner. Therefore, remote post-processing with independent software enables researchers to use CT *ex situ*. There are several post-processing software packages available which can convert CT datasets to 2D and 3D images and several that can also provide quantitative measurements (Fig. 6).

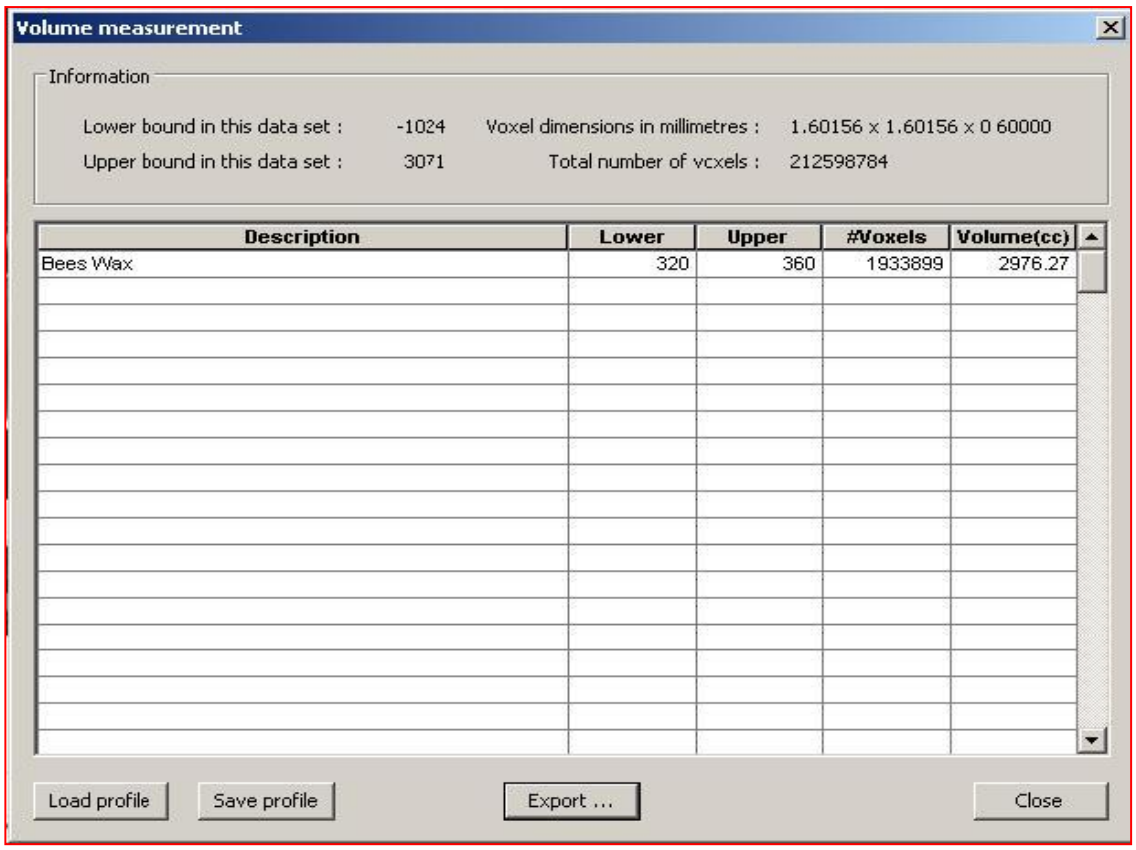

Figure 6: A BeeView post-processing table representing quantitative measurements of wax volume in a managed *A. mellifera* hive.

From personal experience, software packages such as VG STUDIO MAX V1.2 voxel data analysis and visualization software (Volume Graphics GmbH, Wieblinger Weg 92a 69123 Heidelberg Germany) and BeeView 3D rendering software (Disect Systems Ltd Suffolk, UK) produce the highest quality results and are the most versatile. BeeView has been the most affordable and, for the purpose of my experiments, has been the preferred choice of software. I suggest that researchers trial the various software packages available and determine which package is the most appropriate for their requirements. Post-processing is performed as a precursor to data analysis. It is essential that post-processing is performed with both the aims and results of the experiment in mind. For example, production of quantitative volume measurements is not necessary if the experiment requires sophisticated 3D images.

2.11 Data analyses

Data analyses are dependent on the aims of the experiments and can range from simple 2D or complex 3D visualisation of structures to more complex temporal studies of behavioural changes in colony structure or the external and internal morphology of individual insects.

To cover the application of these methods, Table 1 provides a summary the options for scanning insects and their colonies, their implications and which method is the most appropriate for the scientific investigation being considered.

CHAPTER 3

Application of CT to morphology of locusts, ladybirds and butterflies

---

3.0 General Introduction

The research described in this chapter will show the usefulness of CT for examining insects non-invasively. I will describe the application of CT for observing the detailed morphology of specimens from three insect genera (*Orthoptera*, *Coleoptera* and *Lepidoptera*). The first section will describe the intricate tracheolar respiratory system that delivers oxygen directly to tissues and cells which is a distinctive feature of many arthropods including the insects (Chapman 1998; Lease et al. 2006). Then I will describe in detail the malpighian tubules in insects using the ladybird beetle (*Coccinella septempunctata*). Finally, I will show the changes to the tracheal system of insects that occurs during metamorphosis using the blue morpho butterfly (*Morpho menelaus*) as a representative insect.

3.1 CT of the locust

3.1.1 Introduction

In insects, the tracheal system plays a vital role in delivering oxygen from the atmosphere directly to cells via the haemolymph and in expelling carbon dioxide derived from cellular respiration back into the atmosphere. In 2006, Lease et al. determined that the tracheal volume (V_T) should be considered as the total volume of air in an insect's tracheae and air sacs combined. Since the vast majority of insects have a paucity of the oxygen-carrying respiratory proteins haemocyanin and haemoglobin (Chapman, 1998); V_T greatly determines the amount of oxygen available during insect respiration (Lease et al. 2006).

Different methods have been used to determine V_T in insects including a) water displacement (Wigglesworth, 1950) b) use of inert gases (Bridges et al. 1980; Lease et al. 2006) c) Stereology (Schmitz and Perry 1999; Hartung et al. 2004) and d) Stereology in combination with synchrotron X-ray imaging (Kaiser et al. 2007; Greenlee et al. 2009; Socha et al. 2010 and Kirton et al. 2012). All have potential advantages and disadvantages. Because of the high resolution factor, insect imaging is being revolutionised by the use of X-ray Synchrotron imaging (Kaiser et al. 2007; Greenlee et al. 2009; Socha et al. 2010; Greco et al. 2011; Greco et al. 2012; Kirton et al. 2012) however, adequate long term access to synchrotron facilities is a limiting factor for entomologists who require non-invasive approaches to their research.

Visualising the anatomy of an entire insect tracheal system including the use of modern stereomicroscopes remains notoriously difficult (Vinal 1919; Snodgrass 1935; Albrect 1953; Albrecht 1956; Miller 1960a; Clarke and Richards 1976). In 1919 Vinal eloquently illustrated the respiratory system of the Carolina Locust, *Dissosteira carolina* and summarised and referenced much of the earlier work on locust tracheal systems. The paper included Malpighi's discovery of the respiratory system of the silk worm in 1669 and the beautifully illustrated work of Swammerdam (1758) on honey bee anatomy. Vinal (1919) also details the work of others including Lyonet (1762) on the goat moth *Cossus cossus*, Strauss-Durckheim (1828) on the cockchafer *Melolontha vulgaris* and Denny's studies of the Cockroach and finally the studies of Alt (1912) on the great diving beetle *Dytiscus marginalis.*

Much of the research on insect respiration from the 1970's onwards (Imms 1970; Chapman 1998; Klowden 2007; Nation 2008) continues to refer back to the early research of Swammerdam (1758), Vinal (1919) and Snodgrass (1935) and research on respiratory physiology on the mechanisms of insect ventilation and flight frequently refers to research from Hamilton (1937), Weis-Fogh (1952), Weis-Fogh (1956a), Weis-Fogh (1956b), Weis-Fogh (1956c), Miller (1960a), Miller (1960b), Miller (1960c), Weis-Fogh (1964a), Weis-Fogh (1964b), Weis-Fogh (1964c) and Weis-Fogh (1967) and on the detailed light and electron microscopic studies of tracheal and air sac anatomy of Maina (1989) and Hartung et al. (2004). This common practise of referring

to historical studies reflects the continuing difficulties with dissecting extremely small (10-20µm) and delicate tracheae and air sacs (Vinal 1919). Such problems include a) obstruction or alteration of exact anatomical and spatial relationships due to air sacs expanding and shifting as soon as the insect is opened (particularly with the insect under water or a preservative liquid) and b) air sacs/tracheae are often situated between several muscle layers in the thorax or fat bodies and ovaries in the abdomen and it is almost impossible to dissect these out without severing much of the connecting tracheal network. Subsequently, alternative methods to demonstrate tracheal anatomy such as direct injection of various dyes into the tracheal system (Wigglesworth 1950) and corrosion casting plus scanning electron microscopy (Meyer 1989) have been attempted.

X-ray Computerised Tomography (X-ray CT) as well as X-ray micro-Computerised Tomography (X-ray microCT) are being increasingly used to study both insect colony behaviour (Greco et al. 2005; Grimaldi and Engel 2005; Greco et al.2006; Greco et al. 2008; Greco et al. 2009; Greco et al. 2011a) and also individual insect anatomy (Hörnschemeyer et al. 2002; Greco et al. 2008; Al-Harbi et al. 2008; Engel MS 2011; Greco et al. 2011b; Greco et al. 2012). The phrase 'Diagnostic Radioentomology' (DR) has been adopted to describe such studies.

Thus it was hypothesised that micro-CT would be a suitable method for visualising the insect tracheal system. The Desert Locust (*Schistocerca gregaria*) was chosen because its anatomy and that of several similar acrididae have been well documented (Vinal 1919; Snodgrass 1928 and 1935; Misra 1945, 1946, 1947).

3.1.2 Methods

3.1.2.1 The Insect

A 10 day-old male *S. gregaria* was randomly selected from a stock of caged experimental locusts that were kept at 26°C and 40% relative humidity. The 10 day-old male adult insect was euthanised by freezing at – 20°C and then micro-CT scanning approximately 2 days later.

3.1.2.2 Micro-CT scanning

The scanned insect was suspended vertically in a 30 mm acrylic tube that was mounted tightly on the micro-CT's inclination stage. This stage was used to ensure that the rotation axis was at 90 degrees to the x-ray source.

Exposure factors were: kVp = 50, µA = 198.

The data were isotropic 16 bit 2000X2000 with 1048 rows. Pixel size was 10.469 µm.

3.1.2.3 Image reconstruction and viewing

Skyscan NRecon software version 1.5.1.4 was used to reconstruct the projection data (Tarplee and Corps 2008). Having obtained the projection data in the form of an image stack of 2-D TIFF files the data was viewed as a 3-D model using disect software, DISECT Systems Ltd, www.disectsystems.com (Greco et al. 2012).

3.1.2.4 Masking and Segmenting

The TIFF image stacks were loaded into the masking and segmenting software "Tomomask" (www.tomomask.com) at full resolution. The application of the masking features within the software enabled "virtual" removal of the acrylic tube surrounding the locust scan before performing various "virtual" dissections to remove the legs and

wings. Tomomask's segmenting feature was used to segment and remove the tracheae/air sacs of the legs, wings, head, thorax and abdomen.

3.1.2.5 Production of 3-D printed models

The files were saved and converted to STL format within the Tomomask software. The STL files can be either viewed in 3-D using freely available software (e.g. Meshlab) or alternatively printed out as 3-D models at different magnifications using a 3D printer such as the Z-Corps 450.

3.1.3 Results

3.1.3.1 Imaging

Initially, the 3-D views of the insect were obscured by the acrylic tube (Fig 7a) however; masking and segmentation of the tube (Fig 7b) enabled full visualisation of the locust externally including cuticular details. High Attenuation Structures (HAS) within the muscular tissues of the head; thorax and proximal metathoracic femora and a notable absence of HAS in the abdomen were observed (Fig7c). At greater magnification (Fig 7d) details of the ramiform nature of some of the intra-thoracic HAS can be seen.

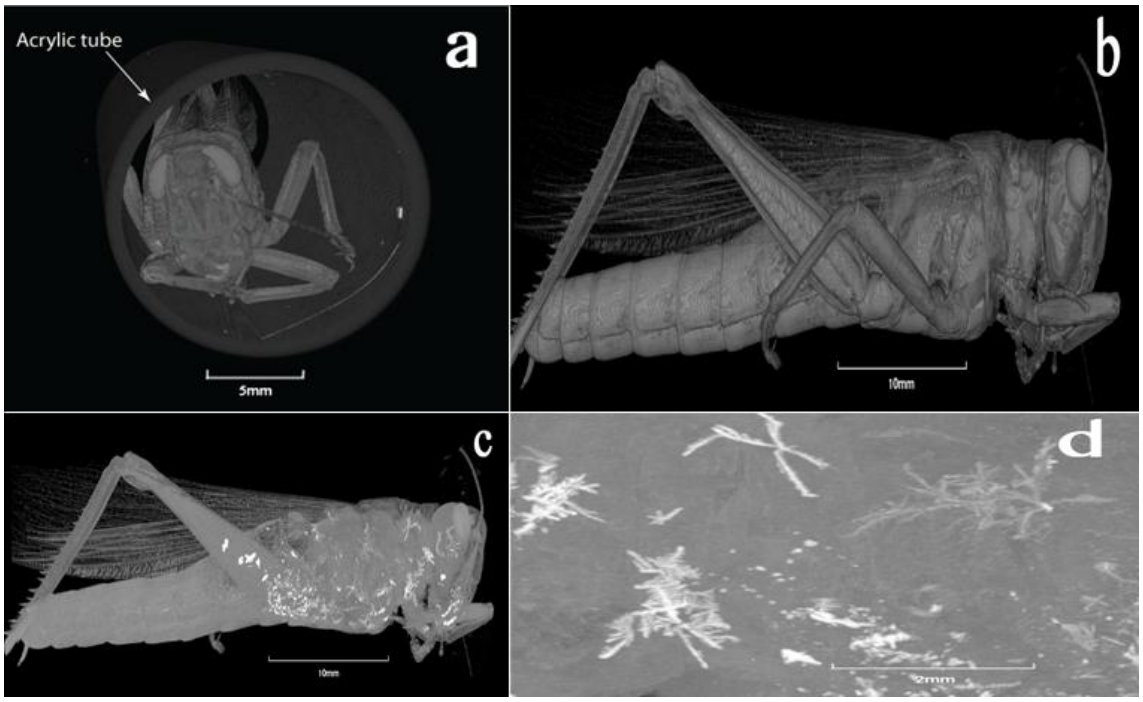

Figure 7: Four 3-D views of the desert locust *(S. gregaria*). a) obscured by the acrylic tube, b) after masking and segmenting the tube showing cuticular details, c) evidence of the High Attenuation Structures (HAS) as white ramiform structures within the muscular tissues of the head, thorax and proximal metathoracic femora but not in the abdomen and d)greater magnification of the HAS to show detail of the ramiform patterns.

High, medium and low attenuation structures varying from very dense structures (grey scale between 36,230 and 36,230) such as the Zinc-containing mandibles (Hillerton 1982, Al-Harbi et al. 2008) to very low density air filled structures (grey scale between 0 and 4,000) such as air sacs and larger tracheae were observed (Fig 8a). The grey scale values for soft tissue structures such as muscle and the brain ranged (from 30,279 to 35,300) and were visualised as various shades of grey. Figure 8b shows a) the tergo-ventral muscles b) dorsal longitudinal muscles c) air sacs and d) tracheae clearly in a 3-D transverse section through the prothorax at the level of the first thoracic spiracle (larger arrow). The hollow 'pegs' (smaller arrows) arising from the pleural surface of the prothorax which keep the pronotum clear of the spiracular orifice were also clearly seen. Figure 8c demonstrates the software's ability to produce oblique, 3-D cut away virtual 'dissections' at an infinite number of different angles (Greco et al. 2005). This enabled a longitudinal oblique view with removal the legs to demonstrate the orifices of the first and second thoracic and first abdominal spiracles. Figure 8d accurately demonstrates the cryptic tympanum, which is difficult to visualise without physical dissection, including the tympanic membrane, camera tympanum and thoracic air sacs positioned between them.

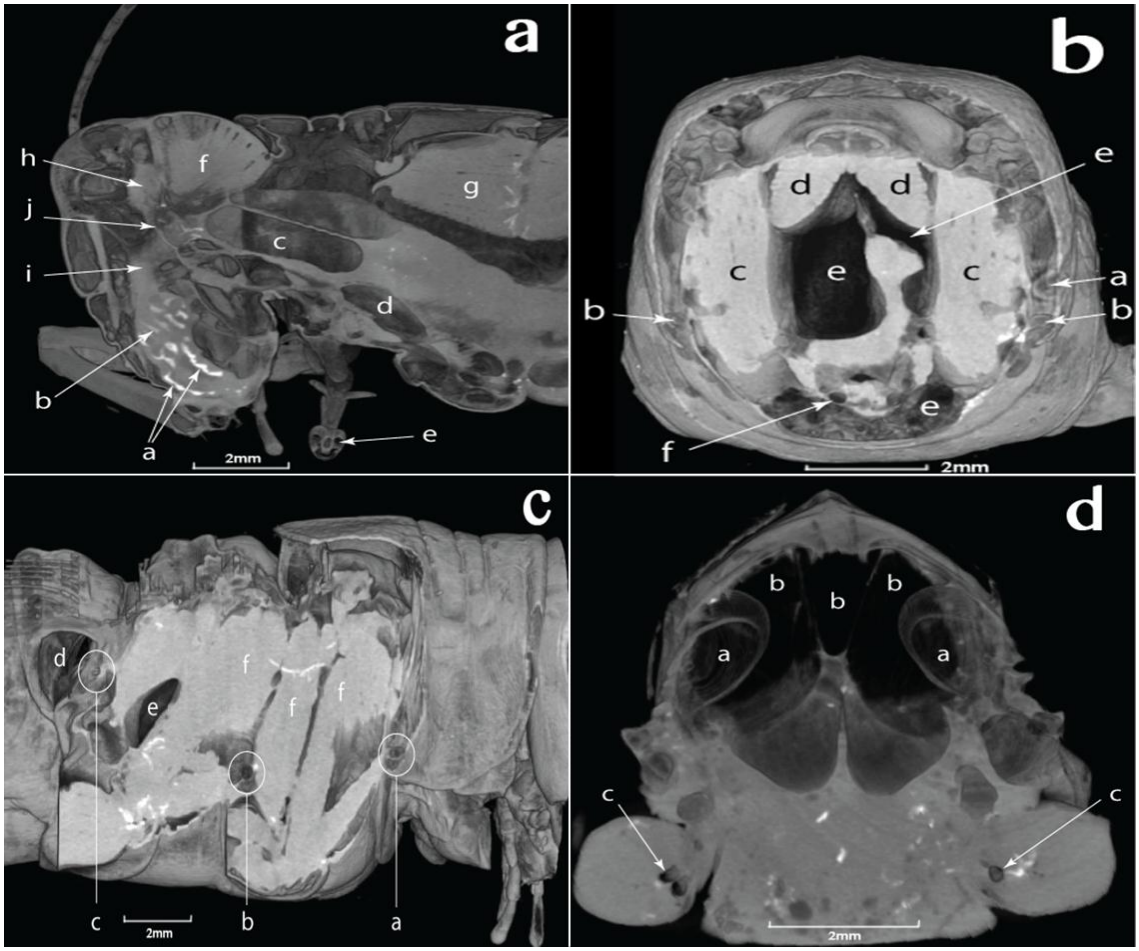

Figure 8: Four 3-D views of the head and thorax. a) Sagittal view of the mandibular incisors (a), mandibular molars (b) , air in the oesophagus (c), air sacs (d), tracheae (e), mandibular adductor muscles (f), prothoracic dorsal longitudinal muscles (g), brain (h), pharynx (i) the circumoesophageal commissures (j). b) transverse view through the prothorax at the level of the first thoracic spiracle showing the hollow 'pegs' (a) arising from the pleural surface of the prothorax (b), tergo-ventral muscles (c), dorsal longitudinal muscles (d), air sacs (e) and tracheae (f). c) Oblique longitudinal view with legs and wings segmented showing the orifices of the first & second thoracic and first abdominal spiracles respectively (a)-(c), camera tympanum(d), thoracic air sacs (e) tergo-ventral muscles and interposed air sacs with one of the HAS traversing them(f). d) transverse view at the level of the first abdominal section showing fine detail of the camera tympanum (a) abdominal air sacs between the tympana (b) and tracheae in the proximal metathoracic femora (c).

Figure 9 shows a 3-D view of the locust's head and thorax. a) have been virtually dissected transversely at the level of the cervix, b) virtually dissected horizontally at the level of the posterior cibarium/anterior oesophagus and c) virtually dissected transversely at the mid thoracic level. The tracheae and air sacs are masked in yellow and the fat bodies in dark grey. The ring of perivisceral trachea surrounding the gut are particularly well shown as are those in the proximal metathoracic legs.

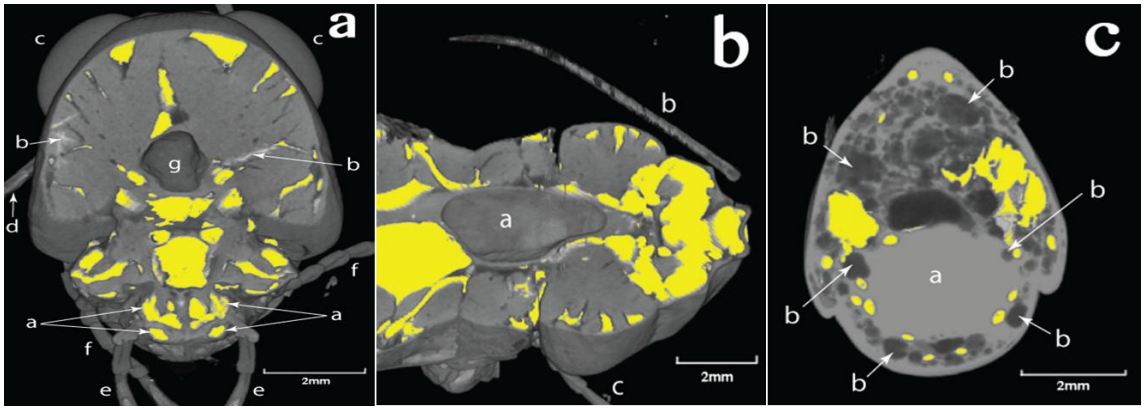

Figure 9: Three views of the head and thorax. a) 3-D transverse view of small air sacs within the labium (a), the HAS (b), compound eyes (c), left antenna (d) labial palps (e) maxillary palps (f) and air in the gut (g) are clearly visualised. b) 3-D horizontal view of head, cervix and anterior prothorax showing air in the crop (a) left antenna (b) and right maxillary palp (c). The tracheae and air sacs (in yellow) were also well visualised. c) 2-D transverse view through the abdomen. c) a 2-D transverse section through the abdomen showing the tracheal system (yellow) with the visceral tracheal plexus surrounding the gut (a) and the fat bodies (b) dispersed throughout the abdomen.

The entire 3-D segmented tracheal system was demonstrated including some of the HAS (Fig 10a) and an enlarged 3-D view of the thoracic section to show finer detail of tracheoles (Fig 10b).

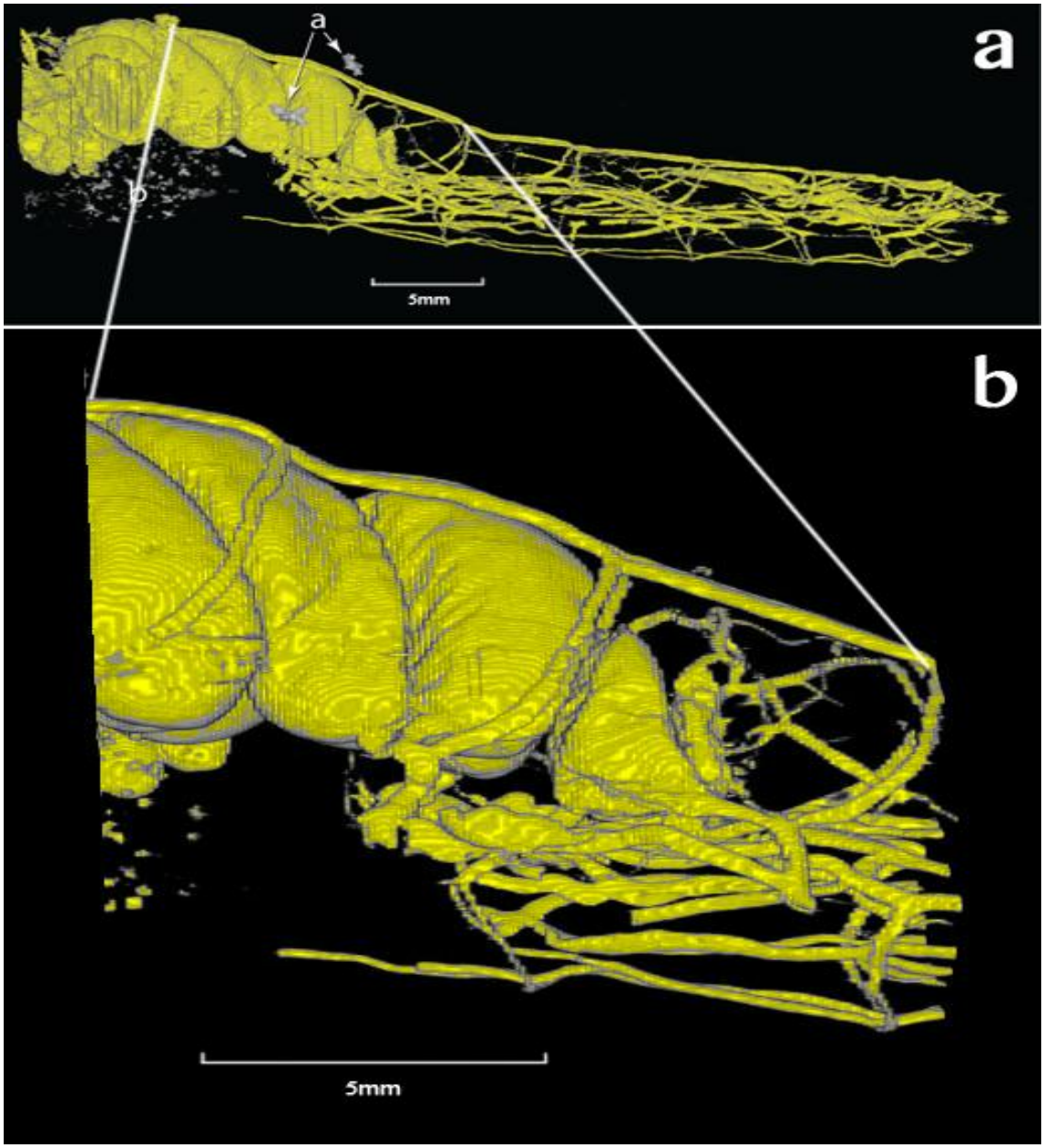

Figure 10: Two 3-D views of the segmented tracheal system. a) a 3-D view of the segmented thoracic and abdominal tracheae with the HAS in the proximal metathoracic femora (a) and meta and mesothoracic muscles (b). b) an enlarged 3-D section of the distal thoracic and proximal abdominal tracheal system to show fine structural details.

Details of legs, HAS and tracheae including the left prothoracic leg tracheal system and prothoracic HAS (Fig 11a), the mesothoracic HAS and tracheal system of the

corresponding right leg (Fig 11b) and the metathoracic HAS and the tibial spur tracheae of the left metathoracic leg (Fig 11c) were shown.

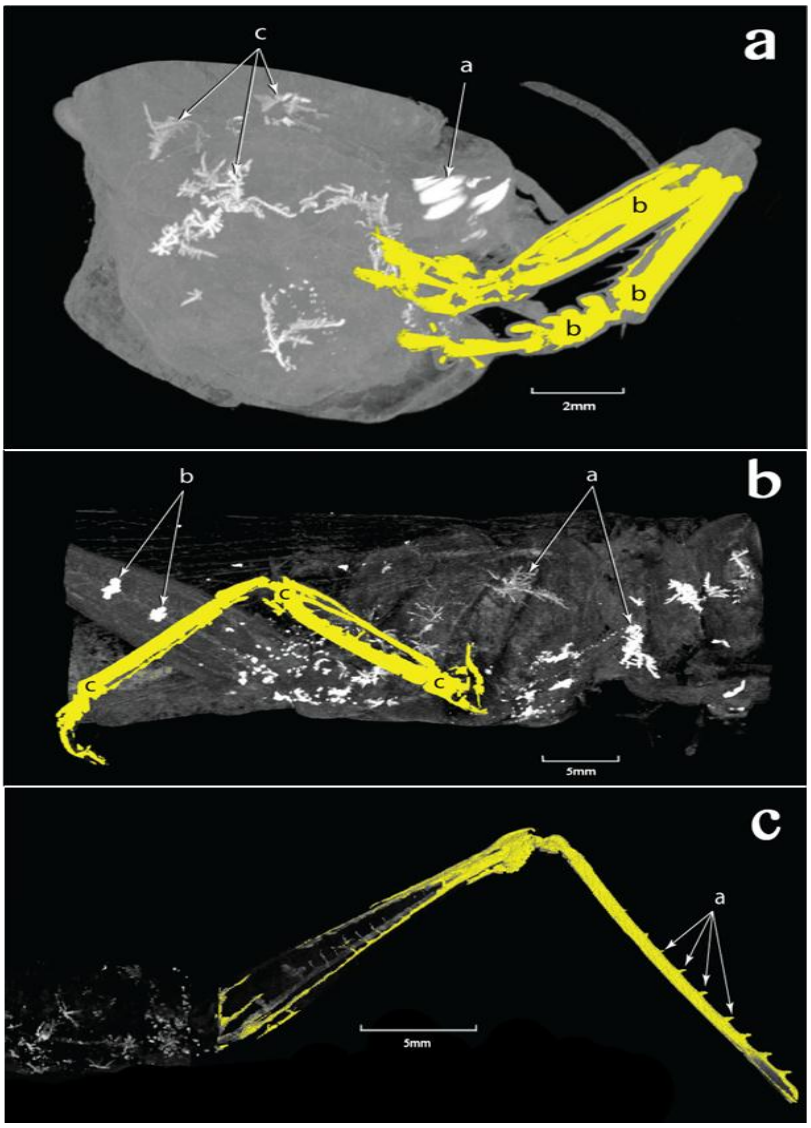

Figure 11: Three MIP volume rendered images of the thorax including details of legs, HAS and tracheae. a) the mandibular teeth (a), the left prothoracic leg tracheal system (b) and prothoracic HAS (c). b) the mesothoracic HAS (a), the metathoracic leg HAS (b) and tracheal system of the corresponding right leg (c). c) the metathoracic HAS and the tibial spur tracheae of the left metathoracic leg (a).

The left forewing segmented to reveal the left tympanum (a) and 1st abdominal spiracle (Fig 12a) and for greater detail, the fine tracheae in the hind wing was masked in yellow (Fig 12b). The estimated combined Tracheal volume of the legs, two wings, head, thorax and abdomen was 253 µL.

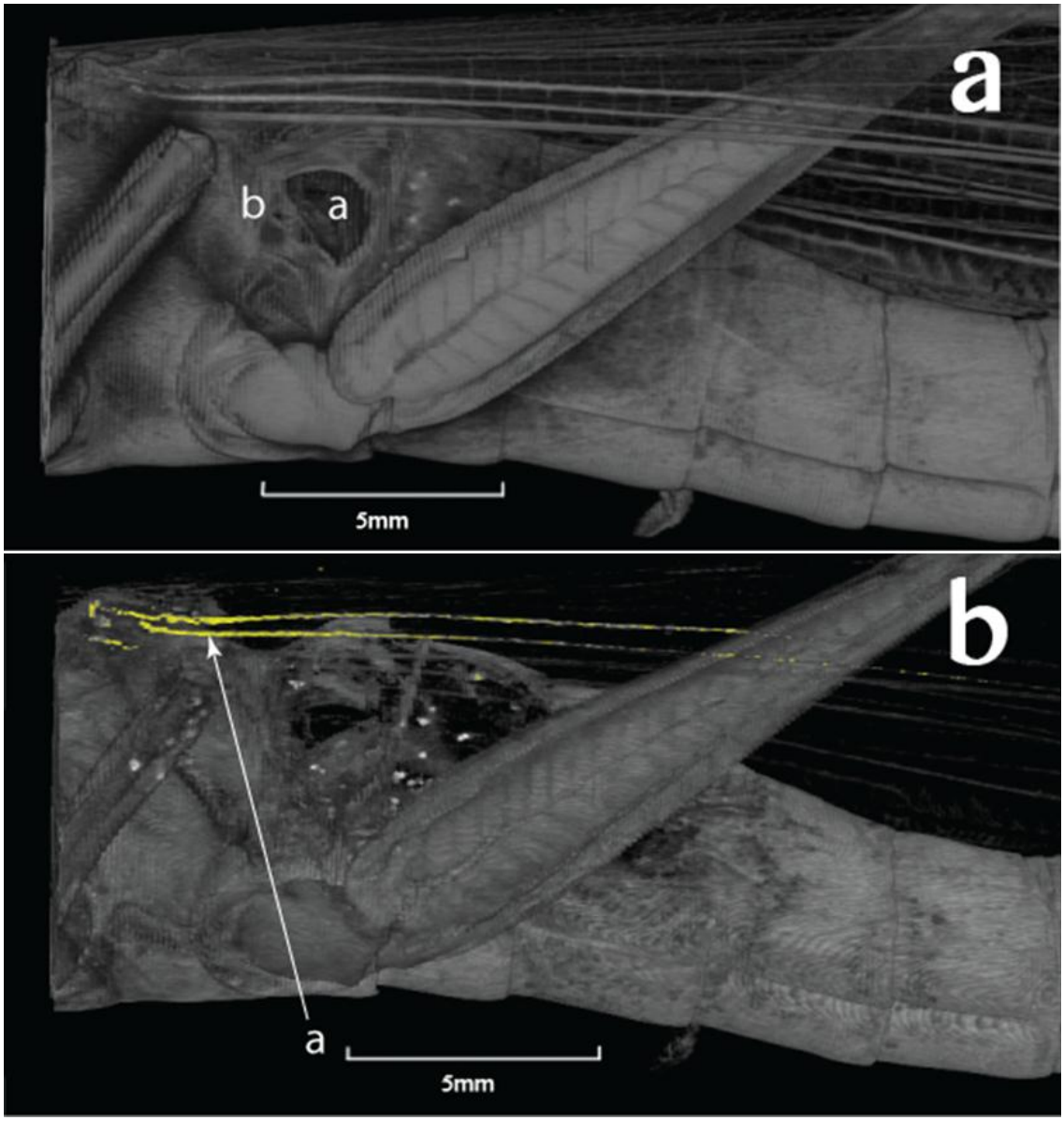

Figure 12: Two 3-D views of the metathorax and anterior abdomen. a) the left forewing segmented to reveal the left tympanum (a) and 1st abdominal spiracle (b). b) for greater detail, the fine tracheae in the hind wing has been masked in yellow (a).

3.1.3.2 The 3-D printed model

Examples of the interactive STL files that were reconstructed (Fig 13) can be downloaded at

www.fishersideas.co.uk/Papers/LocustTrachea/LocustTrachea.html.

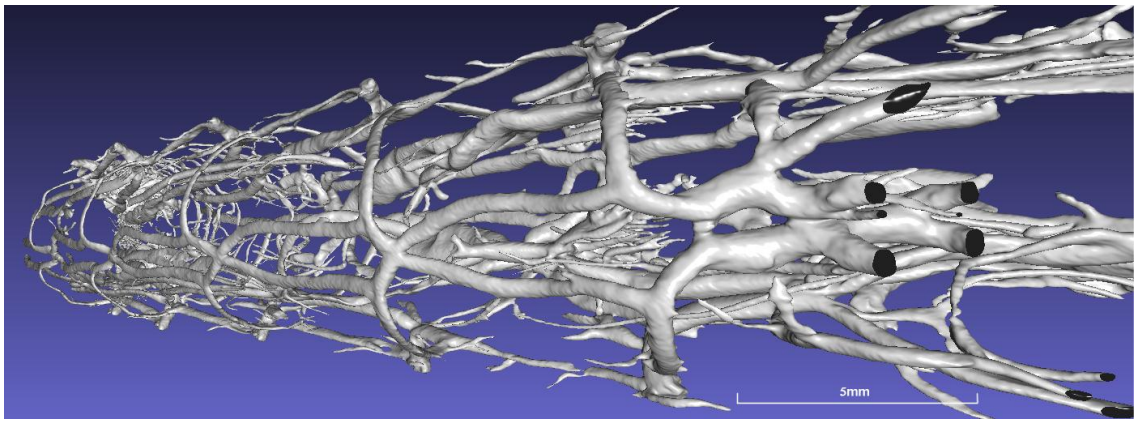

Figure 13: STL file of the segmented tracheal system of the locust's abdominal tracheal system.

An STL file of one and a half abdominal segments of the locust with suitable structural support added prior to printing was reconstructed (Fig 14a) and a physical powder 3-D model produced using Zp150 powder (Fig 14b).

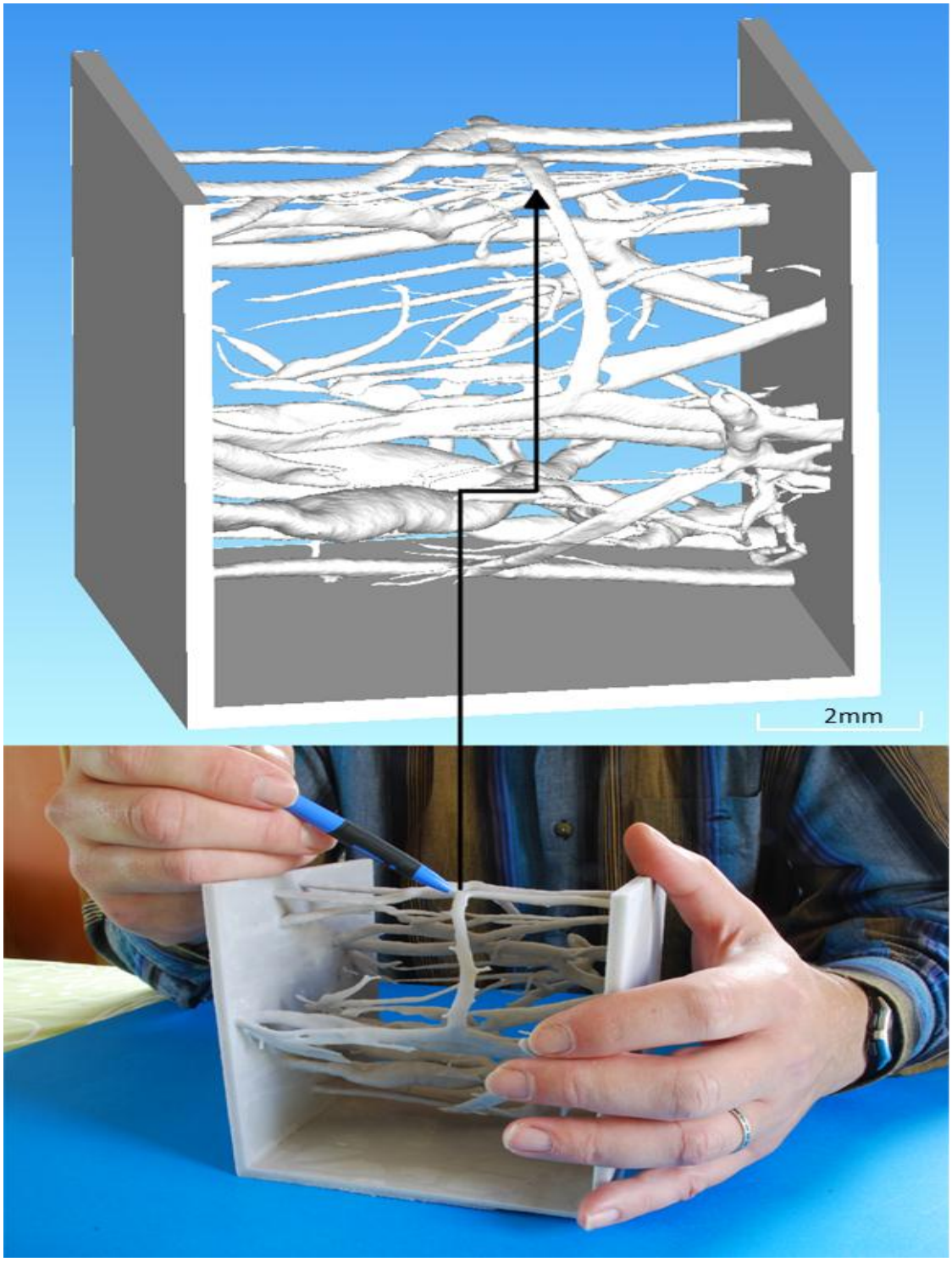

Figure 14: The STL image of a section of the segmented tracheal system of the locust's abdominal tracheae (a) and a photograph of the physical 3-D model which can be used as a teaching aid (b).

3.2 CT of the Ladybird

3.2.1 Introduction

Wigglesworth (1950) summarised in his excellent monograph of insect physiology that the malpighian tubules were the chief excretory organs in insects. The malpighian tubules are relatively simple tubular glands which open at the junction of the mid-gut and the hind-gut. They are exceedingly variable in form: sometimes being numerous (e.g. 100) and short, sometimes few in number (e.g. 2) and long; sometimes simple and sometimes branched; occasionally anastamosing to form closed loops; while sometimes more than one type may be present. Their histological structure is no less variable.

For this research, ten over wintering *C. septempunctata* were scanned using MicroCT with particular focus on their malpighian tubules and it includes a dissecting light microscopy examination of a further 5five *C. Septempunctata* to confirm that the structures highlighted by microCT were indeed the insects' malpighian tubules. Also, the possible nature of the dense, radio-opaque material found in some of the ladybirds' malpighian tubules is discussed.

3.2.2 Methods

Ten specimens of overwintering *C. septempunctata* were euthanised on the 23rd of December 2009 by freezing at -20^{0}C for 12 hours and then stored in 70% ethanol until scanned using the SkyScan 1174 X-ray microCT. The overwintering *C. septempunctata* were collected from a wooden window frame of a house set in a rural village in Suffolk, East Anglia, UK surrounded by agricultural land (52^{o}N:1^{o}35'E).

An additional five non-overwintering *C. septempunctata* were collected in September 2011 in a garden near Bury St Edmunds in Suffolk (52^{o}15'N:00^{o}43'E) and were subjected to dissecting light microscopy examination after euthanising using Ethyl Acetate.

A SkyScan 1174 bench-top X-ray microCT scanner was used for the scans (Tarplee and Corp 2008).

The ladybird samples were contained in plastic tubes and scanned at several different energy levels varying from 30-50 kVp with and without the addition of a topically applied iodinated radiographic contrast agent.

The Malpighian tubules were masked (Bell et al. 2012), segmented and cropped using TomoMask software, (www.tomomask.com).

3.2.3 Results

The first two dissections were female *C. septempunctata* with their abdomens containing eggs. In each case, removal of the abdominal section of the alimentary tract revealed the presence of what appeared to be two sets of malpighian tubules with the proximal ends of each set attached to the gut. Neither of these two sets of tubules had the form of gastric caecae found in some insects (which tend to originate near the distal portion of the crop, are relatively short, are of greater diameter than a malpighian tubule and essentially resemble a fold in the gut wall (Gullen and Cranston 2000).

The next dissection was a male specimen. Removal of the elytra, posterior wings and abdominal tergites revealed well-developed fat bodies (Fig 15).

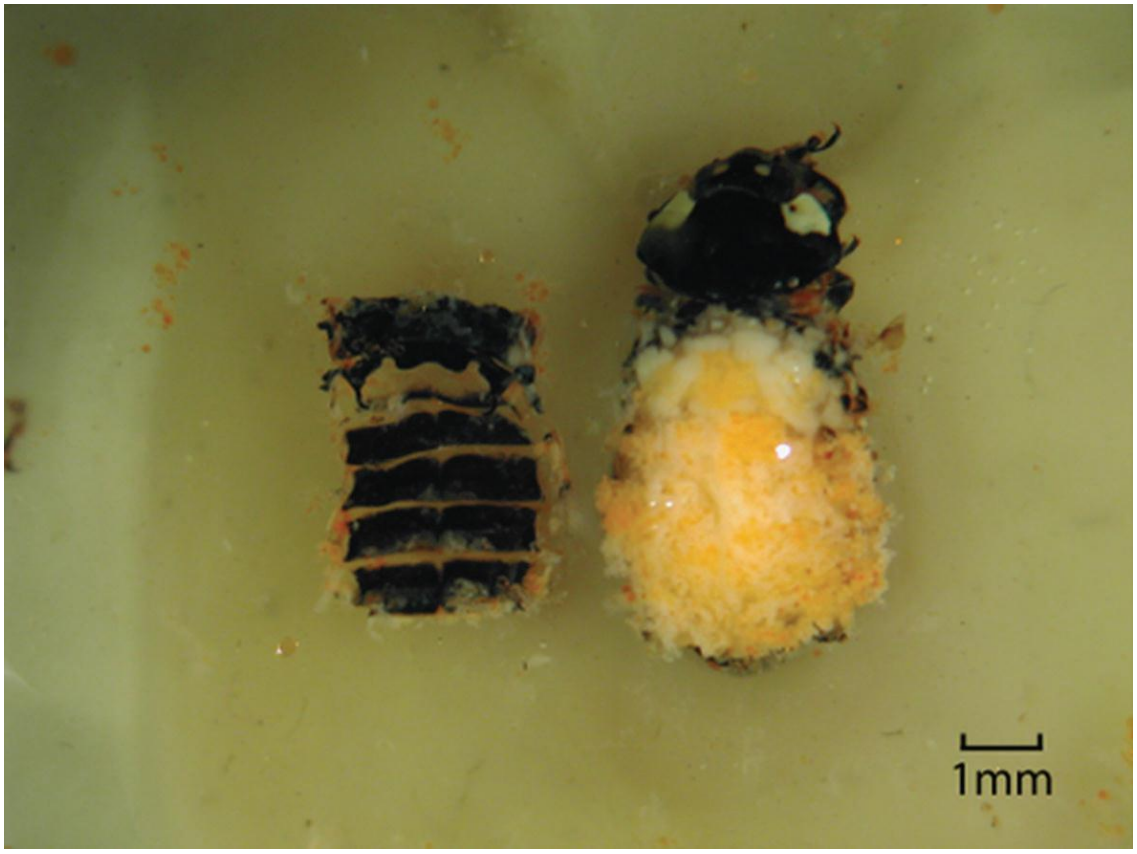

Figure 15: Photomicrograph of "stage 1" dissection of *C. septempunctata* with elytra and tergites removed which enabled in situ visualization of the dorsal aspect of gross internal anatomy.

The intricate separation of the surrounding soft tissue revealed the entire length of two of the malpighian tubules (Fig 16).

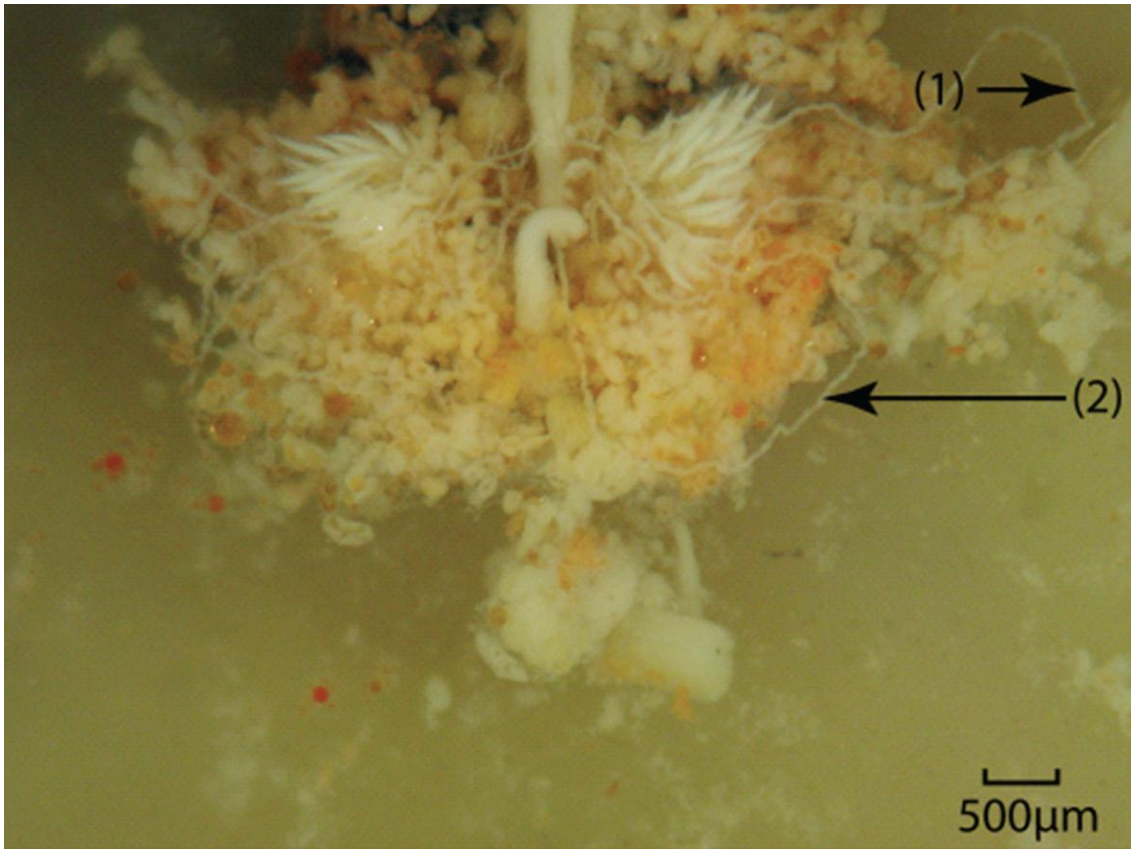

Figure 16: Photomicrograph of "stage 2" dissection of *C. septempunctata* detailing the abdominal portion of the alimentary tract. Two complete malpighian tubules (1) and (2) were physically unfolded for improved examination.

It is clear from the two photomicrographs shown in Figures 15 and 16 that each malpighian tubule forms a complete loop; attachment at the anterior end is around the junction of the mid gut and ileum (i.e. hind gut) whilst the posterior end appears closely attached to the lower alimentary tract

Figures 17 and 18 show a further photomicrograph and diagram of specimen 4 in which the thoracic and abdominal section of the alimentary tract have been removed. In total, there appear to be six individual malpighian tubules in *C. septempunctata*.

Figure 17: Photomicrograph of the resected thoracic and abdominal sections of the alimentary tract of C. septempunctata, with proximal and distal ends of the malpighian tubules attached.

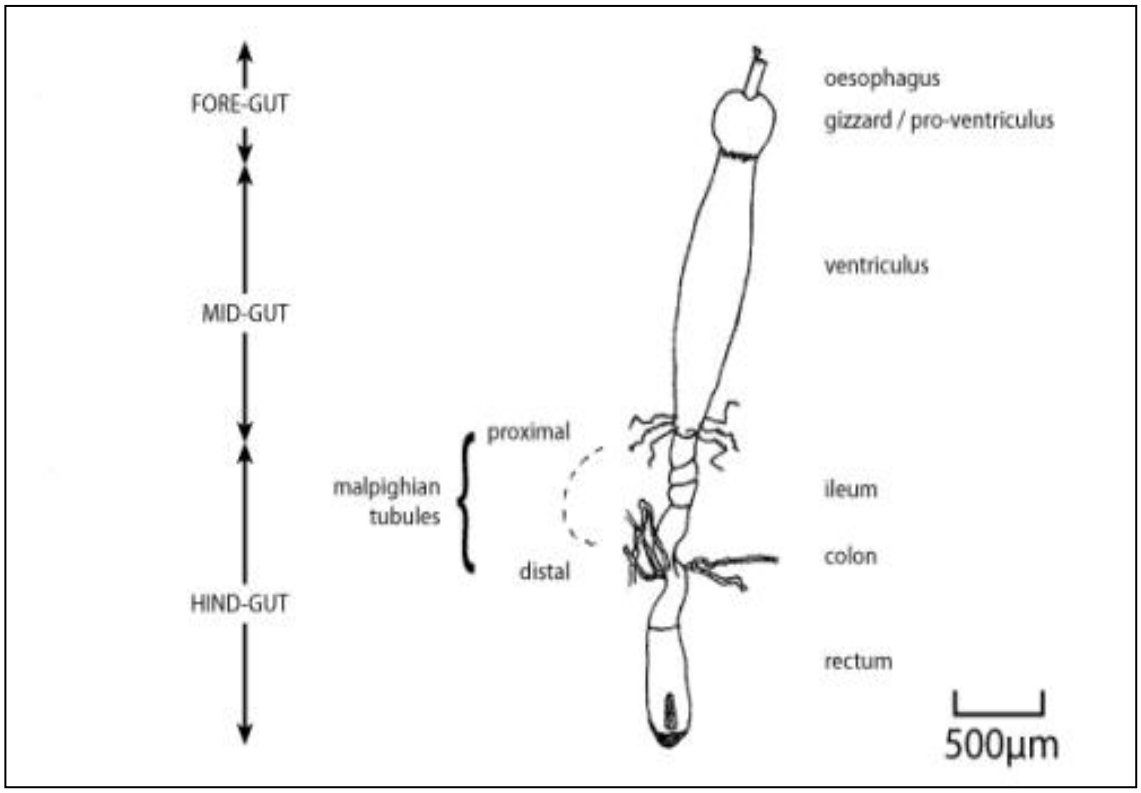

Figure 18: Schematic diagram of thoracic and abdominal sections of the alimentary tract of *C. septempunctata*.

Figures 19-21 show various views of some of the male and female overwintering *C. septempunctata* specimens scanned. While Figure 22 shows just the malpighian tubules after the use of Tomomask to segment out the radio-opaque malpighian tubules.

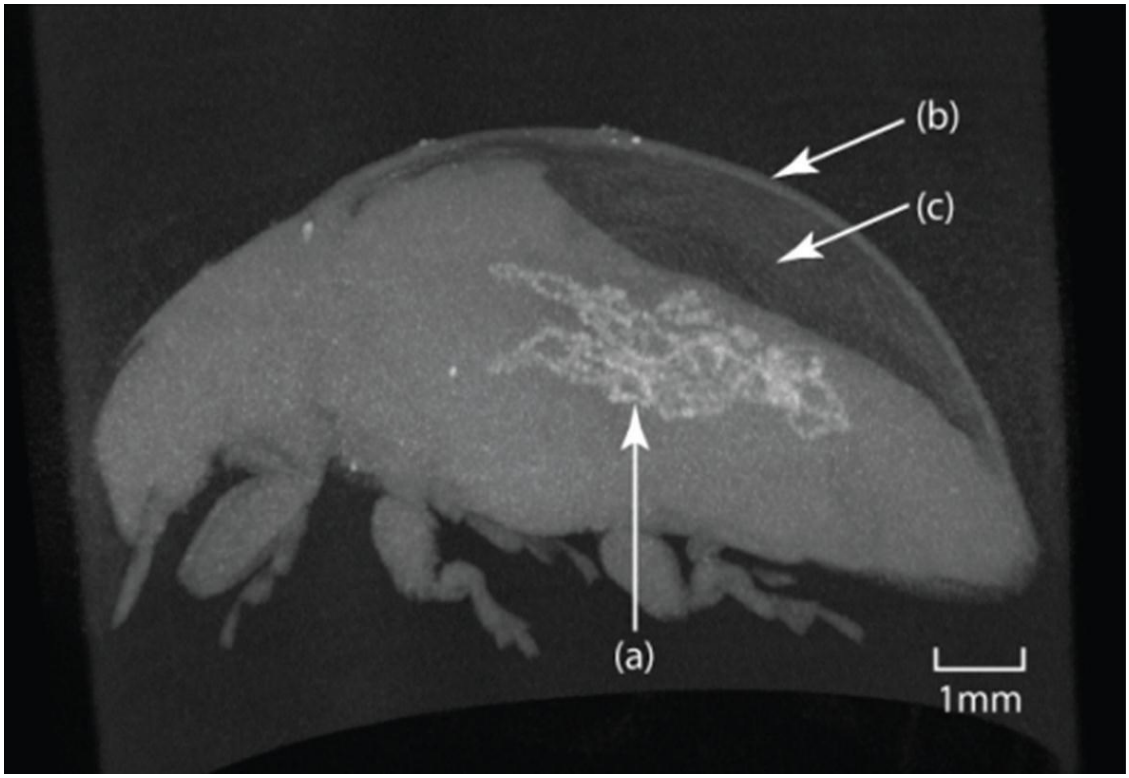

Figure 19: A 3D, volume rendered, micro-CT image of a male *C. septempunctata* using Maximum Intensity Projection (MIP) showing (a) radio opaque malpighian tubules, (b) elytra, and (c) folded wings in the air space between elytra and tergites.

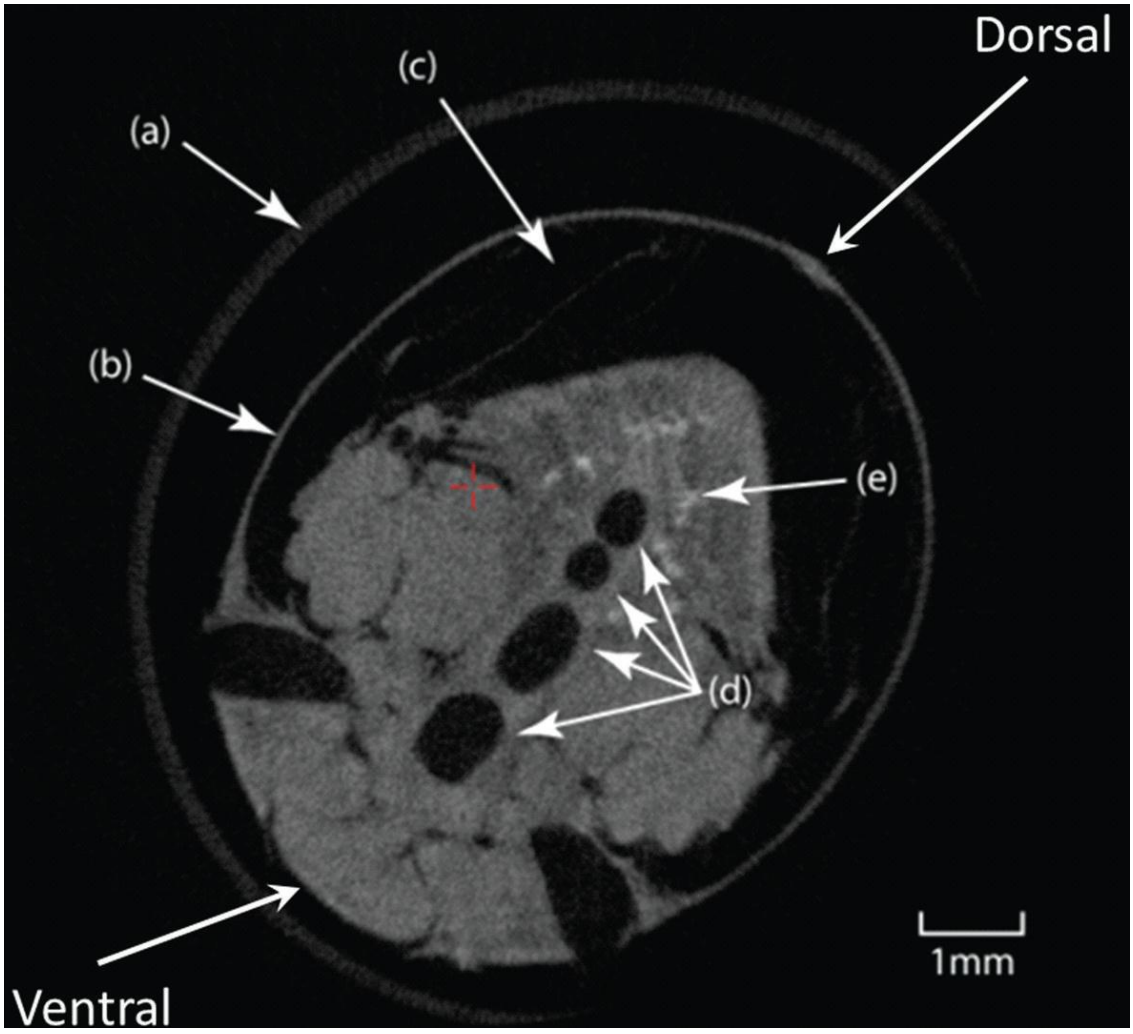

Figure 20: A 2D micro-CT image showing a transverse section through a *C. septempunctata* abdomen with details of (a) wall of plastic tube-mount, (b) elytra, (c) air space containing folded wings between elytra and dorsal tergites, (d) air sacs, and (e) malpighian tubules.

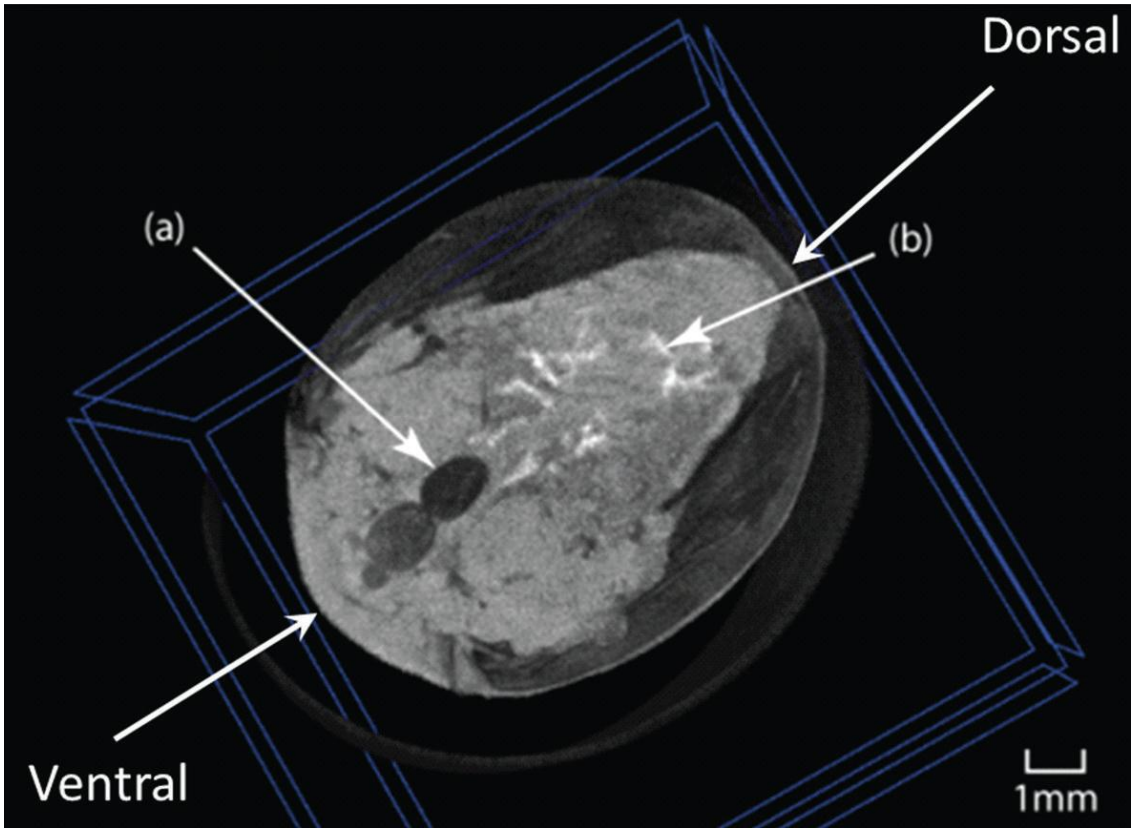

Figure 21: A 2D micro-CT image showing a transverse section through a *C. septempunctata* abdomen showing (a) non-dense "black" radio-lucent air-sacs and (b) dense "white" radio-opaque malpighian tubules. Blue lines indicate the selectable cutting planes.

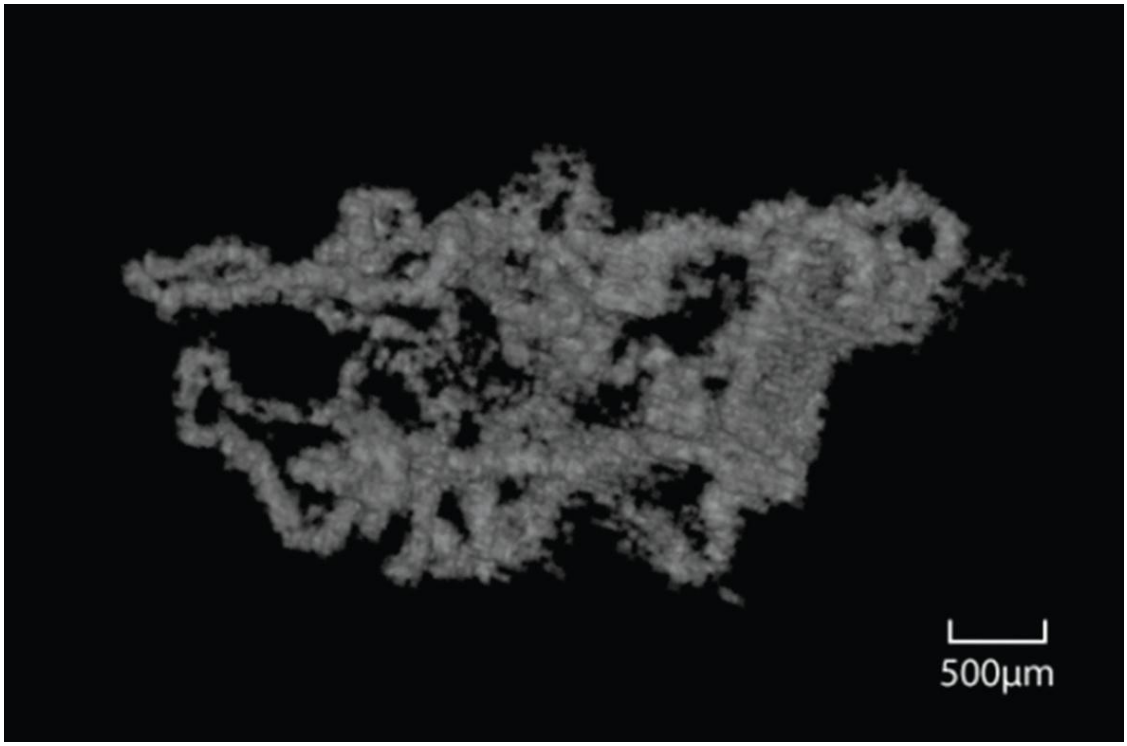

Figure 22: A 3D, volume-rendered and segmented image of the radio-opaque malpighian tubules in *C. septempunctata*.

An estimation of the relative density of the material in the malpighian tubules when compared with the ladybird's exoskeleton or internal organs can be illustrated by the 'Advance' feature of the 'window and levelling tool of 'Disect'. When using the 16 bit TIFF data loaded into 'Disect', the degree of radio-opacity can be viewed on a histogram on a scale of 0-65,536. By making the 'window size' just 1 unit wide and 'levelling up and down (i.e. effectively binarising the data) one can see when a particular structure either first begins to appear or conversely when it starts to disappear as one levels up from 0 upwards: thereby obtaining a range estimate. Using the data illustrated in Figure 19 the range of values were 6,930-14,000 for the plastic tube, 12,770-21,760 for the elytra, 13,860-30,400 for the internal organs and from 34,000 to 44,870 for the radio-opaque material in the malpighian tubules. These values demonstrate that microCT gray scale (density) data can be useful in diagnosing, segmenting and studying insect malpighian tubules.

In agreement with the dissection and photomicrograph results, the microCT data suggest that there are 6 malpighian tubules and that they are of the cryptonephridial in type.

3.3 CT of the Butterfly

3.3.1 Introduction

All insects in the *Pterygota* undergo a marked change in form from immature to adult. This process is termed metamorphosis. These insects display two types of metamorphosis. One group displays hemimetabolous (partial) development, and they undergo an incomplete metamorphosis. Development in this group proceeds in repeated stages of growth and ecdysis (moulting); these stages are called instars. The different immature instar stages resemble small versions of the adult form (nymphs) but without fully formed wings or genitalia. The differences between nymphs in different instars are small, often just differences in body proportions and the number of segments, although external wing buds will form in later instars (Gullan & Cranston 2005). The other group displays holometabolous (full) development, whereby they undergo a complete metamorphosis, including a pupal or resting stage between the larval and adult forms (Gullan & Cranston 2005). Holometabolous insects pass through a larval stage, then enter an inactive state called a pupa, or chrysalis, and finally emerge as adults. This process is called "complete" metamorphosis. It is theorised that the pupal stage is the evolutionary compaction of all the nymphal stages of their hemimetabolous ancestors, while the larval stage is an extended, mobile form of the developing embryo (Gullan & Cranston 2005).

There have been many publications on insect metamorphosis however most have addressed details of the external anatomy. For the following study, it was hypothesised that MicroCT would be useful for visualising internal metamorphic changes from larva to adult in the butterfly *Morpho menelaus* with particular focus on the tracheal system.

3.3.2 Methods

Three individuals of *M. menelaus*, a late-stage caterpillar (larva), a mid-stage chrysalis (pupa) and a late-stage chrysalis (adult) were euthanised by placing them in -20^{0}C for 2hr and then drying at 21^{0}C for 24hr prior to scanning. The late stage chrysalis was euthanised on the day that it was expected to eclose therefore; although the wings were folded, the chrysalis was essentially a fully formed adult (Fig 23).

Figure 23: A late stage *M. menelaus* caterpillar (a), a late stage *M. menelaus* chrysalis (b) and an adult *M. menelaus* butterfly (c). Adult butterfly image downloaded from:

http://www.google.co.uk/imgres?imgurl=http://www.butterflyutopia.com/BIG/137-blue_morpho_didius.jpg&imgrefurl=http://www.butterflyutopia.com/blue_morpho.html&h=329&w=404&sz=90&tbnid=C8cnfzmE8MPk_M:&tbnh=90&tbnw=111&zoom=1&usg=__j4ISo8PZ1PbqnPs37g1LlFbWPwc=&docid=sV8leBcBv-E9xM&hl=en&sa=X&ei=yZISUZTVFeXb0QX1-4DYAw&sqi=2&ved=0CEcQ9QEwBA&dur=0 on 29th January 2013.

The MicroCT scans were performed on a Skyscan 1172. The scanned insects were suspended vertically in a 20 mm polystyrene tube that was mounted tightly on the micro-CT's inclination stage. This stage was used to ensure that the rotation axis was at 90 degrees to the x-ray source.

Exposure factors for the scans were:

Caterpillar:

Source Voltage = 59kV, Source Current = 167µA, Image Pixel Size = 9.83µm;

Mid Stage Chrysalis:

Source Voltage = 59 kV, Source Current = 133 µA, Image Pixel Size = 9.83 µm;

Late Stage Chrysalis:

Source Voltage = 59 kV, Source Current = 167 µA, Image Pixel Size = 6.93 µm.

Skyscan NRecon software version 1.5.1.4 was used to reconstruct the projection data (Tarplee and Corps 2008). Having obtained the projection data in the form of an image stack of 2-D TIFF files the data were viewed as a 3-D model using disect software, DISECT Systems Ltd, www.disectsystems.com (Greco et al. 2012). The TIFF image stacks were loaded into the masking and segmenting software "Tomomask" at full resolution. The application of the masking features within the software (www.tomomask.com) enabled "virtual" filling of the tracheal system and removal of all other anatomical features.

3.3.3 Results

The scans showed marked metamorphic changes between the caterpillar and chrysalis stages however, there were only moderate changes between the mid and late stage chrysalis' (Fig. 24). The images showed ten spiracles on either lateral side of the caterpillar and only seven on either side of the chrysalis. The teeth clearly evident on the caterpillar were completely gone in the chrysalis. The extensive tracheal system in the caterpillar was replaced by a less elaborate tracheal system including large abdominal air-sacs in the mid and late stage chrysalis.

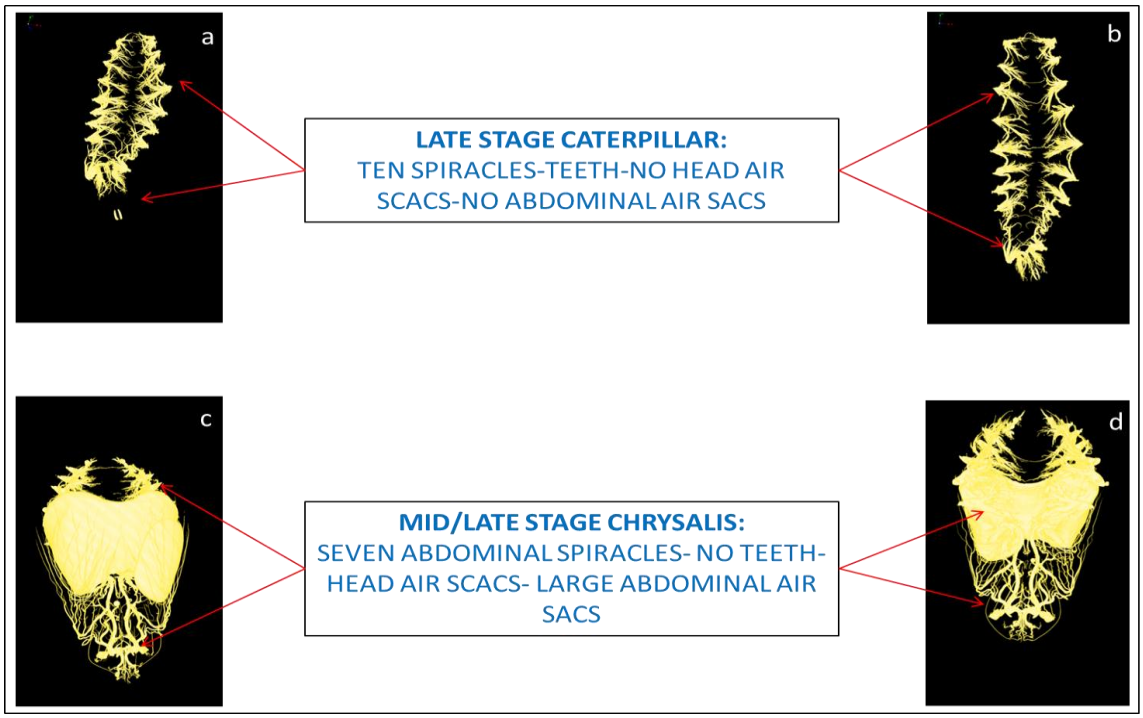

Figure 24: Four 3-D images of *M. menelaus*. The late stage caterpillar showing the absence of air-sacs and presence of teeth (a & b) and the mid and late stages of the chrysalis showing large air-sacs and absence of teeth (c & d).

3.4 Discussion

3.4.1 The locust

To my knowledge, at time of printing this thesis these methods show the first account of non-invasive measurements of insect tracheal volumes and detailed, physical 3-D models of the anatomy of an individual insect's respiratory system. All previous attempts have been produced with prior knowledge gained from physical dissections or other destructive methods. Thus by definition, those approaches are estimations and prone to large errors. The results show that using a microCT with appropriate software researchers can study tracheal anatomy in insects. Also, the conversion of the image stack data to STL format allows the complex 3-D anatomy of the respiratory system in locusts to be visualised non-invasively.

The Tracheal volume of 253µL is in accordance with published methods such as a) water displacement (Wigglesworth, 1950) b) inert gases (Bridges et al. 1980; Lease et al. 2006) c) Stereology (Schmitz and Perry 1999; Hartung et al. 2004) and d) Stereology in combination with Synchrotron X-ray imaging (Kaiser et al. 2007, Greenlee et al. 2009, Socha et al. 2010 and Kirton et al. 2012).

Also, when segmenting out the air-filled tracheal system there was no filling of other air filled spaces within the locust such as air in the crop or the extra oral space. Thus, removing the potential errors involved. However, there were some 'leaks' from inside out at a few predictable places due to the 'partial volume' effect (Tarplee and Corps 2008). These occur where the membranous non-sclerotized exoskeleton of the insect is extremely thin e.g. at the tympanum and the membranous periarticular regions of several of the smaller joints of the legs. This problem was easily solved by using the 'paint' function within Tomomask set at an attenuation of 8,000 to 'patch over' any such potential defects and thus rendering the insect 'leak-proof'.

When 3-D voxels are located between regions of different x-ray attenuation they inherently contain partial volume errors. Since the voxel size for this study was 10 µm the method described above of total respiratory system volume determination would underestimate the volume because the voxels were bigger than some of the tracheoles

and therefore would be located between different x-ray attenuation regions (e.g. air/muscle). However, using this total respiratory system volume determination method for time series studies in the same live anaesthetised insect (Al-Harbi et al. 2008) or killed groups of insects (e.g. fed versus unfed), then the theoretical underestimation of total respiratory system would be the same in all groups.

Synchrotron micro-CT (Greco et al. 2012; Kirton et al. 2012) inherently provides the highest resolution however; a limiting factor for synchrotron imaging is that there are few available for usage. In the United Kingdom there is currently only one Synchrotron scanner and so UK based research might typically have to wait several months for an opportunity to use it. The nature of the high attenuation areas (HAS) described in this experiment is at this stage unclear however it is feasible that they are: desiccated cells accumulated in sections of the tracheae; Calcium deposits/scarring after localised infections; aggregations of the locust tracheal mite e.g. *Locustacarus locustae* or *Locustacarus buchneri*); infected glandular tissue; accumulated debris from external airborne impurities. They may also be effete tracheal structures as described by Miller et al. (1960c).

3.4.2 The ladybird

The results in the over wintering seven spotted ladybird, *C. septempunctata* clearly showed that the malpighian tubules contain an unknown extremely radio-opaque material. The fact that there were six such structures with the distal ends in close contact with the rectum is in agreement a) with our findings with dissecting light microscopy and b) the literature which suggests that most polyphagic coleopterans such as ladybirds have cryptonephridial malpighian tubules (Marcus 1930; Wigglesworth 1950; Maddrell 1971; Imms 1977; Bell 1977; Bell & Anstee 1977; Gullen and Cranston 2000; Klowden 2007; Nation 2008).

More detailed studies are required to elucidate a) the nature of the radio-opaque material demonstrated in the overwintering *C. septempunctata* malpighian tubules and b) discern whether this phenomenon is confined just to this species of ladybird or whether it is a

common phenomenon in other beetle species. The material in the tubules is so radio-opaque that it must contain a significant amount of some metal compound such as Calcium, Magnesium or as in the case of the locusts' mandibles Zinc (Al-Harbi et al. 2008).

3.4.3 The butterfly

The scans showed marked metamorphic changes between the caterpillar and chrysalis stages however, there were only moderate changes between the mid and late stage chrysalis'. The images showed ten spiracles on either lateral side of the caterpillar and only seven on either side of the chrysalis. The teeth clearly evident on the caterpillar were completely gone in the chrysalis. The extensive tracheal system in the caterpillar was replaced by a less elaborate tracheal system including large abdominal air-sacs in the mid and late stage chrysalis. Future studies will include microCT scans conducted at more frequent intervals e.g. daily to better demonstrate the tracheal system changes from caterpillar to adult during metamorphosis.

3.5 Future Directions

The methods described in this chapter have provided new ways for observing internal morphology of insects non-invasively. The tracheal system was explored in the locust and butterfly with both volume estimations and metamorphic changes described and the malpighian tubes in the ladybird were segmented and imaged in 3-D without physical dissection. These techniques have opened up new areas of research such as live scanning of "internal" metamorphic changes and organ characterisation in live insects. It is envisaged that these methods will be used in developmental experiments where individual insects can be scanned daily over several weeks to observe metamorphic changes. Other experiments will involve treating individuals with pathogens or nutritional variations in diets to observe insect development. In particular, the malpighian tubules of ladybird beetles can now be examined in live insects to describe

their physiological function over time while being exposed to different diet regimes. Their HU can now be determined to estimate the types of solid materials that accumulate in them. The non-invasive aspects of the new methods will now enable these experiments to be conducted on the same individuals over time thus reducing bias errors that occur when observing different individuals.

CHAPTER 4

A specific case for CT "Plasticity in the live honeybee brain"

4.1 Introduction

The European honey bee *A. mellifera*, worker brain weighs approximately 0.001 g, has a volume of approximately 1 mm^3, and has approximately one million neurons (Ribi et al. 2008). The main parts of the brain are the optic lobes, the antennal lobes, the mushroom bodies, and the central complex. The optic and antennal lobes are responsible for processing vision and olfaction, respectively. The mushroom bodies and the central complex constitute the most important centres for behaviour, instinct, and memory (Hourcade et al. 2010). Other known parts of the brain include the sub-oesophageal ganglion, tritocerebrum, and ventral cord and it is thought that complex behaviour is based on overarching brain networks superimposed on smaller local networks controlling individual responses. Since simple environmental manipulations can both accelerate and delay brain growth in young bees, and since brain volume is sensitive to behaviour throughout life, the honey bee has great potential as a model for exploring the interactions between environment, behaviour, and brain structure. Experience related changes in brain structure are believed to be an important part of the memory engram (Kolb and Whishaw 1998; Kim and Diamond 2002; Mohammed et al. 2002; Gerber et al. 2004; Kim et al. 2006; Liston et al. 2006), and understanding the relationships between experience and brain structure is key to understanding the relationships between brain and behaviour (Kolb and Whishaw 1998). A worker honey bee's natural behavioural change is associated with conspicuous growth of the mushroom bodies in the brain (Withers et al. 1993; Farris et al. 2001; Ismail et al. 2006). The mushroom body calyx is larger in forager bees than same-aged nurse bees that have not left the hive (Withers et al. 1993; Farris et al. 2001). This structural change may be part of the memory engram for the many foraging-related and navigational tasks learned by a forager bee (Farris et al. 2001; Fahrbach et al. 2003).

Phenotypic plasticity in the adult bee brain has been demonstrated in previous experiments using various techniques, such as the Cavalieri or computer volume segmentation methods (Gunderssen & Jenson 1987; Michel & Cruz-Orive 1988; Withers et al. 1993; Brown et al. 2000; Ribi et al. 2008; Maleszka et al. 2009). In all cases, dead bees were used to collect data, which invariably led to inherent differences among individuals.

This research was conducted to identify limitations and potentials for MicroCT scanning of live bees to be used as a comprehensive, non-invasive method for studying brain plasticity.

4.2 Methods

The SYRMEP beamline facilities at the ELETTRA synchrotron in Trieste, and a SCANCO μCT40 bench-top scanner at the University of Bern, were used to scan the bees. At the beamline, newly emerged, adult bees were scanned once daily over five days to observe differential brain plasticity produced by asymmetric environmental stimuli. Scans on live bees at the beamline facility were performed using phase contrast with the following parameters: 15keV X-ray energy, 20 cm sample to detector distance, a number of projections (over 180°) of 1800, 9 μm isotropic voxel size, 0.9 seconds exposure time, 1 hour 48 minutes measurement time.

To enhance tissue differentiation, bolus injections of radiographic contrast medium were delivered directly into the haemolymph, between the dorsal abdominal terga, via a 30G needle (Fig. 25).

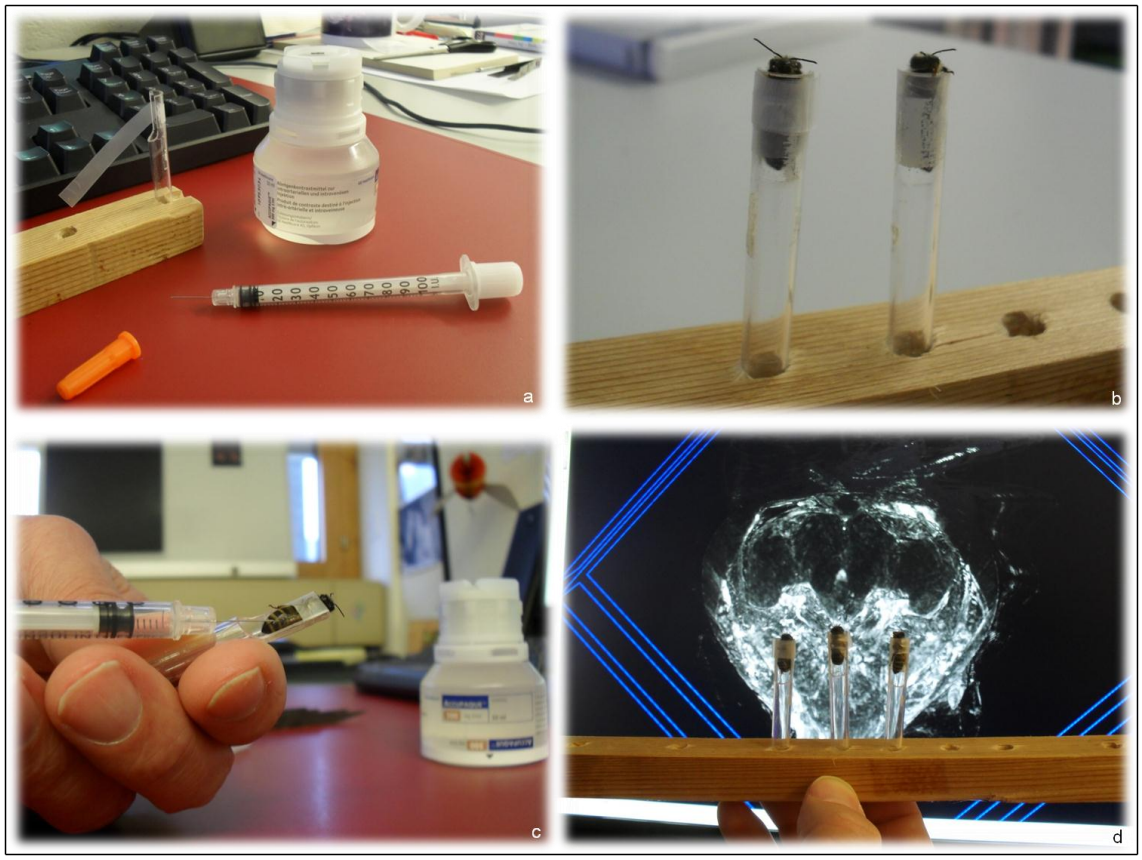

Figure 25: To enhance brain tissue differentiation, bolus injections of radiographic contrast media were delivered via a 30G needle (a) directly into the haemolymph, between the dorsal abdominal terga, of live bees that were previously secured for scanning (b and c). The 3D rendered brain (d) showed that contrast had perfused into tissue to enable improved structural differentiation.

For visual comparisons of gross anatomical features of the brain, MicroCT scans of an ancient bee trapped in amber were also performed on the bench-top scanner, using absorption techniques. The tube operating conditions were set at 45kV, and 177μA. The other parameters were: high resolution mode (1000 Projections/180°), 2048 × 2048 pixels image matrix, 10μm size isotropic voxel, 3 seconds integration time, 610 total slices, 2 hours and 30 minutes measurement time.

Images and brain volume data (Fig. 26) were measured using BeeView volume rendering software (DISECT Systems Ltd).

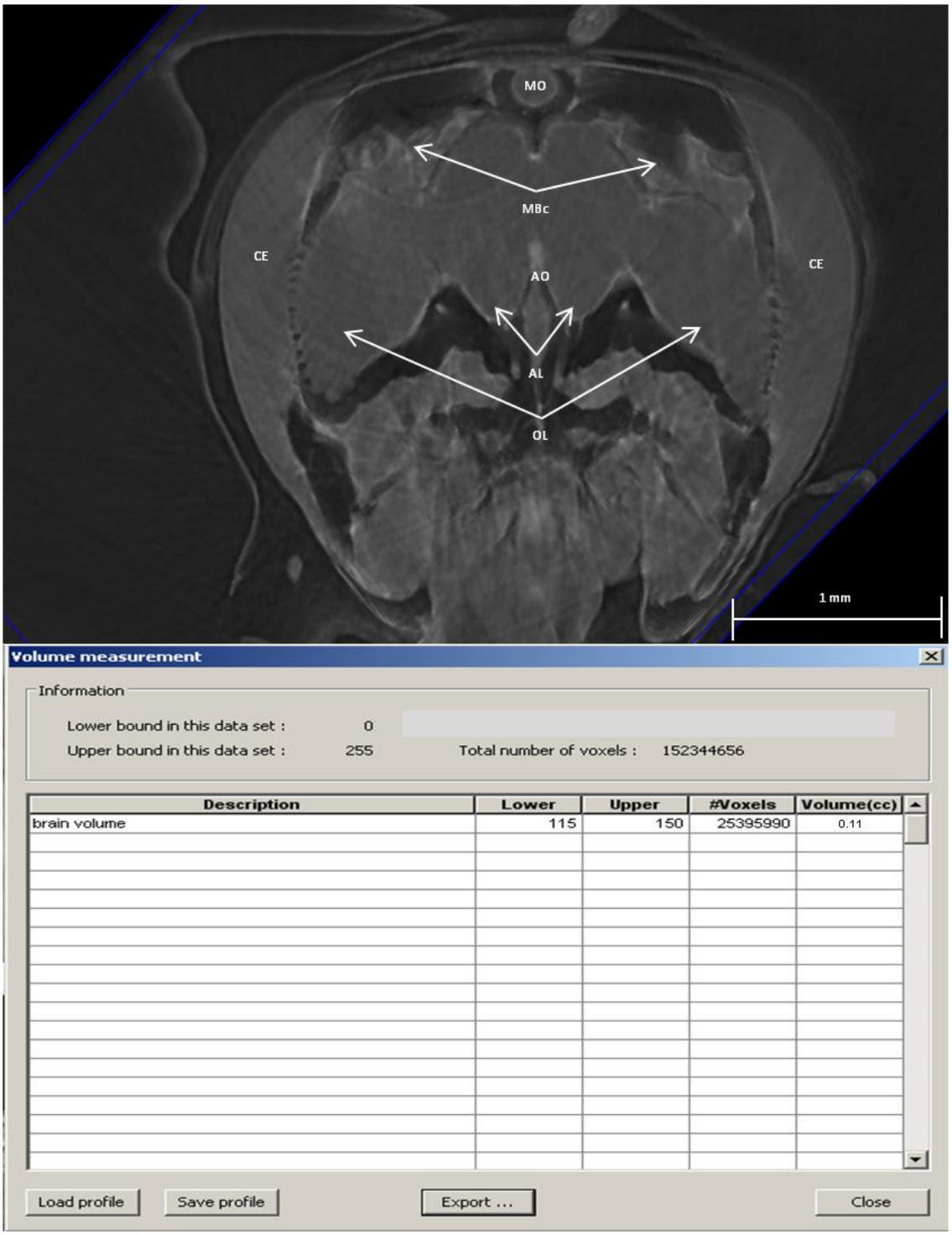

Figure 26: A 3D volume rendered image of a live honey bee's head capsule showing gross morphological structures such as the optic lobes (OL), antennal lobes (AL), aorta (AO), mushroom body calyces (MBc), and median ocellus (MO). The compound eyes (CE) are visualised immediately adjacent and lateral to the optic lobes.

4.3 Results

Gross brain morphology, such as the optic lobes, antennal lobes, aorta, mushroom body calyces, and median ocellus, were visualised in 2D and 3D projections. Brain volume measurements (Fig. 26) enabled estimates of plasticity. Scanning of live bees enabled minimally-invasive imaging of physiological processes (for the first time), such as passage of contrast from gut to haemolymph (Fig. 27), as well as preliminary brain perfusion and plasticity studies (Fig 27a).

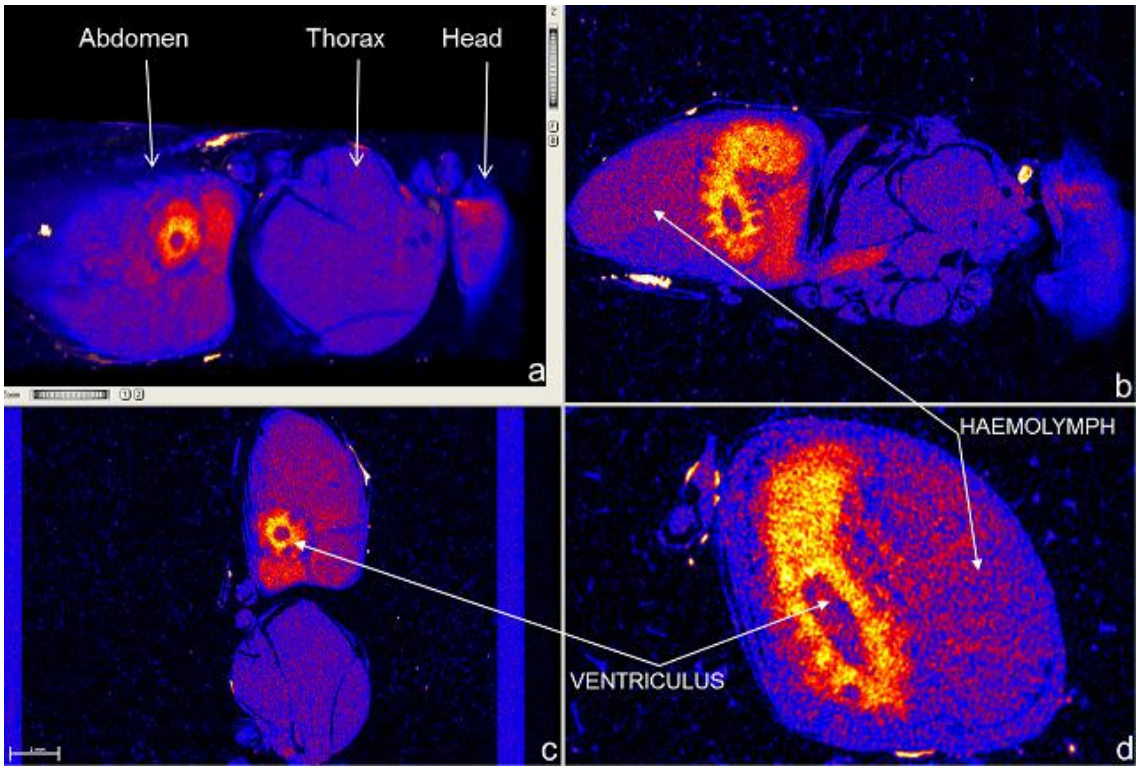

Figure 27: A 3D volume rendered image with BeeView software of a live honey bee showing the three body segments (a) and orthogonal, 2D images (b, c, and d) showing the passage of radiographic contrast from the ventriculus (true stomach) to the haemolymph in the coelom. Images were rendered 1.5 hours after ingestion of contrast.

The image in Figure 28a shows comparisons of brain images from live extant bees and the 20 million year old bee *Proplebeia abdita* showed little variation in gross morphological features (Fig. 28b).

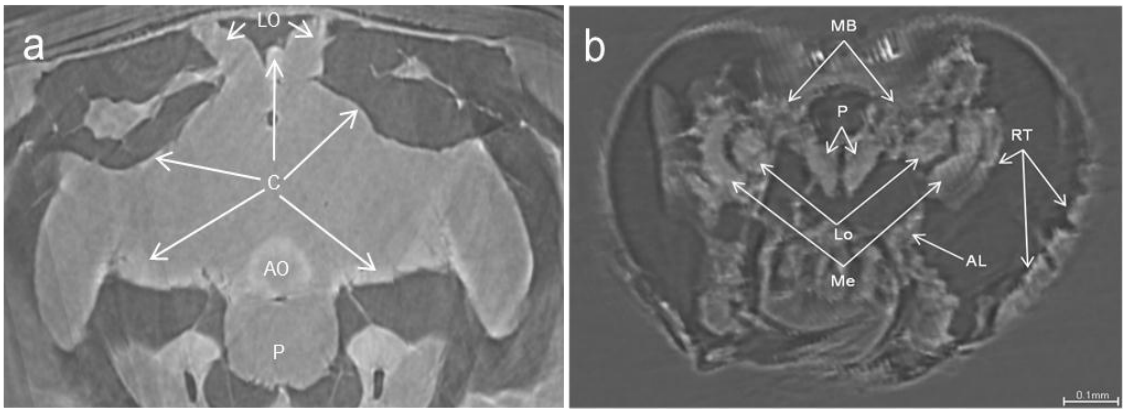

Figure 28: (a) A 2D axial view of a live honey bee brain showing perfusion of contrast medium (C) into peripheral regions. Arrows indicate areas of higher concentration. At 30 minutes post bolus injection into the haemolymph, the lateral ocelli (LO) and aorta (AO) contained more contrast than the sub oesophageal ganglion (SOG). (b) An axial view of the head capsule of an ancient stingless bee *Proplebeia abdita* (Greco et al. 2011) trapped in amber. The brain of this 20 million years old bee was particularly well preserved, as evidenced by the optic lobes including the medullae (Me) and lobulae (Lo), antennal lobes (AL), protocerebral lobes (P), and the mushroom bodies (MB). The retinal zone (RT) was also well preserved.

4.4 Discussion

Results from this study indicate that it is feasible to observe plasticity of the honey bee brain 'in vivo' using DR, and that progressive, real-time observations of these changes can be followed in individual live bees in association with environmental stimuli. Plasticity in the adult bee brain has been demonstrated in previous experiments using various techniques, such as the Cavalieri or computer volume segmentation methods. In all cases previous to this study, dead bees were used. However, the use of ex-vivo samples increases the chances of fundamental errors in correlation data analyses due to inherent differences among individuals. Movement errors were not a major limitation of this study, because it was possible to completely immobilize the bees, heads. However, haemolymph flow within the head capsule continued and this caused exposure variations between data capture events and thus also between tomographic slices on the resultant

image. The exposure variations were easily corrected by using the intensity averaging function during image reconstruction. The greatest challenge for this study was achieving adequate brain tissue differentiation, and it was clear that although radiographic contrast showed promise for improving tissue visualisation, further improvements on reconstruction algorithms are required to better separate brain structures. It is clear that bee brain imaging studies from Ribi et al. (2008) and Rybak et al. (2010) are still of superior quality; however, the results in this experiment demonstrate great potential for in-vivo, non-invasive DR imaging of the honey bee for future research in brain plasticity.

4.5 Future Directions

The non-invasive aspects of the methods described in this chapter will now enable live bee brain experiments to be conducted on the same individuals over time thus reducing bias errors that occur when observing different individuals. It is also worth mentioning that there are no restrictions from animal ethics committees on using insects for scientific research purposes and that once the sensitivity of determining the different brain neuropils is increased to that similar to MRI, it will be feasible to conduct live brain plasticity volume measurements on individual bees. Although insects are not vertebrates, the bee brain contains all the rudimentary functional portions of the vertebrate brain which enables comparisons to the corresponding portions of the vertebrate brain possible. Therefore, these new methods will enable a whole new area of research to into brain function and animal behaviour to develop. The methods also described, for the first time, the passage of food from the insect gut to the haemolymph in a live insect. Nutritional and pathogen treatments can now observed in live individuals on a temporal scale. These experiments will shed light on areas such as how nutrition or pathogens affect the immune response in insects.

CHAPTER 5

Application of CT to Insect Behaviour

5.1 Introduction

Many factors influence the evolutionary fitness of honeybees *Apis mellifera* (Hymenoptera: Apidae). Factors like foraging strategies are mediated by natural selection (Emlen 1966; MacArthur and Pianka 1966; Waddington and Holden 1979; Charlton and Houston 2010) and, as a consequence of net energy efficiencies, decision making strategies in individual bees which better exploit optimum food Vs. energy expenditure ratios, such as floral constancy, develop over time and impact on the long term survival of colonies (Betts 1935; Wells & Wells 1983; Slaa et al. 1997; Hassell and Southwood 1978; Kobayashi-Kidokoro and Higashi 2010). Bees gain most of their energy from simple carbohydrates when ingesting nectar or honeydew. Honeydew is a sweet exudate produced by various sap-sucking insects, mainly in the order Hemiptera, such as scale insects (Coccoidea) and aphids (Aphidoidea) (Eickwort and Ginsberg 1980). The carbohydrates serve for metabolic processes, flight and normal activity and are converted to glycogen or fat for storage in repositories called fat bodies during times of excess energy intake and honey storage (Gmeinbauer and Crailsheim 1993; Panzenböck and Crailsheim 1997; Romoser and Stoffolano 1998; Suarez et al. 2005; Standifer 2007). The predominant constituents of nectars, produced by floral and extra-floral nectaries on plants, are the sugars sucrose, glucose and fructose (Roubik 1995; Somerville 2005; Standifer 2007; Brodschneider and Crailsheim 2010). On occasions when nectar or honeydew are not available, bees collect sweet juices from mature fruit that is open or weeping and from other natural plant exudates (Roubik 1995; Michener 2000; O'Toole and Raw 2004; Standifer 2007). Nectar, honeydew, juices and exudates vary in the amount and type of sugars (and therefore energy) they contain, depending on the plant and insect species from which they are derived (Percival 1961) and the amount of water present in them differs with temperature and time of day (Bartareau 1996; de Bruijn and Sommeijer 1997). Bees can detect various food constituents such as amino

acids and cations (Waller 1972; Dress et al. 1997; Inouye and Waller 1984; Alm et al. 1990) and will avoid foraging on unsuitable nectar such as from onions, which contain high concentrations of potassium ions (Waller 1972; Williams and Free 1974; Gary et al., 1977; Kumar and Gupta 1993).

Bees expend energy when foraging for food and like many other organisms, follow optimal foraging strategies (Emlen 1966; MacArthur and Pianka 1966; Waddington and Holden 1979) to conserve energy. Optimal foraging strategies such as floral constancy (Grant 1950; Waser 1986; Slaa et al., 2003) improve a colony's chances of survival however, although there has been significant research on nectar processing and trophallaxis (Free 1957 & 1959; Ribbands 1953; Crailsheim 1998) there has been only limited research on nectar storage (Park 1925; Seeley 1992; Grueter and Farina 2007; Johnson and Baker 2007) and to our knowledge, none on decision making for optimal storage strategies. The benefits for optimisation strategies such as efficient honeybee foraging behaviour has been demonstrated by mathematical modelling and computer simulations (Schmickl and Crailsheim 2008; Thenius et al. 2008; Schmickl et al. 2010). If optimal storage strategies exist, decision making would be performed by storage bees that take food from incoming foragers, honey processing bees and from storage sources inside the hive (Nunez 1966; Farina 1996; De Marco & Farina 2001; Pirez & Farina 2004; Grueter & Farina 2007). Natural selection would favour bees with more efficient/optimal honey storage behaviour therefore colonies whose individuals exhibit efficient honey storage behaviour will have better chances of survival. For example, if bees were to store nectar of similar sugar concentrations in cells that were close to each other the dehydration phase of the ripening process would be more efficient than for that in groups of cells that contained nectar of varying concentrations (Pers comm. Tom Seeley 2010). Thus, colonies which exhibit optimal storage behaviour would conserve energy and have an evolutionary advantage and improved colony survival expectations over less efficient colonies.

For a detailed description of how honey is processed prior to final storage refer to (Nunez 1966; Farina 1996; De Marco & Farina 2001; Pirez & Farina 2004; Grueter & Farina 2007) and see (Fig. 29) for a description of the pathways involved.

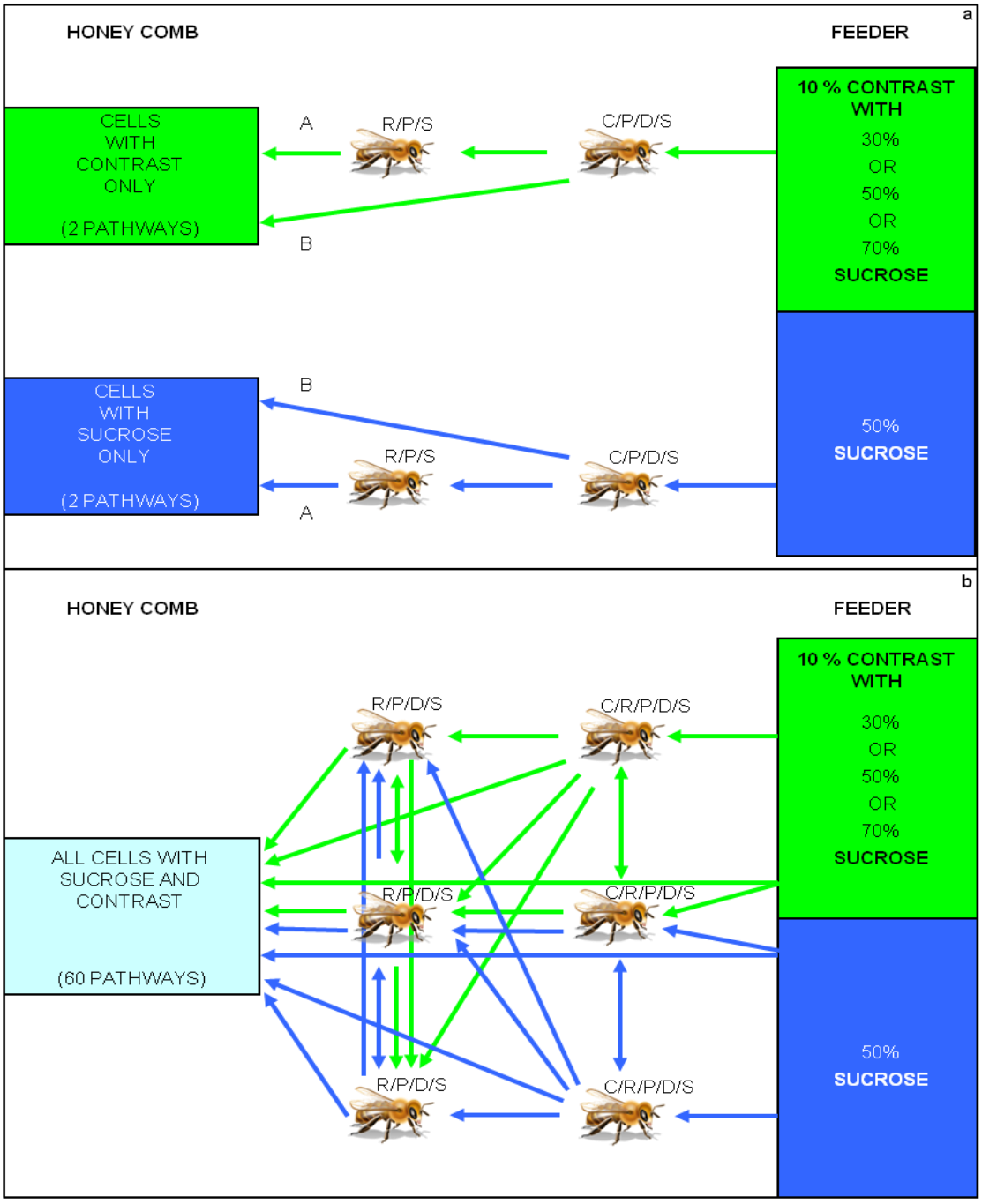

Figure 29: A schematic diagram of the three possible pathways as evidenced by the empirical data. There are only two pathways possible for either labelled (green) or unlabelled (blue) nectar to enter a cell unmixed (a) and sixty pathways possible for a mixture of labelled and unlabelled nectar to enter a cell (b). The random theoretical multinomial probabilities distribution of these pathways gives a cell ratio of 1:30:1 for the three categories of stored nectar.

Therefore more efficient honey storage behaviour has the potential to reduce energy expenditure, improve the honey ripening process and ultimately impact on a colony's chances of long term survival. In this study, the honey storage behaviour of bees from nine *A. mellifera* colonies that were fed solutions with three different sugar concentrations was explored using CT.

5.2 Methods

5.2.1 Hive preparation

Nine colonies containing one mated/physogastric, actively laying queen and approximately 1000 workers aged between 1 and 28 days in Apidea hives (Transidea AG, Dentenbergstrasse 50, 3076, Worb, Switzerland) were prepared by removing brood and honey combs and then adding only foundation combs and labelled and unlabelled food inside the hives. The hives were closed during daylight hours, to prevent bees foraging on external food sources, and opened for one hour after sunset for hive hygiene. The food was liquid sucrose solutions in feeders that had a separator to prevent labelled and unlabelled food from mixing (Fig. 30). Solutions were labelled with Visipaque 320 radiographic contrast agent (GE Healthcare Inc, 3135 Easton Turnpike Fairfield, CT 06828-0001 United States).

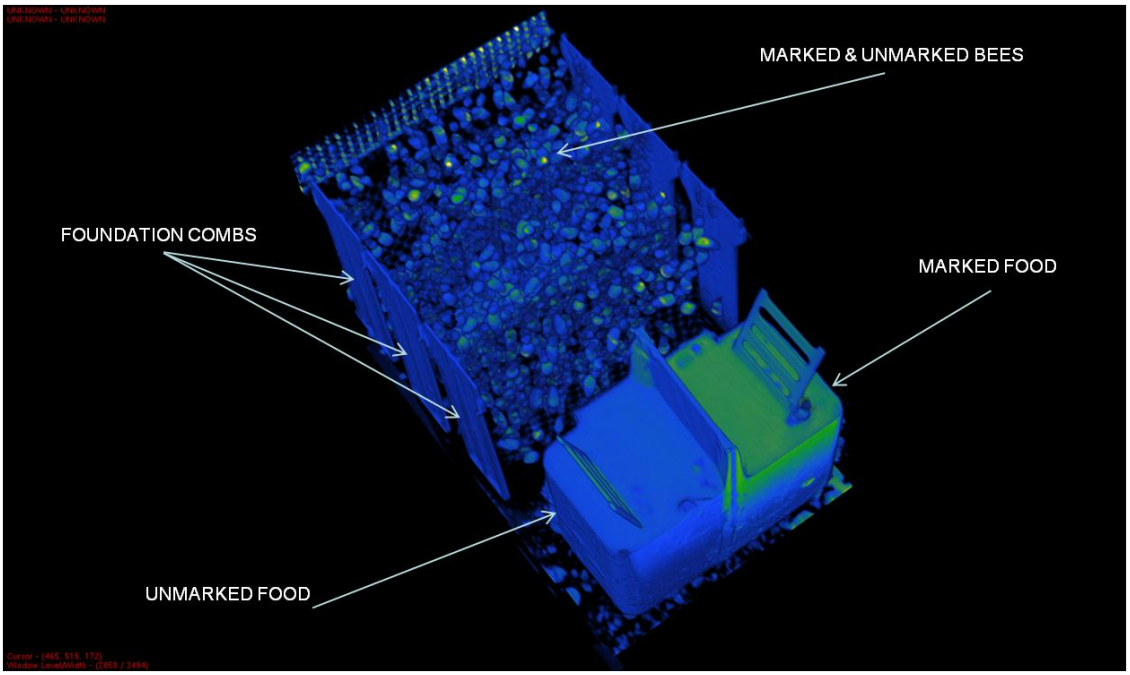

Figure 30: A 3D CT scan of an Apidae hive as prepared for mapping the in-hive honey distribution patterns. This scan was performed at the start of the experiment, just before the bees commenced building cells.

The internal feeders in hives 1, 2 & 3 contained solutions with Treatment-1 (T1): 30% sucrose solution-10% Visipaque 320 and Control: 50% sucrose, hives 4, 5 & 6 contained solutions with Treatment-2 (T2): 50% sucrose solution-10% Visipaque 320 and Control: 50% sucrose and hives 7, 8 & 9 contained solutions with Treatment-3 (T3): 70% sucrose solution-10% Visipaque 320 and Control: 50% sucrose. Workers tested for food acceptance showed no preference between 50% sucrose solution-10% Visipaque 320 or 50% sucrose solution and there was no toxic effect of Visipaque 320 for concentrations of up to 20% on adult worker bees (unpublished data).

5.2.2 Diagnostic Radioentomology (CT)

The labelled food enabled the bees' honey storage behaviour to be traced and mapped using CT on a Philips Brilliance CT 16-slice scanner (Philips Healthcare, 5680 DA Best, The Netherlands). Each cell containing honey was allocated vector co-ordinates (υ_1, υ_2 and υ_3) using BeeView 3D visualisation software (Disect Systems Ltd, Suffolk, United Kingdom) and the Hounsfield Units (HU) for the honey in the cell was recorded using *e*FilmLite version 1.5.0.0-DICOM (Digital Imaging and Communications in Medicine NEMA). Scans were performed at 48 hours after introduction of bees, combs and food. This enabled time for the bees to construct cells and commence honey storage. Scans performed after three days showed that, although there was still space available on the combs the bees stopped storing honey, probably because the food was readily available from the feeders inside the hive. Workers in small colonies have been observed behaving similarly with 50% sugar solutions placed inside apidea hives (pers comm. Laurent Gautier 2010).

5.2.3 Statistics

In utilizing the standard curve which was generated for this and future experiments (Fig. 31), each honey storage cell was allocated one of the three HU categories: Category-1 (C1) = 0-400HU, category-2 (C2) = 401-700HU and category-3 (C3) = 701- 1500.

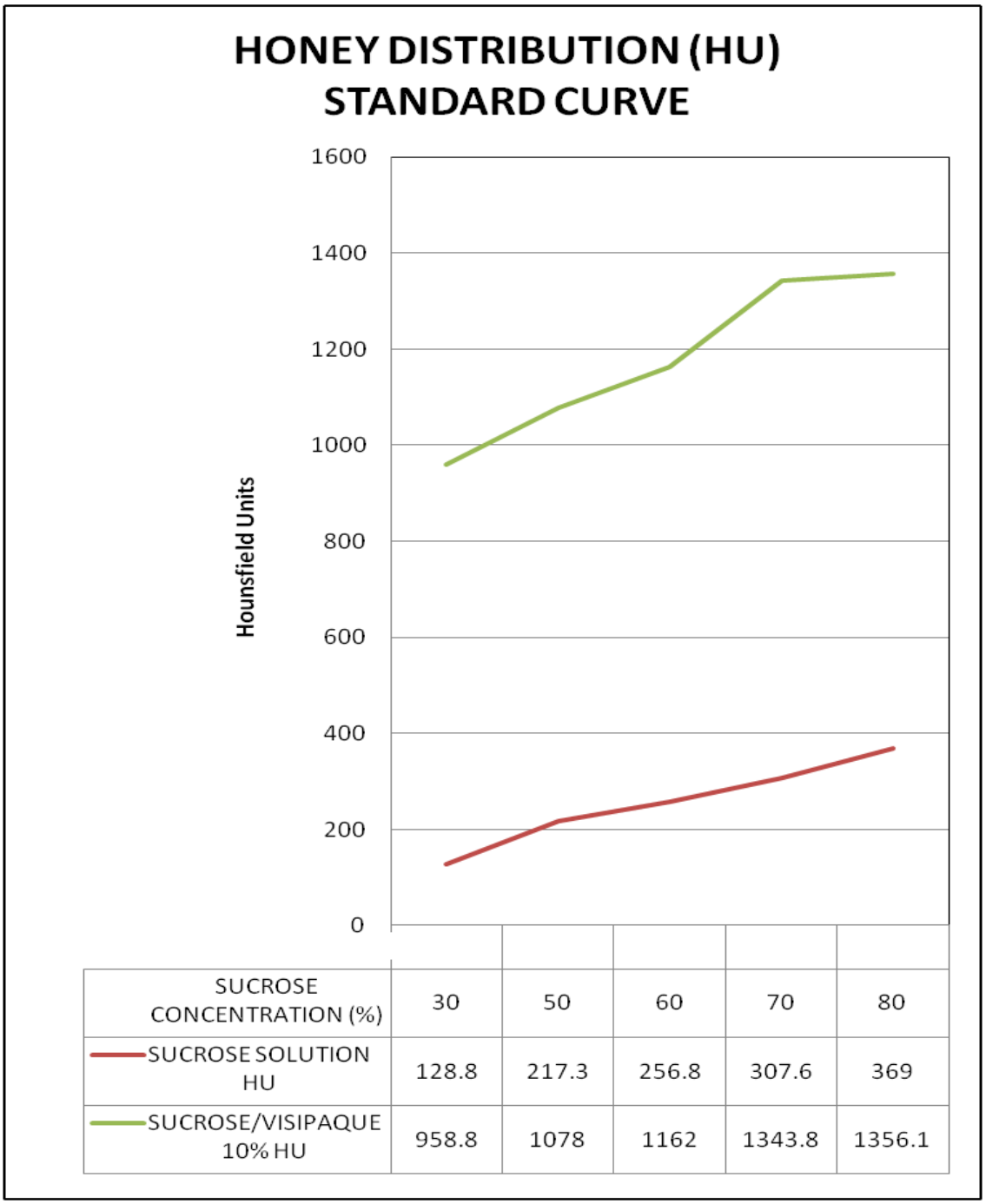

Figure 31: The standard curve produced for this experiment plotting Hounsfield Units (HU) according to sugar concentrations, without 10% Visipaque contrast agent (red) and with 10% Visipaque contrast agent (green).

Therefore, C1 cells contained honey without contrast, C2 cells contained honey with a combination of non-contrast and contrast honey and C3 cells contained only honey with contrast. The frequencies of cells for C1, C2 and C3 to the theoretical random honey storage frequency ratio (1:30:1) for the nine hives were compared.

5.2.4 Distribution of storage cells on combs

The distribution of labelled and unlabelled honey containing radiographic contrast (as measured by the HU's) on combs from the nine hives (within treatment groups) was also tested for uniformity. The "uniformity" here was not the statistical uniform distribution HU ~ U(min, max). The uniformity tested was given by the null hypotheses that the HU of the honey is the same in each cell (plus a random fluctuation). This in fact is the case for a normal distribution with constant mean μ and variance σ^2. Therefore the null hypothesis reads H_0: HU ~ N(μ, σ^2) and the tests performed were tests on normal distribution of HU (Shapiro-Wilk, Anderson-Darling and Kolmogorov-Smirnov-Lilliefors).

5.2.5 Sugar concentration versus distance from brood centre

Correlations between sugar concentrations (HU) within the honey containing cells and their Euclidean vector distances ($\|u\| = \sqrt{u_1^2 + u_2^2 + u_3^2}$) from the brood centre were then tested. Brood centre was established by locating the centre of the three dimensional brood (on-screen) and allocating 0,0,0 values for the x, y and z brood centre co-ordinates respectively. The brood centre co-ordinates and u_1, u_2 and u_3 were acquired with BeeView's on screen linear callipers. Spearman correlations and Kruskal-Wallis tests for T1, T2, T3 and pooled results were performed to compare the honey sugar concentrations in cells with Euclidean vector distances and their components u_1, u_2 and u_3 from brood centre.

5.3 Results

5.3.1 Honey storage frequency ratios

The theoretical polynomial distribution of honey storage frequency ratio for this experiment was (1:30:1) for (C1:C2:C3). The honey storage frequency ratios recorded from the empirical data for T1, T2 and T3 were statistically different from (1:30:1) at, 1:2:1, 3:1:3 and 1:2:4 respectively (Table 2). This was confirmed by Chi-square tests for T1, T2 and T3 being, χ^2: 128.8, 226.3, and 9358.9 respectively, with 2 df and p values of < 0.001 for all three treatments (Table 2). Thus, the null hypothesis that the honey storage distribution ratio of the three treatments follows the polynomial (1:30:1) distribution was rejected. Therefore, the honey storage frequency for all three treatments was not random.

5.3.2 Distribution of storage cells on combs

The null hypothesis, H_0: HU ~ N(μ, σ^2), that the sugar concentration of the honey was the same in each cell (plus a random fluctuation) was not rejected for T1, which could be related to smaller sample size leading to low power for the test for T1, however the null hypothesis was rejected for T2 and T3. Therefore, at least for T2 and T3 the labelled food was not deposited randomly by the bees. In addition, Figure 4 shows the distribution of cells containing honey of differing concentrations to have localized, patchy spatial distributions. The patchy cell distribution was not evidenced for T2 (50% labelled - 50% unlabelled) indicating, as expected, that the bees could not detect differences in sugar concentrations in T2 and also that they did not show preferences for labelled or unlabelled food.

5.3.3 Sugar concentration versus distance from brood centre

The honey sugar concentrations in cells for T2 and T3 were statistically different and there were cells grouped together that contained honey with similar sugar concentrations

for all three treatments (Fig. 32). There were some significant correlations between honey sugar concentrations within cells and their Euclidian distances from the brood centre for the three treatments (Table 3) however the correlations were very weak.

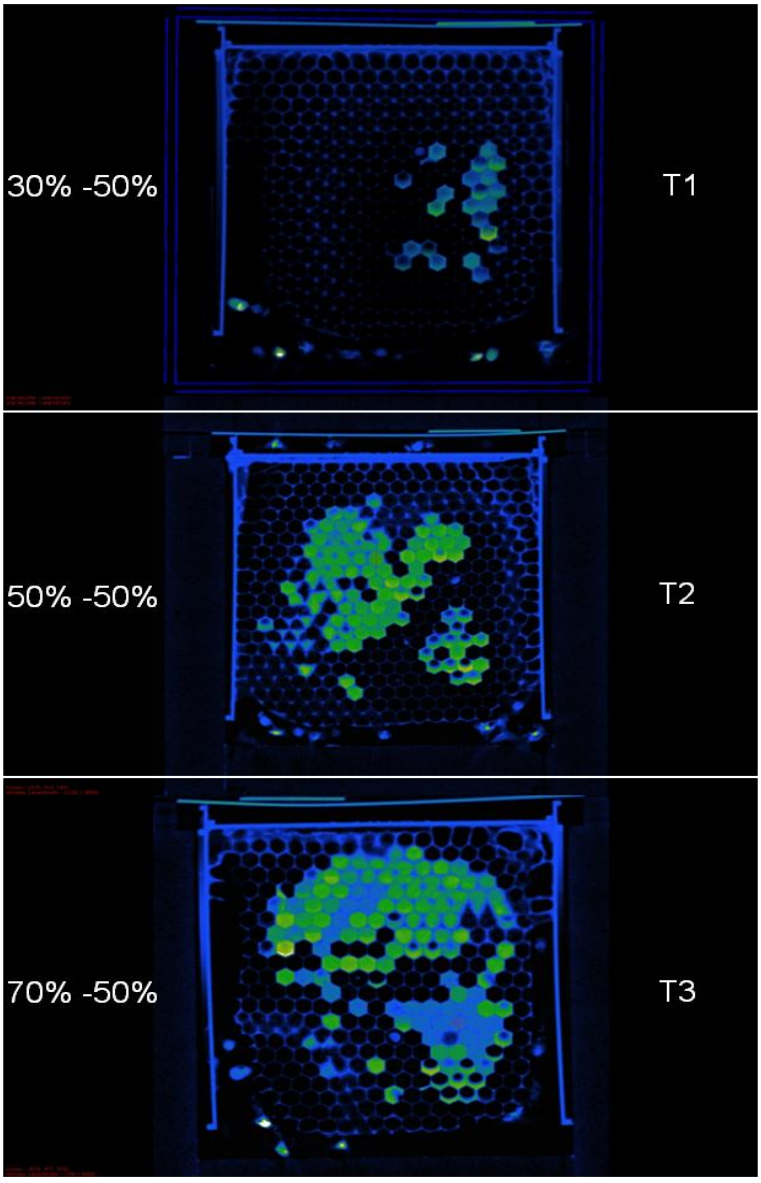

Figure 32: A 2D CT scan showing patchy distribution of cells containing honey with differing sugar concentrations (T1 & T2) and uniform distribution of cells containing honey with similar sugar concentrations (T2). The sugar concentration of Treatment 1 (T1) food was 30% labelled (green) and 50% unlabelled (blue), Treatment 2 (T2) food was 50% labelled (green) and 50% unlabelled (blue) and Treatment 3 (T3) food was 70% labelled (green) and 50% unlabelled (blue).

These results indicate that, at least for this experiment, there were no significant relationships between honey sugar concentrations and a cell's distance from the brood centre.

5.4 Discussion

The results suggest that decision making in storer bees is influenced by nectar sugar concentrations and that the bees store carbohydrates in groups of cells with similar sugar concentrations in a non-random way. This behaviour, as evidenced by the patchy spatial cell distributions, might help to hasten the ripening process (Pers comm. Tom Seeley 2010) by reducing the distance between cells of similar sugar concentrations. Indeed, storing nectar of similar sugar concentrations (and therefore water content) in cells that are close to each other would make the dehydration phase of the honey ripening process more efficient for those cell groups (Pers comm., Tom Seeley 2010). Thus, colonies which exhibit optimal storage behaviours such as these would have an evolutionary advantage and improved colony survival expectations over less efficient colonies.

When storing honey from the internal feeders, the bees in our experiment had three foraging-storage pathways to follow (Fig. 28). Therefore, assuming that there were no behavioural influences acting on these pathways, the random theoretical multinomial probabilities distribution for C1:C2:C3 would follow a honey storage frequency ratio of 1:30:1 for the three categories. However, the honey storage frequency ratios for C1:C2:C3, as calculated from the empirical data in this experiment, were significantly different from this random theoretical multinomial probabilities distribution as follows:

T1 (30% - 50%) had a honey storage frequency ratio for C1:C2:C3 of 1:2:1 ($p < 0.001$)

T2 (50% - 50%) had a honey storage frequency ratio for C1:C2:C3 of 3:1:3 ($p < 0.001$)

T3 (70% - 50%) had a honey storage frequency ratio for C1:C2:C3 of 1:2:4 ($p < 0.001$).

The significant differences in these ratios suggest that there were behavioural influences, such as decisions on where to place honey of similar concentrations, occurring. It is

therefore likely that the bees were depositing nectar according to contextual information (Seeley 1998), such as the location of other cells in the hive containing honey of similar sugar concentrations. Therefore, behaviours influencing the honey storage frequency ratios are most probably based on decisions for achieving optimal storage strategies. Camazine (1991) suggested that the honey storage pattern in honeybees was random. Although there were no significant relationships between honey sugar concentrations and a cell's distance from the brood centre in this experiment our data indicate, as do those of Free & Williams (1974) and Johnson and Baker (2007), that honeybees show a preference for storing honey according to sugar concentrations in the nectar. In another study, De Grandi-Hoffman and Hagler (2000) found that, up to 24 hours after introduction of labelled nectar, honeybees stored at least 20% of unlabelled nectar separately. In addition, although Seeley and Tovey (1994) discussed search time for foragers unloading to receivers, the principle follows that when using sugar concentration as a cue, search time for nectar deposition would be a consequence of storing bees returning to a cell patch containing nectar of similar sugar concentrations. Therefore, one optimal storage strategy would be for storer bees to return to cell patches containing cells with similar sugar concentrations until all the cells in those patches were full. This strategy would reduce search time and thus increase storing behaviour efficiency. The CT images in this study clearly show that honeybees are producing such cell patches with similar sugar concentrations (Fig 32).

It is feasible that storing honey in cell patches has benefits other than for those of ripening honey. Nectars collected by honeybees from different foraging patches (either natural or agricultural patches) can have differing sugar concentrations simply because the plants in these patches are growing under different local ambient conditions. In light of the current trend in global colony losses, it is crucial to mention here that the nectar from these plants might also contain other differences in constituents such as lethal or sub-lethal levels of toxins from agrochemicals and other sources (Sur and Stork 2003; Rogers et al.. 2007; Cloyd and Bethke 2010). Decision making in honeybees is based on information which is acquired and processed in order to make choices between two or more alternatives (Seeley 2010). Honey storage strategies, like those shown in this experiment, would be based on information such as sensing sugar concentrations in

incoming nectar and in ripening honey. Although it is not clear whether honeybees can detect agrochemicals in nectar or honey, as was shown in this experiment, honeybees might store toxin-containing nectars separately from toxin-free nectars indirectly by way of sensing the nectars' differing sugar concentrations. This would be an effective way to prevent all the honey from being contaminated and it would reduce widespread toxin contamination in the hive and help prevent bee losses. vanEngelsdorp et al. (2009), also suggest that honeybees store pollen with high levels of chlorothalonil separately in entombed cells which might be a phenomenon similar to the honey storage pattern behaviour shown in this experiment. In addition, there are plants in several genera from at least 11 families (Adler 2001; Robertson et al., 2010) that naturally produce nectars which contain constituents that have varying degrees of toxicity to bees (and humans) and there are plants that produce toxic pollen (Kevan and Ebert, 2005; Mesquita et al., 2010). Foragers bring these naturally occurring nectars and pollens back to the hive. It is feasible that the naturally occurring toxins in pollen and nectar have provided the selective pressure for honeybees to improve their food storage strategies. Thus colonies that exhibit storage strategies which separate toxic from non-toxic food would have an evolutionary advantage over colonies whose bees store food indiscriminately.

CT was used to acquire data and analyse results from this study and it is important to note that statistics were applied (2790 data points) to verify results. These results were however immediately visible and obvious prior to applying the statistical tests because the CT images highlighted the behavioural patterns as soon as the data were reconstructed. It is also important to note that although bees were marked with Visipaque 320, it was not possible to accurately establish the number of marked and unmarked bees because of bee movement errors. Nevertheless, research on overcoming these CT limitations to enable fast (full hive scans that take less than 20sec) and accurate results for future entomological experiments continues. For example, as with medical radiology where specialists use human visual pattern recognition techniques to diagnose pathology such as tumours or calculi, radio-entomology will be able to diagnose pathology (AFB, EFB, Nosema etc.) or behavioural patterns (Fig. 32) by visual diagnosis. Similarly, as with medical radiologists, radio-entomologists will able to view

the results instantaneously and perform diagnoses without the need to run extensive statistics on each case.

5.5 Future Directions

The methods described in this chapter have shown features of honeybee behaviour that were not possible to observe by any other method to date. The discovery of the non-random honey distribution has led us to re-examine how worker bees interact with each other within the hive. Future experiments will test for decision making between different patriline groups within the same colony and the effects of nectar sugar concentrations on honey distribution behaviour in storer bees. The non-invasive aspects of the methods will now enable experiments to be conducted on live colonies over time thus observing their behaviour in a quasi-natural setting. This will enable the most “real to life” scenario for full colony observations ever. It will be feasible to observe honey distribution behaviour for the first time, trophallaxis behaviour and nursing behaviour. We will be able to track individuals and groups of bees simultaneously and measure hive component changes over time. It also envisaged that whole hive treatments such as treating the hive with oxalic acid to remove parasitic mites will be monitored by MacroCT scanning to observe the distribution of the treatment over time.

CHAPTER 6

Conclusion and Future Research

Given the need to develop new methods for the study of insects, the overall aim of my thesis was to test the hypotheses that:

1. MacroCT can be used to non-destructively image behaviour in insect colonies;
2. MicroCT can be used to image the anatomical features of insects;
3. CT facilitates the study of insect physiology

The research described in this study was conducted as proof of concept for testing the three hypotheses above.

Thus, the overall objective that X-ray CT would be useful for non-invasive studies in entomology was achieved. The research has also advanced our knowledge of bee morphology and honeybee behaviour and has provided new research leads. These include the possibility of discovering new species, studying physiology in live insects non-invasively and developing better management regimes for honeybees. The research has also highlighted that it is necessary to explore insect behaviour such as honey storage patterns and determine if the honey storage frequency ratios shown have significant efficiencies of scale as do other honeybee behaviour optimisation strategies such as floral constancy. If they do, then these efficiencies will have important evolutionary implications for the long term survival of honeybee colonies and beekeepers will be able to select colonies that exhibit these preferred traits.

This research has shown that X-ray CT has great potential in entomology for studying insects (collectively termed: Diagnostic Radioentomology). It is envisaged that research will continue to improve the methods described in this thesis. Discussions with senior researchers from the Department of Mathematics at the University of Bath have led to

two MSc project proposals on developing sophisticated component differentiation algorithms and one PhD project proposal to develop algorithms to compensate for motion artefacts in tomography. The MSc projects will apply to real life data sets on live beehives and will be beneficial for differentiating and quantifying the various components within a beehive e.g. honey, wax, larvae or pollen. The need for greater accuracy in measuring these components is increasing (Sur and Stork 2003; Rogers et al,. 2007; Cloyd and Bethke 2010) and the MSc projects following on from the work carried out in this thesis will help to provide these accuracies. The PhD project will apply sophisticated motion correction algorithms to real life beehive tomography datasets. It is envisaged that these algorithms will, for the first time, enable bees within a live colony to be accurately counted. Although the methods described in Chapter 2 of this thesis have already been described as the **"GOLD STANDARD"** for estimating strength parameters of *A. mellifera* colonies (Delaplane et al. 2013) the improvements produced during the proposed PhD project will have the potential to supersede current manual estimations.

The methods described in this chapter have also provided new ways for observing internal morphology of insects non-invasively. The tracheal system was explored in the locust and butterfly with both volume estimations and metamorphic changes described and the malpighian tubes in the ladybird were segmented and imaged in 3-D without physical dissection. These techniques have opened up new areas of research such as live scanning of "internal" metamorphic changes and organ characterisation in live insects. It is envisaged that these methods will be used in developmental experiments where individual insects can be scanned daily over several weeks to observe metamorphic changes. Other experiments will involve treating individuals with pathogens or nutritional variations in diets to observe insect development. In particular, the malpighian tubules of ladybird beetles can now be examined in live insects to describe their physiological function over time while being exposed to different diet regimes. Their HU can now be determined to estimate the types of solid materials that accumulate in them. The non-invasive aspects of the new methods will now enable these experiments to be conducted on the same individuals over time thus reducing bias errors that occur when observing different individuals.

The non-invasive aspects of the methods described in this chapter will now enable live bee brain experiments to be conducted on the same individuals over time thus reducing bias errors that occur when observing different individuals. It is also worth mentioning that there are no restrictions from animal ethics committees on using insects for scientific research purposes and that once the sensitivity of determining the different brain neuropils is increased to that similar to MRI, it will be feasible to conduct live brain plasticity volume measurements on individual bees. Although insects are not vertebrates, the bee brain contains all the rudimentary functional portions of the vertebrate brain which enables comparisons to the corresponding portions of the vertebrate brain possible. Therefore, these new methods will enable a whole new area of research to into brain function and animal behaviour to develop. The methods also described, for the first time, the passage of food from the insect gut to the haemolymph in a live insect. Nutritional and pathogen treatments can now observed in live individuals on a temporal scale. These experiments will shed light on areas such as how nutrition or pathogens affect the immune response in insects.

The methods described in this chapter have shown features of honeybee behaviour that were not possible to observe by any other method to date. The discovery of the non-random honey distribution has led us to re-examine how worker bees interact with each other within the hive. Future experiments will test for decision making between different patriline groups within the same colony and the effects of nectar sugar concentrations on honey distribution behaviour in storer bees. The non-invasive aspects of the methods will now enable experiments to be conducted on live colonies over time thus observing their behaviour in a quasi-natural setting. This will enable the most “real to life” scenario for full colony observations ever. It will be feasible to observe honey distribution behaviour for the first time, trophallaxis behaviour and nursing behaviour. We will be able to track individuals and groups of bees simultaneously and measure hive component changes over time. It also envisaged that whole hive treatments such as treating the hive with oxalic acid to remove parasitic mites will be monitored by MacroCT scanning to observe the distribution of the treatment over time.

The recent acquisition of a MicroCT scanner in the Department of Mechanical Engineering has provided opportunities to further extend the research in this thesis. Discussions with research engineers have led to projects to improve tissue differentiation in live insect brains. Tomography at the micrometre level on live insect brains requires 30min to2hours. The long scan time increases the motion artefacts in live specimens. Future research will attempt to compensate for these errors. It is also worth mentioning that the developments from this research will apply to other fields such as medical and veterinary X-ray tomography. Radiologists are continually faced with motion artefacts and tissue differentiation limitations while reading patient tomographic images.

The research described in this thesis has also determined that the sensitivity of the data produced from the new imaging techniques requires further engineering developments to produce more useful results. The sensitivity of tissue differentiation needs to improve so that it becomes comparable to MRI methods. Thus because of the faster speed and higher resolution of CT to MRI, it will be a much more powerful tool for entomologists. Further developments to make scanners more portable will also enable them to be taken to hive sites rather than taking hives to the scanner. Some hospital scanners are already portable within ward units however mechanical modifications to wheels and gantries would need to be made to enable them to be taken out into the field. Taking scanners into the field will provide more flexibility for experimental procedures and also provide a more “natural” setting for the observations. This new field of Diagnostic Radioentomology brings with it improvements in image quality, image manipulations, reduction of potential errors, flexibility in experimental protocols and new methods for observing live insects. The benefits this research brings to apicultural practices to increase the health and long-term survival of bees plus the benefits to the scientific process of observing insects justify continuation of this line of research for the development of improved methods for agriculturalists and imaging scientists.

Literature Cited

Adler, L. S. 2001. The ecological significance of toxic nectar. - Oikos 91: 409–420.

Albrecht FO. (1953) The anatomy of the migratory Locust. University of London, The Athlone Press.

Albrecht FO. (1956) The anatomy of the Red Locust (*Nomadacris septemfasciata* Serville). Anti-locust Research Centre. 1 Princes Gate, London SW7.

Al-Harbi J, Hunt V, Charnley K, Heatley D, Bell GD, Corps N. (2008) X-ray micro-CT enables high-resolution 3-D imaging of the internal anatomy of live locusts. Poster presentation at the World Congress of Entomology, South Africa. July 2008 http://www.fishersideas.co.uk/Papers/WorldCongressOnEntomologyJuly08.pdf.

Alm, J., Ohnmeiss, T.E., Lanza, J. and L. Vriesenga. 1990. Preference of cabbage white butterflies and honey-bees for nectar that contains amino-acids. Oecologia 84:53–57.

Alt W. (1912) Ueber das Respirationssystem von 'Dytiscus marginalis'. Ein Beitrag zur Morphologie des Insektenkoerpers. Inaugural-Dissertation... von Willy Alt,... Breitkopf und Härtel.

Araujo, V.A., U. Zama, H. Dolder and J. Lino-Neto (2005). Morphology and ultrastructure of the spermatozoa of Scaptotrigona xanthotricha Moure (Hymenoptera: Apidae: Meliponini). Brazilian Journal of Morphological Science 22: 137–141.

Atkinson, C. H. and Soria, J. (2007). Algebraic Reconstruction Techniques for Tomographic Particle Image Velocimetry. In: Peter Jacobs, Tim McIntyre, Matthew Cleary, David Buttsworth, David Mee, Rose Clements, Richard Morgan and Charles Lemckert, 16th Australasian Fluid Mechanics Conference (AFMC). *16th Australasian Fluid Mechanics Conference (AFMC)*, Gold Coast, Queensland, Australia, (191-198). 3-7 December, 2007.

Bartareau, T. (1996). "Foraging Behaviour of Trigona carbonaria (Hymenoptera: Apidae) at Multiple-choice feeding stations." Australian Journal of Zoology 44: 143-153.

Bell DM (1977) Studies on the malpighian tubules of *Locusta migratoria migratorioides* (R +F), with particular reference to the role of Na +-K+ activated ATPase in fluid secretion. A thesis submitted for the degree of Doctor of Philosophy of the University of Durham January 1977.

Bell DM, Anstee JH. (1977) A study of the malpighian tubules of *Locusta migratoria* by scanning and transmission electron microscopy. Micron, Vol 8: 123-134.

Bell GD, Woolnough L, Mortimore M, Corps N, Hudson DM, Greco MK. A Preliminary Report on the Use of Bench-Top X-Ray Micro-Computerised Tomography to Study the Malpighian Tubules of the Overwintering Seven Spotted Ladybird *Coccinella septempunctata L*. (Coleoptera: Coccinellidae. Psyche ,2012; Article ID 348348, 6 pages doi:10.1155/2012/348348.

Betts, A. D. (1935) The constancy of pollen collecting bees. – Bee World 16: 11 1-1 13.

Bettuzzi, M.S., F. Casali, S. Cornacchia, M. Rossi, E. Paltrinieri, M.P. Morigi, R. Brancaccio and D. Romani (2004). A new linear array detector for high resolution and low dose digital radiography. Nuclear Instrumentation and Methodology B 213: 227–230.

Betz, O. and G. Koelsch (2004). The role of adhesion in prey capture and predator defence in arthropods. Arthropod Structure and Development 33: 3–30.

Bocage, A.E.M. (1921) Procede et dispositfs de radiografie sur plaque en movement. French patent 536, 464

Bracewell, R.N. (1965). The Fourier Transform and its Applications (New York: McGraw-Hill).

Brenner, D.J. & E.J. Hall (2007). Computed Tomography — An Increasing Source of Radiation Exposure. N Engl J Med Vol 357:2277-2284. DOI: 10.1056/NEJMra072149.

Bridges CR, Kestler P, Scheid P. (1980) Tracheal volume in the pupa of the saturniid moth *Hyalophora cecropia* determined with inert-gases. Respir. Physiol Vol 40:281-291.

Brodschneider R. and Crailsheim K. (2010) Nutrition and Health in the Honeybee (Review). Apidologie 41: 278-294.

Brooks, R. and Di Chiro, G. (1976). Review Article: Principles of Computer Assisted Tomography (CAT) in Radiographic and Radioisotopic Imaging PHYS. MED. BIOL., Vol: 21(5), 689-732.

Brown SM, Napper RM, Mercer AR. (2000) Analysis of Structural Plasticity in the Honey Bee Brain using the Cavalieri Estimator of Volume and the Disector Method. *Image Analysis and Stereology* 19: 139-144.

Bust, G. S., T. L. Gaussiran, and D. S. Coco (1997), Ionospheric observations of the November 1993 storm, J. Geophys. Res., 102, 14,293–14,304.

Camargo J.M.F., Grimaldi D.A. and Pedro S.R.M. 2000. The extinct fauna of stingless bees (Hymenoptera: Apidae: Meliponini) in Dominican amber: Two new species and redescription of the male of Proplebeia dominicana (Wille and Chandler). Am. Mus. Novitates 3293: 1-24.

Camazine S. 1991. Self-organizing pattern-formation on the combs of honey bee colonies. Behav. Ecol. Sociobiol. 28: 61 – 76.

Censor, Y. (1983), Finite series expansion methods, Proc. IEEE, 71, 409–419.

Chapman RF. The Insects: Structure and Function.1998. Cambridge: Cambridge University Press.

Charlton, N.L. and Houston, A.I. (2010). What Currency Do Bumble Bees Maximize? PLoS ONE 5(8): e12186. doi:10.1371/journal.pone.0012186.

Clarke WM, Richards MM. (1976) The Locust as a typical Insect. Published by John Murray, 50 Albemarle Street, London.

Cloyd, R.A. and J.A. Bethke (2010) Impact of neonicotinoid insecticides on natural enemies in greenhouse and interiorscape environments. (wileyonlinelibrary.com) DOI 10.1002/ps.2015.

Crailsheim, K. (1998) Trophallactic interactions in the adult honeybee (Apis mellifera L.). Apidologie 29: 97 – 112.

de Bruijn, L. L. M. and M. J. Sommeijer (1997) Colony foraging in different species of stingless bees (Apidae, Meliponinae) and the regulation of individual nectar foraging. Insectes Sociaux 44(1): 35-47.

De Grandi-Hoffman, G. and J. Hagler (2000) The flow of incoming nectar through a honey bee (Apis mellifera L.) colony as revealed by a protein marker. Insectes soc. 47 302–306.

Delaplane K.S., Jozef van der Steen J. and E. Guzman-Novoa (2013) Standard methods for estimating strength parameters of Apis mellifera colonies. Journal of Apicultural Research 52(1): (2013) © IBRA 2013 DOI 10.3896/IBRA.1.52.1.03

De Marco, R.J. and Farina, W.M. (2001) Changes in food source profitability affect the trophallactic and dance behaviour of forager honeybees (Apis mellifera L.). Behav. Ecol. Sociobiol. 50: 441 – 449.

Dollin, A. (1996a) Introduction to Australian Native Bees. North Richmond, Native Bees of Australia Series, Booklet 1. The Australian Native Bee Research Centre; North Richmond, Australia, 10 pp.

Dollin, A. (1996b). Behaviour of Australian stingless bees. North Richmond, Australian Native Bee Research Centre.

Dress, W. J., S. J. Newell, A. J. Nastase, and J. C. Ford. (1997) Analysis of amino acids in nectar from pitchers of Sarracenia purpurea (Sarraceniaceae). Am. J. Bot 84:1701–1706.

Eickwort, G. and H. Ginsberg (1980) Foraging and Mating Behaviour in Apoidea. Annual Reviews of Entomology 25: 421-426.

Elsinga G.E., Scarano F., Wieneke B. and van Oudheusden B. W. (2006) Tomographic particle image velocimetry. Experiments in Fluids, 41, 2006, 933–947.

Emlen, J. M. (1966) The role of time and energy in food preference. American Naturalist, 100: 611-617.

Engel M.S. 1995. Neocorynura electra, a new fossil bee species from Dominican amber (Hymenoptera: Halictidae). J. N.Y. Entomol. Soc. 103: 317-323.

Engel M.S. 1996. New augochlorine bees (Hymenoptera: Halictidae) in Dominican amber, with a brief review of fossil Halictidae. J. Kansas Entomol. Soc., Suppl. 69: 34-345

Engel M.S. 1997. A new fossil bee from the Oligo-Miocene Dominican amber (Hymenoptera: Halictidae). Apidologie 28: 97-102

Engel M.S. 2000. A new interpretation of the oldest fossil bee (Hymenoptera: Apidae). Am. Mus. Novitates 3296: 1-11.

Engel M.S. 2001. A monograph of the Baltic amber bees and evolution of the Apoidea (Hymenoptera). Bull. Am. Mus. Nat. Hist. 259: 1-192.

Engel M.S. 2005. Family-group names for bees (Hymenoptera: Apoidea). Am. Mus. Novitates 3476: 1-33.

Engel M.S. (2011) Systematic melittology: Where to from here? Syst. Entomol. 36: 2-15.

Fahrbach SE, Farris SM, Sullivan JP, Robinson GE. (2003) Limits on volume changes in the mushroom bodies of the honey bee brain. *Journal of Neurobiology* 57:141–151.

Farina W.M. (1996) Food-exchange by foragers in the hive – A means of communication among honey bees? Behav. Ecol. Sociobiol. 38: 59 – 64.

Farris SM, Robinson GE, Fahrbach SE. (2001) Experience-and age related outgrowth of the intrinsic neurons in the mushroom bodies of the adult worker honey bee. *Journal of Neuroscience* 21(16):6395–6404.

Feeney, D.S., J.W. Crawford, T. Daniell, P.D. Hallett, N. Nunan, K. Ritz, M. Rivers and I.M. Young (2006). Three-dimensional microorganisation of the soil– root–microbe system. Microbiology and Ecology 52: 151–158.

Free, J.B. (1957) The transmission of food between worker honeybees. Br. J. Anim. Behav 5: 41 – 47.

Free, J.B. (1959) The transfer of food between the adult members of a honeybee community. Bee world 40: 193 – 201.

Free J.B. and Williams I.H. 1974. Factors determining food storage and brood rearing in honeybee (Apis mellifera) comb. J. Ent. (A) 49: 47 – 63.

Fuchs, A., A. Schreyer, S. Feuerbach and J. Korb (2004). A new technique for termite monitoring using computer tomography and endoscopy. International Journal of Pest Management 50: 63–66.

Gary, N.E., Witherell, P.C., Lorenzen, K. and J.M. Marston (1977) Area fidelity and intra field distribution of honey bees during the pollination of onions. Environmental Entomology Vol. 6 (2): 303-310.

Gerber B, Tanimoto H, Heisenberg M. (2004) An engram found? — evaluating the evidence from fruit Xies. *Current Opinion in Neurobiology* 14:737–744.

Gerling D. and Hermann H.R. 1978. Biology and mating behaviour of Xylocopa virginica L. (Hymenoptera: Anthophoridae). Behav. Ecol. Sociobiol. 3: 99-111.

Gerling D., Hurd P.D. Jr. and Hefetz A. 1981. In-nest behaviour of the carpenter bee, Xylocopa pubescens Spinola (Hymenoptera: Anthophoridae). J. Kansas Entomol. Soc. 54: 209-218.

Gmeinbauer R. and Crailsheim K. (1993) Glucose utilisation during flight of honeybee workers, drones and queens. J. Insect Physiol. 39: 959-967.

Gordon, R., R. Bender, and G. T. Herman (1970), Algebraic Reconstruction Techniques (ART) for three dimensional electron microscopy and X-ray photography, J. Theor. Biol., 29, 471– 481.

Grant, V. (1950) The flower constancy of bees. The Botanical Review: 379-398.

Greco MK, Spooner-Hart R, Holford P. (2005) A new technique for monitoring *Trigona carbonaria* nest content, brood and activity using X-ray computerised tomography. Journal of Apicultural Research Vol 44(3): 97-100

Greco MK, Bell M, Spooner-Hart R, Holford P. (2006) X-ray computerised tomography as a new method for monitoring *Amegilla holmesi* nest structures, nesting behaviour, and adult female activity. Entomologia Experimentalis et Applicata Vol 120:71-76

Greco MK, Jones A, Spooner-Hart R, Holford P. (2008) X-ray computerised microtomography (microCT): a new technique for assessing external and internal morphology of bees. Journal of Apicultural Research and Bee World Vol 47(4):286-291.

Greco MK, Hoffmann D, Dollin A, Duncan M, Spooner-Hart R, Neumann P. (2009) The alternative Pharaoh Approach: Stingless bees encapsulate beetle parasites alive. Naturwissenschaften Vol 97(3):319-323

Greco MK, Spooner-Hart RN, Beattie GAC, Barchia I, Holford P. (2011a) Australian stingless bees improve greenhouse Capsicum production. Journal of Apicultural Research Vol 50(2):102-115

Greco MK, Welz PM, Siegrist M, Ferguson J, Gallman P Roubik DW, Engel MS. (2011b) Describing an ancient bee trapped in amber using Diagnostic Radioentomology. Insectes Sociaux Vol 58(4):487-494

Greco MK, Tong J, Soleimani M, Bell GD, Schafer MO. (2012) Imaging live bee brains using minimally-invasive Diagnostic Radioentomology. Insect Science Vol 12: Article 89 1-7. http://www.insectscience.org/12.89.

Greenlee KJ, Henry JR, Kirton SD, Westneat MW, Fezzaa K, Lee W-K, Harrison JF. (2009) Synchrotron imaging of the grasshopper tracheal system and physiological

components of tracheal hypermetry. Am J Physiol Regul Integr Comp Physiol Vol 297:1343-1350.

Grimaldi D., Bonwich E., Delannoy M. and Doberstein S. 1994. Electron microscopic studies of mummified tissues in amber fossils. Am. Mus. Novitates 3097: 1-31.

Grimaldi D, & Engel MS (2005) Evolution of the Insects. Cambridge University Press; Cambridge, UK.

Grueter C. and Farina W.M. (2007) Nectar distribution and its relation to food quality in honeybee (Apis mellifera) colonies. Insectes Sociaux 54: 87 – 94.

Gullen PJ, Cranston PS. (2000) The Insects, An Outline of Entomology page 68. Blackwell.

Gullen PJ, Cranston PS. (2005) The Insects, An Outline of Entomology page 68. Blackwell.

Gundersen HJG, Jensen EB. (1987) The efficiency of systematic sampling in stereology and its prediction. Journal of Microscopy 147: 229–263.

Hamilton AG. (1937) The mechanism of respiration of locusts and its bearing on the problem of inhalation of poison dusts. Bull. ent. Res Vol 28:53-68.

Harrison, R.D., Gardner, W.A., Tollner, W.E. and Kinard, D.J. (1993) X-ray computed tomography studies of the burrowing behaviour of fourth-instar pecan weevil (Coleoptera: Curculionidae). Journal of Economic Entomology 86: 1714–1719.

Hartung DK, Kirton SD, Harrison JF. (2004) Ontogeny of tracheal system structure: a light and electron-microscopy study of the metathoracic femur in the American locust *Schistocerca Americana* . J. Morphol Vol 262:800-812

Hassell, M. P. and T. R. E. Southwood (1978) "Foraging strategies of insects." Annual Review of Ecology and Systematics 9: 75-98.

Heethoff M, Helfen L. and R.A. Norton. (2009). Description of *Neoliodes dominicus* n. sp. (Acari, Oribatida) from Dominican Amber, aided by synchrotron x-ray microtomography. Journal of Palaeontology, Vol 83(1): 153-159.

Hillerton JE, Vincent JFV. (1982) The specific location of Zinc in Insect Mandibles. J.Exp.Biol Vol 101:333-336

Hinojosa-Dı´az I.A. and Engel M.S. 2008. Juxtocellar structures in euglossine bees: A new character for corbiculate studies (Hymenoptera: Apidae). Beitr. Entomol. 58: 97-105.

Hönnickea MG, Foersterb LA, Navarro-Silvab MA, Menkc R-H, Rigond L, Cusatisa C. 2005. Preliminary studies of enhanced contrast radiography in anatomy and embryology of insects with Elettra synchrotron light. *Nuclear Instruments and Methods in Physics Research* 548: 207–212.

Hörnschemeyer T, Beutel RG, Pasop F. 2002. Head Structures of *Priacma serrata* Leconte (Coleoptera, Archostemata) Inferred From X-ray Tomography. *Journal of Morphology* 252: 298–314.

Hounsfield, G. (1973). Computerized transverse axial scanning (tomography): Part I. Description of system. British Journal of Radiology, 46, 1016-1022.

Hourcade B, Muenz TS, Sandoz J-C, Rössler W, Devaud J-M. (2010) The Long-Term Memory Leads to Synaptic Reorganization in the Mushroom Bodies: A Memory Trace in the Insect Brain? *Journal of Neuroscience* 30(18): 6465-6461.

Hsieh, J. (2003) Computed Tomography: principles, design, artifacts and recent advances. SPIE, Washington. ISBN: 0-8194-4425-1.

Imms' General Textbook of Entomology Tenth Edition Volume One. Edited by Richards OW and Davies RG. Chapman and Hall . 1977 London.

Inouye D.W. and G.D. Waller (1984) Responses of honey bees Apis mellifera to amino acid solutions mimicking nectars, Ecology 65: 618–625.

Ismail N, Robinson GE, Fahrbach SE. (2006) Stimulation of muscarinic receptors mimics experience-dependent plasticity in the honey bee brain. *Proceedings of the National Academy of Sciences of the United States of America* 103:207–211.

Johnson B.R. & Baker N. (2007) Adaptive spatial biases in nectar deposition in the nests of honey bees. Insectes Soc. 54, 351–355. doi:10.1007/s00040-007-0953-6.

Johnson SN, Read DB, Gregory PJ. 2004. Tracking larval insect movement within soil using high resolution X-ray microtomography. *Ecological Entomology* 29(1): 117–122.

Kaiser A, Klok JC, Socha JJ, Lee W-K, Quinlan MC, Harrison JF. (2007) Increase in tracheal investment with beetle size supports hypothesis of oxygen limitation on insect gigantism. PNAS Vol 104:13198-13203.

Kak A.C. (1979) Computerized tomography with x-ray emission and ultrasound Sources. Proc. IEEE, Vol. 67: 1245-1272.

Kak A.C. and Slaney M. (1988) *Principles of Computerized Tomographic Imaging*, IEEE Press.

Kanao, T, Okamoto T, Miyachi Y and Nohara N (2003) Parental exposure to low dose x-rays in Drosophila melanogaster induces early emergence in offspring, which can be modulated by transplantation of polar cytoplasm. Mutation Research 527: 1–6.

Kevan, P.G. and T. Ebert (2005) Can almond nectar and pollen poison honey bees? American Bee Journal 145(6): 507-509.

Kim JJ, Diamond DM. (2002) The stressed hippocampus, synaptic plasticity and lost memories. *Nature Reviews Neuroscience* 3:453–462.

Kim JJ, Song EY, Kosten TA. (2006) Stress effects in the hippocampus: synaptic plasticity and memory. *Stress* 9:1–11.

Kirton SD, Hennessey LE, Duffy B, Bennett MM, Lee W-K, Greenlee GJ. (2012) Intermolt development reduces oxygen delivery capacity and jumping performance in the American Locust (*Schistocerca Americana*). J. Comp Physiol B Vol 182:217-230.

Klowden MJ (2007) Physiological Systems in Insects. Second Edition, Elsevier, Amsterdam. Boston. Heidelberg. London.

Kobayashi-Kidokoro, M. and Higashi, S. (2010) Flower Constancy in the Generalist Pollinator *Ceratina flavipes* (Hymenoptera: Apidae): An Evaluation by Pollen Analysis, Psyche, vol. 2010, Article ID 891906, 8 pages, 2010. doi:10.1155/2010/891906.

Kolb B, Whishaw IQ. (1998) Brain plasticity and behaviour. *Annual Review of Psychology* 49:43–64.

Kumar, J. and J.K. Gupta (1993) Nectar sugar production and honey bee foraging activity in three species of onion (Allium species) Apidologie 24(4): 391-396.

Lak M., Ne´raudeau D., Nel A., Cloetens P., Perrichot V. and Tafforeau P. 2008. Phase contrast X-ray synchrotron imaging: Opening access to fossil inclusions in opaque amber. Microsc. Microanal. 14: 251-259.

Lak M., Fleck G., Azar D., Engel M.S., Kaddumi H.F., Neraudeau D., Tafforeau P. and Nel A. 2009. Phase contrast x-ray synchrotron microtomography and the oldest damselflies in amber (Odonata: Zygoptera: Hemiphlebiidae). Zool. J. Linn. Soc. 156: 913-923.

Lease HM, Wolf BO, Harrison JF. (2006) Intraspecific variation in the tracheal volume in the American locust, *Schistocerca americana*, measured by a new inert gas method. J.Exp.Biol. Vol 209:3476-3483.

Liston C, Miller MM, Goldwater DS, Radley JJ, Rocher AB, Hof PR, Morrison JH, McEwen BS. (2006) Stress-induced alterations in prefrontal cortical dendritic morphology predict selective impairments in perceptual attentional set-shifting. *Journal of Neuroscience* 26(30):7870-4.

Lyonet, P. (1762). Traité anatomique de la chenille qui ronge le bois de Saule. Gosse and Pinet, La Haye.

Maddrell SHP. (1971) The mechanism of Insect Excretory Systems. Adv. Insect physiol Vol 8:199-331.

Maina JN. (1989) Scanning and Transmission Electron Microscopic Study of the Tracheal Air Sac System in a Grasshopper *Chrotogonus senegalensis* (Kraus)-Orthoptera: Acridae: Pyromorphinae. The Anatomical Record Vol 223:393-405. MacArthur, R.H. and Pianka, E. R. (1966). On the optimal use of a patchy environment. The American Naturalist, 100 (916): 603-609.

Maleszka J, Barron AB, Helliwell PG, Maleszka R. (2009) Effect of age, behaviour and social environment on honey bee brain plasticity. *Journal of Comparative Physiology A Neuroethology Sensory Neural And Behavioural Physiology* 195:733–740.

Marcus BA. (1930) malpighian tubules : Coleoptera . Z. Morph. Oekol. Tiere, Vol 1: 609-77.

Mesquita, L.X., Maracaja, P.G., Sakamoto, S.M. and Soto-Blanco, B. (2010) Toxic evaluation in honeybees (Apis mellifera) of pollen from selected plants from the semi-arid region of Brazil. Journal of Apicultural Research 49(3): 265-269.

Meyer EP. (1989) Corrosion casts as a method for investigation of the insect tracheal system. Cell and Tissue Research Vol 256:1-6.

Michel RP, Cruz-Orive LM. (1988) Application of Cavalieri principle and vertical sections method to lung: estimation of volume and pleural surface area. *Journal of Microscopy* 150:117–136.

Michener, C. D. (1982). A new interpretation of fossil social bees from the Dominican Republic. Sociobiology 7 (1): 37-45 [42] (as Trigona domiciliorum, comparative notes).

Michener, C.D. (2000). The bees of the world. The John Hopkins University Press,

Baltimore, MD, USA.

Miller PL. (1960a) Respiration in the Desert Locust 1. The control of ventilation . J.Exp.Biol Vol 37:224-36.

Miller PL. (1960b) Respiration in the Desert Locust II. The control the spiracles. J.Exp. Biol;37:237-263.

Miller PL. (1960c) Respiration in the Desert Locust III Ventilation and the spiracles during flight.. J.Exp. Biol;37:264-278.

Misra DM. (1945) Studies on the somatic musculature of the desert locust, *Schistocerca gregaria* (Forskal). Part I The head. Indian Journal of Entomology Vol 7(1-2) 103-138.

Misra DM. (1946) Studies on the somatic musculature of the desert locust, *Schistocerca gregaria* (Forskal). Part 2. The neck and prothorax. Indian Journal of Entomology Vol 8(1) 1-29.

Misra DM. (1947) Studies on the somatic musculature of the desert locust, *Schistocerca gregaria* (Forskal). Part III. The pterothorax. Indian Journal of Entomology Vol 9(1) 19-72.

Mitchell, C. N., I. K. Walker, S. E. Pryse, I. Kersley, I. W. McCrea, and T. B. Jones (1998), First complementary observations by ionospheric tomography, the EISCAT Svalbard radar and the CUTLASS HF radar, Ann. Geophys., 16, 1519–1522.

Mohammed AH, Zhu SW, Darmopil S, Hjerling-LeZer J, Ernfors P, Winblad B, Diamond MC, Eriksson PS, Bogdanovic N. (2002) Environmental enrichment and the brain. *Progress in Brain Research* 138:109–133.

Nation JL. (2008) Insect Physiology and Biochemistry. Second Edition. CRC Press, Taylor & Francis Group Boca Raton. London/ New York.

Nunez J.A. (1966) Quantitative Beziehungen zwischen den Eigenschaften von Futterquellen und dem Verhalten von Sammelbienen. Z. vergl. Physiol. 53: 142 – 164.

Oliveira F.F. 2002. The mesotibial spur in stingless bees: A new character for the systematics of Meliponini (Hymenoptera: Apidae). J. Kansas Entomol. Soc. 75: 194-202.

O'Toole, C. and A. Raw (2004). Bees of the world. London, Cassell Illustrated.

Panzenböck, U. & Crailsheim, K. 1997. Glycogen in honeybee queens, workers and drones 375 (Apis mellifera carnica). Journal of Insect Physiology, 34, 155-165.

Park, W. (1925) The storing and ripening of honey by honeybees. Journal of Economic Entomology 18: 405-410.

Percival, M. S. (1961) Types of nectar in Angiosperms. New Phytologist 60: 235-281.

Perna, A., C. Jost, E. Couturier, S. Valverde, S. Douady and G. Theraulaz (2008). The structure of gallery networks in the nests of termite Cubitermes spp. revealed by X-ray tomography. Naturwissenschaften 95(9): 877-884.

Pirez, N. and Farina, W.M. (2004). Nectar-receiver behaviour in relation to the reward rate experienced by foraging honeybees. Behav. Ecol. Sociobiol. 55: 574 – 582.

Ribbands, C.R. (1953) Food sharing. In: The Behaviour and Social Life of Honeybees (C.R. Ribbands, Ed). London, Bee Research Association, Ltd., pp 191 – 194.

Ribi W, Sendenb TJ, Sakellariou A, Limayec A, Zhang S. (2008). Imaging honey bee brain anatomy with micro-X-ray-computed tomography. *Journal of Neuroscience Methods* 171: 93–97.

Robertson, L.M., Edlin, J.S. and Edwards, J.D. (2010) Investigating the importance of altitude and weather conditions for the production of toxic honey in New Zealand. New Zealand Journal of Crop and Horticultural Science. 38(2): 87-100.

Rogers MA, Krischik VA and Martin L.A. (2007). Effect of soil application of imidacloprid on survival of adult green lacewing, Chrysoperla carnea (Neuroptera: Chrysopidae), used for biological control in greenhouse. Biol Cont 42:172–177.

Romoser, W. S. and J. G. Stoffolano (1998). The Science of Entomology. Singapore, McGraw Hill.

Roubik, D. W. (1995) Pollination of Cultivated Plants in the Tropics. FAO Bulletin of Agricultural Services 118: 1-194.

Rozen J.G. Jr (1996). A new species of the bee Heterosarus from Dominican amber (Hymenoptera: Andrenidae; Panurginae). J. Kansas Entomol. Soc. Suppl. 69: 346-352.

Rybak J, Kuß A, Lamecker H, Zachow S, Hege H-C, Lienhard M, Singer J, Neubert K, Menzel R. (2010) The digital bee brain: integrating and managing neurons in a common 3D reference system. *Frontiers in Systems Neuroscience* 4:30.

Schlüter T. and Stürmer W. (1982). X-ray examination of fossil insects in Cretaceous amber of N.W.-France. Ann. Soc. Entomol. France 18: 527-529.

Schmickl T., Crailsheim K. (2008) TaskSelSim: A Model of the Self-Organisation of the Division of Labour of Honeybees. Mathematical and Computer Modelling of Dynamical Systems 14: 101 – 125.

Schmickl T., Thenius R., Crailsheim K. (2010) Swarm-Intelligent Foraging in Honeybees: Benefits and Costs of Task-Partitioning and Environmental Fluctuations. Neural Computing and Applications. DOI 10.1007/s00521-010-0357-9.

Schmitz A, Perry SF. (1999). Stereological determination of tracheal volume and diffusing capacity of the tracheal walls in the stick insect *Carausius morosus* (Phasmatodea, Lonchodidae). Physiol. Biochem. Zool. Vol 72:205-218.

Seeley, T.D. (1992) The tremble dance of the honey bee: message and meanings. Behav. Ecol. Sociobiol. 47: 311–316.

Seeley, T.D. (1998) Thoughts on information and integration in honey bee colonies. Apidologie 29: 67–80.

Seeley, T.D. and Tovey, C.A. (1994) Why search time to find a food-storer bee accurately indicates the relatives rates of nectar collection and nectar processing in honey bee colonies. Anim Behav 47: 311-316.

Seeley, T.D. 2010. Honeybee Democracy. Princeton University Press.

Serrao, J.E. (2001). A comparative study of the proventricular structure in corbiculate apinae (Hymenoptera, Apidae). Micron 32: 379–385.

Serrao, J.E. (2005). Proventricular structure in solitary bees (Hymenoptera: Apoidea). Organisms Diversity and Evolution 5: 125–133.

Shepp, L.A. and Logan, B.F. (1974) IEEE Trans . Suc l . Sc i . , NS-21 (3), 21-43

Slaa, E.J., Tack, A.J.M. and Sommeijer, M.J. (2003) The effect of intrinsic and extrinsic factors on flower constancy of stingless bees. Apidologie 34: 457-468.

Snodgrass, R.E. 1928. Morphology and evolution of the insect head and its appendages. Smithsonian Misc. Coll. 81: 1-158.

Snodgrass RE. Principles of Insect Morphology. (1935) New York: McGraw-Hill Book Co.

Socha JJ, Forster TD, Greenlee KJ. (2010) Issues of convection in insect respiration: Insights from synchrotron X-ray imaging and beyond. Respiratory Physiology and Neurobiology Vol 173S:S65-S73.

Somerville, D. (2005). Fat bees - skinny bees. A manual on honey bee nutrition for beekeepers. Goulburn, AUS, Australian Government Rural Industries Research and Development Corporation: 1-142.

Straus Durkheim. (1828) Considérations sur l'Anatomie compare des animaux (Anatomie du Hanneton). Paris.

Standifer, L. N. (2007) Honeybee nutrition and supplemental feeding. Beekeeping in the United States.

Suarez, R.K., Darveau, C.A., Welch, Jr, K.C., O'Brien, D.M., Roubik, D.W. and P.W. Hochachka (2005). Energy metabolism in orchid bee flight muscles: carbohydrate fuels all. J. Exp. Biol. 208, 3573-3579.

Sur, R. and A. Stork A (2003) Uptake, translocation and metabolism of imidacloprid in plants. Bull Insectol 56:35–40.

Swammerdam, J., 1737–38. Bybel der Natuure. Severinus, Vander Aa and Vander Aa, Leiden. 2 vols. Translated as The Book of Nature, 1758, Seyffert, London. 2 vols, 236 & 153 pp.

Tafforeau, P., Boistel,R., Boller, E., Bravin, A., Brunet, M., Chaimanee, Y., Cloetens, P., Feist, M., Hoszowska, J., Jaeger, J-J., Kay, R.F., Lazzari, V., Marivaux, L., Nel, A., Nemoz, C., Thibault, X., Vignaud, P. and S. Zabler (2006). Applications of X-ray synchrotron microtomography for non- destructive 3D studies of paleontological specimens. Applied Physics A, Vol 83(2): 195-202.

Tafforeau, P. (2007) Palaeontologists Get X-Ray Vision. *Science* 318: 1546-1547.

Tarplee M, Corps N. (2008) Skyscan 1072 Desktop X-ray microtomography – sample scanning, reconstruction, analysis and visualisation (2-D & 3-D) protocols. Guidelines, notes, selected references and F.A.Q. May 2008 http:/www.geog.qmul.ac.uk/docs/staff/4952.pdf.

Thenius R., Schmickl T., Crailsheim K. (2008) Optimisation of a honeybee-colony's energetics via social learning based on queuing delays. Connection Science 20 (2-3): 193-210.

Tollner, E.W. (1991). X-ray computed tomography applications in soil ecology. Agriculture, Ecosystems and Environment 34: 251–260.

Udupa J.K, and G.T Herman (2000) 3D Imaging in Medicine 2nd Ed, CRC Press.

vanEngelsdorp, D., Evans, J.D., Donovall, L., Mullin, C., Frazier, M., Frazier, J., Tarpy, D.R., Hayes Jr., J and J.S. Pettis (2009) ‘‘Entombed Pollen”: A new condition in honey bee colonies associated with increased risk of colony mortality. Journal of Invertebrate Pathology 101: 147–149.

Velthuis H.H.W. and Gerling D. 1983. At the brink of sociality: Interactions between adults of the carpenter bee Xylocopa pubescens Spinola. Behav. Ecol. Sociobiol. 12: 209-214.

Vinal S.C. (1919) The Respiratory System of the Carolina Locust *(Dissosteira Carolina Linne*). Journal of the New York Entomological Society Vol 27:19-32.

Waddington, K.D. and Holden, L.R. (1979). Optimal Foraging: On Flower Selection by Bees. The American Naturalist 114 (2): 179-196.

Waller, G. D. (1972). Evaluating responses of honey bees to sugar solutions using an artificial-flower feeder. Annual Review of Entomology 65: 857-862.

Waser, N.M. 1986. Flower constancy: definition, cause and measurement. The American Naturalist, 127(5): 596-603.

Weis-Fogh, T. (1952) Fat combustion and metabolic rate of flying insects (*Schistocera gregaria* Forskal). Phil. Trans. B 237, 1-36.

Weis-Fogh, T. (1956a) The ventilatory mechanism during flight of insects in relation to the call for oxygen. Proc. XIV Int. Congr. Zool., 283-5.

Weis-Fogh, T. (1956b) Biology and physics of locust flight. II. Flight performance of the desert locust (*Schistocera gregaria*).). Phil. Trans. B 239, 459-510.

Weis-Fogh, T. (1956c) Biology and physics of locust flight. IV. Notes on sensory mechanisms in locust flight. Phil. Trans. B 239, 555-84.

Weis-Fogh, T. (1964a) Functional design of the tracheal system of flying insects as compared with the avian lung. J.Exp.Biol. 41:207-227.

Weis-Fogh, T. (1964b) Diffusion in insect wing muscle, the most active tissue known. J. exp. Biol. 41: 229-56.

Weis-Fogh, T. (1964c) Biology and physics of locust flight. VIII. Lift and metabolic rate of flying locusts. J. exp. Biol. 41: 257-71.

Weis-Fogh, T. (1967) Respiration and tracheal ventilation in locusts and other flying insects. Exp. Biol. 47:561-587.

Wells, H. & Wells, P. H. (1983) Honey bee foraging ecology: optimal diet, minimal uncertainty or individual constancy? J. Anim. Ecol., 52, 829–836.

Wigglesworth VB. (1950) A new method of injecting the trachea and tracheoles of insects. Q .J. Micros. Sci. Vol 91:113-137.

Wille, A, and L. Chandler. 1964. A new stingless bee from the tertiary amber of the Dominican Republic. Revista de Biologia Tropical 12: 187-195.

Williams, I.H. and J. B. Free (1974) The pollination of onion (Allium cepa L.) to produce hybrid seed. J. appl. Ecol. 11: 409-418.

Wirkner C.S & L. Prendini (2007). Comparative Morphology of the Haemolymph Vascular System in Scorpions- A Survey Using Corrosion Casting, MicroCT and 3D Reconstruction. Journal of Morphology, 268: 401-413.

Withers GS, Fahrbach SE, Robinson GE. (1993) Selective neuroanatomical plasticity and division of labour in the honey bee. *Nature* 364:238–240.

SCIENTIFIC INVESTIGATION	SCANNING OPTIONS	EXPECTED IMPLICATIONS	MOST APPROPRIATE METHOD
Social Insect Colony Behaviour	Non-invasive Visual Inspection	Good surface and external observations	
	Invasive Visual Inspection	Good external and internal observations however colonies are damaged or destroyed during the process	
	MRI	Good external and internal resolution however scanning times (3hrs) produces blurred images	
	MacroCT	Good external and internal observations and short scanning times (20-30sec) produce sharp images	X
Insect Morphology	Light Microscopy	Good surface resolution however sample require dissection for internal observations	
	SEM	Best surface resolution however the sample is destroyed in the process	X
	MicroMRI	Good tissue differentiation however resolution is not as fine as MicroCT	
	MicroCT	High resolution however tissue differentiation is not a sensitive as MicroMRI	X
Insect Physiology on Live Insects	Light Microscopy	Not possible	
	SEM	Not possible	
	MicroMRI	Not possible	
	MicroCT	Can be performed on live insects with good image resolution.	X

Table 1: Options for scanning insects and their colonies, their implications and which method is the most appropriate for the scientific investigation being considered.

T1 (30%)	HU_CAT	Counts	Ratio	Percent	Expected probability	expected counts	Chi^2	p
	C1	**10**	**1**	**27.027**	**0.03125**	**1.156**		
	C2	**18**	**2**	**48.649**	**0.93750**	**34.688**	**128.881**	**0.0000**
	C3	**9**	**1**	**24.324**	**0.03125**	**1.156**		
T1 (50%)	HU_CAT	Counts	Ratio	Percent	Expected probability	expected counts	Chi^2	p
	C1	**9**	**3**	**42.857**	**0.03125**	**0.656**		
	C2	**3**	**1**	**14.286**	**0.93750**	**19.688**	**226.314**	**0.0000**
	C3	**9**	**3**	**42.857**	**0.03125**	**0.656**		
T3 (70%)	HU_CAT	Counts	Ratio	Percent	Expected probability	expected counts	Chi^2	p
	C1	**130**	**1**	**14.908**	**0.03125**	**27.250**		
	C2	**232**	**2**	**26.606**	**0.93750**	**817.500**	**9358.977**	**0.0000**
	C3	**510**	**4**	**58.486**	**0.03125**	**27.250**		

Table 2: Honey storage frequency ratios and χ^2 test statistic for Treatment 1 (T1), Treatment 2 (T2) and Treatment 3 (T3) were (1:2:1), (3:1:3) (1:2:4), and 128.881, 226.314, 9358.977 respectively. The random theoretical (expected) honey storage frequency ratio was (1:30:1). Therefore the storage bees did not distribute honey at random.

T1 (30%)	Spearman Correlation	HU	p	KW Statistic	p
	DIST_ v_1	**0.1650**	**0.329**	**0.321**	**0.852**
	DIST_ v_2	**0.0799**	**0.638**	**0.138**	**0.933**
	DIST_ v_3	**-0.1287**	**0.448**	**1.291**	**0.524**
	EUCL_DIST	**-0.0062**	**0.971**	**1.056**	**0.590**
T2 (50%)	Spearman Correlation	HU	p	KW Statistic	p
	DIST_ v_1	**-0.0494**	**0.831**	**1.913**	**0.384**
	DIST_ v_2	**-0.2000**	**0.385**	**1.154**	**0.561**
	DIST_ v_3	**-0.1844**	**0.424**	**4.502**	**0.105**
	EUCL_DIST	**-0.4623**	**0.035**	**9.945**	**0.007**
T3 (70%)	Spearman Correlation	HU	p	KW Statistic	p
	DIST_ v_1	**-0.0611**	**0.071**	**4.928**	**0.085**
	DIST_ v_2	**-0.0065**	**0.848**	**23.281**	**0.000**
	DIST_ v_3	**-0.0879**	**0.009**	**1.148**	**0.563**
	EUCL_DIST	**-0.114**	**0.736**	**15.958**	**0.000**
POOLED	Spearman Correlation	HU	p	KW Statistic	p
	DIST_ v_1	**-0.0257**	**0.434**	**1.533**	**0.465**
	DIST_ v_2	**0.0052**	**0.874**	**20.903**	**0.000**
	DIST_ v_3	**-0.0914**	**0.0053**	**3.681**	**0.159**
	EUCL_DIST	**-0.0114**	**0.7284**	**13.311**	**0.001**

Table 3: Spearman correlations of Hounsfield Units (HU) vs. distance measures and Kruskal-Wallis tests on C1, C2, and C3 for T1, T2, T3 and pooled results to compare the honey sugar concentrations, as measured in HU from standard curve (Fig. 3), in cells with distance from brood centre. There were some significant, but very weak, correlations between honey sugar concentrations in cells and their distances from the brood centre.

Appendix 1

Imaging live bee brains using Phase Contrast Tomography

ROYAL SOCIETY LONDON 2013

Mark K Greco[1,2], Jenna Tong[2], Manucher Soleimani[2], Duncan Bell[3], Marc O Schäfer[4], Cathryn Mitchell[2]

1 Department of Biology and Biochemistry, University of Bath, BA2 7AY, UK (m.k.greco@bath.ac.uk)
2 INVERT Centre, Department of Electrical and Electronic Engineering, University of Bath, BA2 7AY, UK
3 East Anglian Radiography Research, modelling and 3-D printing Group, School of Science, Technology and Health , University Campus Suffolk, Ipswich IP4
4 National Reference Laboratory for Bee Diseases, Friedrich-Loeffler-Institute, Federal Research Institute for Animal Health, Südufer 10, 17493, Greifswald – Insel Riems, Germany

Introduction

The sensitivity of the honeybee's brain volume and density (plasticity), which is believed to be linked to behavior, makes it a great model for exploring the interactions between experience, behavior and brain structure. Plasticity in the adult bee brain has been demonstrated in previous experiments (Ribi et al. 2008; Maleszka et al. 2009). This experiment was conducted to identify the potentials and limitations of phase contrast MicroCT scanning "live" bees as a more comprehensive, non-invasive method for brain morphology and physiology.

Methods

Bench-top and synchrotron MicroCT were used to scan live bees. For improved tissue differentiation, bees were fed and injected with radiographic contrast (Fig 1) and phase contrast scans were performed (Greco et al. 2012). Images of Optic lobes, ocelli, antennal lobes and mushroom bodies were visualized in 2D and 3D rendering modes (Fig 2).

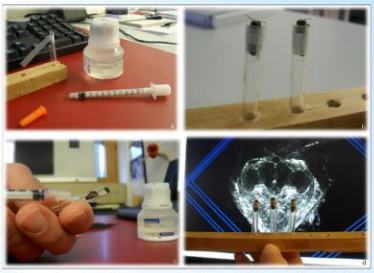

Figure 1: To enhance brain tissue differentiation, bolus injections of radiographic contrast media were delivered via a 30G needle (a) directly into the haemolymph, between the dorsal abdominal terga, of live bees that were previously secured for scanning (b) & (c). The 3D rendered brain (d) showed that contrast had perfused into tissue to enable improved structural differentiation.

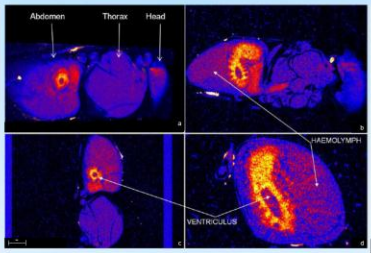

Figure 3: A 3D volume rendered image with BeeView software (www.disectsystems.com) of a live honey bee showing the three body segments (a) and orthogonal, 2D images (b), (c) & (d) showing the passage of radiographic contrast from the ventriculus (true stomach) to the haemolymph in the coelom. Images were rendered 1.5h after ingestion of contrast.

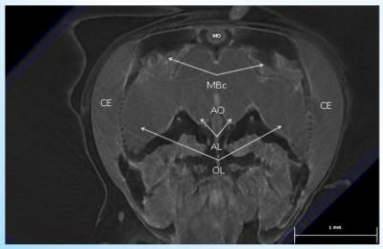

Figure 2: A 3D volume rendered image of a live honey bee's head capsule showing gross morphological structures such as the optic lobes (OL), antennal lobes (AL), aorta (AO), mushroom body calyces (MBc) and median ocellus (MO). The compound eyes (CE) are visualized immediately adjacent and lateral to the optic lobes.

Results

Scanning of live bees (for the first time) enabled minimally-invasive imaging of anatomy and physiological processes such as passage of contrast from gut to haemolymph (Fig 3) and preliminary brain perfusion studies.(Fig 4).

Discussion

The non-invasive methods for studying behaviour, morphology and physiology of insects and their colonies using X-ray CT (collectively termed Diagnostic Radioentomology "DR") is increasing. Our phase contrast results indicate that it is feasible to observe plasticity of the honey bee brain "in vivo" using DR and that progressive real-time observations of these changes can be followed in individual live bees. Although we used phase contrast methods, limitations such as movement errors and poor tissue differentiation due to the pulsating aorta and circulating haemolymph in the live bees were identified. The results are however encouraging for this line of research and we will explore dark field imaging to seek improvements in soft tissue differentiation. This study has demonstrated that there is still great potential for using phase contrast for in-vivo imaging of the honeybee to observe brain morphology and physiology. Research is also planned on the effects of pathogens on bee muscle tissue.

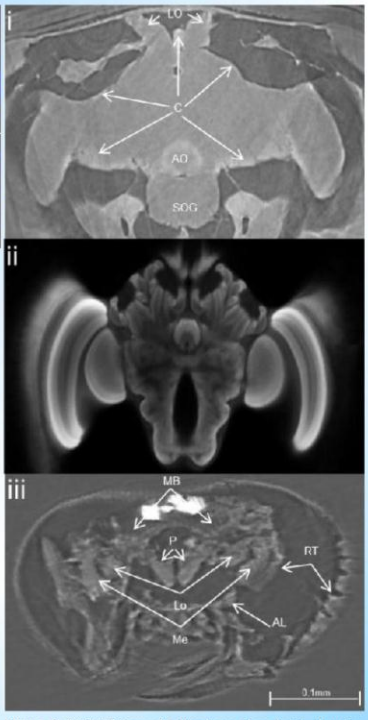

Figure 4: (i) Axial view of a live honey bee brain showing perfusion (C) into peripheral regions. At 30min post bolus injection, into the haemolymph, the lateral ocelli (LO) and aorta (AO) contained more contrast than the sub oesophageal ganglion (SOG). (ii) A comparative axial view from (http://www.neurobiologie.fu-berlin.de/beebrain/Default.html) using two-channel confocal microscopy. (iii) Axial view of the head capsule of 20MA stingless bee *Proplebeia abdita* in amber (Greco at al. 2011). The optic lobes (Me) and (Lo), antennal lobes (AL), protocerebral lobes (P), the mushroom bodies (MB). The retinal zone (RT) was well preserved.

REFS: Ribi W, Sendenb TJ, Sakellariou A, Limayec A, Zhang S. 2008. Imaging honey bee brain anatomy with micro-X-ray-computed tomography. *Journal of Neuroscience Methods* 171: 93–97. **Maleszka J, Barron AB, Helliwell PG, Maleszka R**. 2009. Effect of age, behaviour and social environment on honey bee brain plasticity. *Journal of Comparative Physiology A Neuroethology Sensory Neural And Behavioral Physiology* 195:733–740. **Greco MK, Tong J, Soleimani M, Bell D, Schäfer MO** 2012. Imaging live bee brains using minimally-invasive diagnostic radioentomology. Journal of Insect Science. Vol. 12 : Article 89.